AN INVESTIGATION OF MECHANISMS IN THE PATHOGENESIS OF AMIODARONE-INDUCED PULMONARY TOXICITY

by

ELIZABETH RAFEIRO

A thesis submitted to the Department of Pharmacology and Toxicology

in conformity with the requirements for the

degree of Doctor of Philosophy

Queen's University

Kingston, Ontario, Canada

September, 1997

QUEEN'S UNIVERSITY AT KINGSTON

SCHOOL OF GRADUATE STUDIES AND RESEARCH

PERMISSION OF CO-AUTHOR(S)

I/we, the undersigned, hereby grant permission to microfilm any material designated as being co-authored by me/us in the thesis copyrighted to the person named below:

Name of Copyrighted Author	Signature of copyrighted author
ELIZABETH RAFEIRO	Elizabeth Rafeiro

Name(s) of co-author(s)	Signature(s) of co-author(s)
RANDALL LEEDER	Randall Leeder
ANDREW TAM	Andrew Tam

DATE: Sept 25/97

QUEEN'S UNIVERSITY AT KINGSTON

SCHOOL OF GRADUATE STUDIES AND RESEARCH

PERMISSION OF CO-AUTHOR(S)

I/we, the undersigned, hereby grant permission to microfilm any material designated as being co-authored by me/us in the thesis copyrighted to the person named below:

ELIZABETH RAFEIRO — Elizabeth Rafeiro

Name of Copyrighted Author — Signature of copyrighted author

Name(s) of co-author(s)	Signature(s) of co-author(s)
ROBIN WALKER	Robin M Walker

DATE: Sept 5/97

QUEEN'S UNIVERSITY AT KINGSTON

SCHOOL OF GRADUATE STUDIES AND RESEARCH

PERMISSION OF CO-AUTHOR(S)

I/we, the undersigned, hereby grant permission to microfilm any material designated as being co-authored by me/us in the thesis copyrighted to the person named below:

Name of Copyrighted Author	Signature of copyrighted author
ELIZABETH RAFEIRO	Elizabeth Rafeiro

Name(s) of co-author(s)	Signature(s) of co-author(s)
GUOMAN CHEN	Guoman Chen

DATE: Sept 5/97

ABSTRACT

Elizabeth Rafeiro: An investigation of mechanisms in the pathogenesis of amiodarone-induced pulmonary toxicity. Ph.D. thesis, Department of Pharmacology and Toxicology, Queen's University at Kingston, September 1997.

Amiodarone (AM) is an efficacious antidysrhythmic agent. However, its clinical use is limited by life-threatening pulmonary toxicity. The morphological effects of AM on cultured lung slices, as well as the role of free radicals and the susceptibility of the mitochondrion in AM-induced pulmonary toxicity (AIPT), were studied.

The keto group of AM has been proposed to play a key role in free radical generation and AIPT. At 21 days post-dosing, hamsters treated intratracheally with 1.83 μmol of either AM or des-oxo-amiodarone (DOAM), a synthetic AM derivative lacking its keto oxygen, had increased lung weight, hydroxyproline content, and histological disease index compared to controls. Thus, DOAM possesses fibrogenic properties similar to AM, but appears to be a somewhat less potent pulmonary toxicant.

Using electron spin resonance and the spin trapping agent α-phenyl-N-t-butylnitrone (PBN), AM (2-20 mM) generated a free radical in lung and liver microsomes *in vitro*. The PBN-free radical adduct possessed hyperfine splitting constants (hfsc's) consistent with a carbon centred phenyl radical. In addition, both DOAM and desethylamiodarone, a major AM metabolite, generated radicals with hfsc's very similar to the AM generated radical.

Many agents that initiate toxicity via a radical process induce oxidative stress, reflected by induction of antioxidant enzymes. Since assessment of oxidative stress *in vivo* is complicated by extrapulmonary factors, cultured hamster lung slices were used as a model system to study AIPT. Electron microscopy showed that type I alveolar cells were susceptible to damage in lung slices incubated with 200 μM AM. However, control lung slices developed elevated glutathione reductase activity, which prohibited assessment of AM's ability to induce the enzyme.

AM exerted a biphasic effect (stimulation followed by inhibition) on state 4 respiration of complexes I and II in hamster lung mitochondria *in vitro*.

Overall, this study has shown that the keto group of AM does not play a key role in AIPT, but that AM is capable of generating a free radical in lung and liver microsomes. Furthermore, the type I cell is selectively damaged in cultured lung slices incubated with AM, and AM causes dysfunction of lung mitochondria.

Keywords: amiodarone, pulmonary toxicity, free radicals, electron spin resonance, mitochondria, cultured lung slices, hamster.

CO-AUTHORSHIP

This research was conducted by the candidate Elizabeth Rafeiro, under the supervision of Dr. T.E. Massey.

Dr. Randall L. Leeder assisted with experiments in Chapter 2. This included assistance with intratracheal amiodarone administration, hydroxyproline measurement and sample preparation for HPLC analysis.

Dr. Guoman Chen (University of Guelph) provided advice on experimental design and conducted sample analysis by ESR spectroscopy (Chapter 3).

Dr. Robin M. Walker (Parke-Davis Research Institute) performed electron microscopy on cultured hamster lung slices and provided ultrastructural evaluation (Chapter 4).

Andrew Tam assisted with experiments in Chapter 5. This included assistance with the preparation of isolated hamster lung mitochondria and measurement of mitochondrial oxygen consumption.

ACKNOWLEDGEMENTS

I would like to thank my research supervisor and friend, Dr. T.E. Massey, for his guidance and patience during the course of this research and for providing a friendly environment in which to work.

I am grateful to Dr. Robin M. Walker for allowing me to benefit from his expertise in electron microscopy. Dr. E. Janzen also offered his vast knowledge on electron spin resonance. Both collaborators were very helpful and pleasant to work with.

I would like to thank Dr. James F. Brien for his willingness to offer advice and answer my questions and most of all, for his perpetual enthusiasm. I am also indebted to Dr. William J. Racz for reading my thesis rapidly so that I could meet the submission deadline. I appreciated all the interesting discussions, his unique sense of humour and just being able to walk into his office to get his insight into various matters. All of the professors in the department have been very approachable and eager to assist me with my queries.

Research wouldn't have been as interesting without the contribution of all the freaky personalities in the department, especially the members of my lab, both past and present (Sophia Ali, Sue Im, Patty Donnelly, Rick Stewart, Mike Bolt, Graeme Smith, Andrew Tam, Jeff Card). I've made many special friends and I will have some great memories. I would especially like to thank Lucy Longo for helping me in my moments of panic. I also appreciate all the assistance provided by Bernice Ison, Janet LeSarge, Chris Berga and René Roscher.

Special thanks to my parents, sisters Cathleen, Doreen and Norvinda, and Randy Leeder for their support and encouragement, and for just plain putting up with me.

I would like to acknowledge the following sources for providing financial support toward the completion of this research: the Department of Pharmacology and Toxicology at Queen's University, the School of Graduate Studies and Research at Queen's University, the Ontario Ministry of Colleges and Universities, the Medical Research Council of Canada and the Society of Toxicology.

Dedicated with love to my parents

TABLE OF CONTENTS

CHAPTER 2
A COMPARISON OF THE *IN VIVO* PULMONARY TOXICITY OF DES-OXO-AMIODARONE AND AMIODARONE IN THE HAMSTER.

CHAPTER 3
AN ELECTRON SPIN RESONANCE AND SPIN TRAPPING STUDY OF FREE RADICAL PRODUCTION BY AMIODARONE *IN VITRO*.

CHAPTER 4
AN INVESTIGATION OF AIPT IN CULTURED ADULT PERIPHERAL HAMSTER LUNG SLICES.

CHAPTER 5
EFFECT OF *IN VITRO* AMIODARONE ON LUNG MITOCHONDRIAL RESPIRATION.

CHAPTER 6
GENERAL DISCUSSION AND FUTURE DIRECTIONS

LIST OF TABLES

LIST OF FIGURES

LIST OF ABBREVIATIONS AND SYMBOLS

ADP	adenosine diphosphate
ATP	adenosine triphosphate
ATPase	adenosine triphosphatase
$RO^{\bullet}$	alkoxyl radical
AIPT	amiodarone-induced pulmonary toxicity
AM	amiodarone
ANOVA	analysis of variance
AV	atrioventricular
BALF	bronchoalveolar lavage fluid
BCNU	1,2-bis(2-chloroethyl)-1-nitrosourea
BSA	bovine serum albumin
BHA	butylated hydroxyanisole
Ca^{2+}	calcium ion
CAMIAT	Canadian Amiodarone Myocardial Infarction Arrythmia Trial
CCl_4	carbon tetrachloride
cm	centimetre(s)
CYP450	cytochrome P-450
^{51}Cr	chromium
°C	degrees celsius
DNA	deoxyribonucleic acid

DEA	desethylamiodarone
DOAM	des-oxo-amiodarone
EPR	electron paramagnetic resonance
ESR	electron spin resonance
et al.	et alia (and others)
etc.	et cetera (and others esp. of same kind)
EDTA	ethylenediamine tetraacetic acid
EGTA	ethylene glycol-bis (β-amino ethyl ether) tetraacetic acid
EMIAT	European Myocardial Infarction Amiodarone Trial
eg.	exempli gratia (for example)
G	Gauss
GSH	glutathione, reduced form
GSSG	glutathione, oxidized form
g	gram(s)
HPLC	high performance liquid chromatography
h	hour(s)
HCl	hydrochloride
H_2O_2	hydrogen peroxide
$HOO^{\bullet}$	hydroperoxyl radical
$^{\bullet}OH$	hydroxyl radical
hfsc	hyperfine splitting constant(s)

a^N	hyperfine splitting constant for α-nitrogen atom
$a_\alpha^{^{13}C}$	hyperfine splitting constant for α-^{13}-carbon atom
a_β^H	hyperfine splitting constant for β-hydrogen atom
HOCl	hypochlorous acid
ie.	id est (that is)
G_i protein	inhibitory guanyl-nucleotide binding protein
IU	international units
im	intramuscular
ip	intraperitoneal
it	intratracheal
iv	intravenous
LDH	lactate dehydrogenase
$LO^\bullet$	lipid alkoxyl radical
LOOH	lipid hydroperoxide
$LOO^\bullet$	lipid peroxyl radical
LPO	lipid peroxidation
L	litre(s)
$\bar{x}$	mean
3-MI	3-methylindole
μ	micro
mg	milligram(s)
ml	millilitre(s)

mm	millimetre
mW	milliwatts
min	minute(s)
M	molar
MOPS	3-[N-morpholino]propane-sulfonic acid
MTT	3-[4,5-dimethylthiazol-2-yl]-2,5-diphenyl-
nm	nanometer(s)
pH	negative logarithm of the hydrogen ion concentration
NAD	nicotinamide adenine dinucleotide
NADH	nicotinamide adenine dinucleotide (reduced form)
NADPH	nicotinamide adenine dinucleotide phosphate (reduced form)
$NO^{\bullet}$	nitric oxide
N_2	nitrogen gas
N	normal
n	number (of experiments or subjects)
O_2	oxygen (molecular)
PQ	paraquat
$ROO^{\bullet}$	peroxyl radical
PBN	α-phenyl-N *tert*-butylnitrone
PBS	phosphate buffered saline
±	plus or minus

PMN	polymorphonuclear leukocyte
PUFAs	polyunsaturated fatty acids
K+	potassium ion
p<	probability less than
$R^{\bullet}$	radical
ROS	reactive oxygen species
x g	relative centrifugal force
RCR	respiratory control ratio
rpm	revolutions per minute
sec	second(s)
$^1O_2$	singlet oxygen
M_s	spin orientation of an electron
S	spin quantum number
Na^+	sodium ion
SD	standard deviation
$O_2^{\bullet-}$	superoxide anion radical
SOD	superoxide dismutase
CCl_3	trichloromethyl radical
UV	ultraviolet
v/v	volume per volume
H_2O	water
w/v	weight per volume

in vitro	'within a glass' (outside the living body)
in vivo	within the living body

CHAPTER 1

GENERAL INTRODUCTION

1.1 STATEMENT OF RESEARCH PROBLEM

Amiodarone (AM, Cordarone®, Wyeth-Ayerst Laboratories Inc.) is an efficacious antidysrhythmic agent used to treat a variety of life-threatening cardiac dysrhythmias. However, the use of AM is limited by its propensity to produce a wide variety of adverse effects. The adverse effect of greatest clinical concern is pneumonitis which may progress to life threatening pulmonary fibrosis. The etiology of amiodarone-induced pulmonary toxicity (AIPT) is unknown. However, numerous mechanisms have been proposed (reviewed in Massey *et al.*, 1995; Reasor and Kacew, 1996). The goal of this thesis research was to investigate the initiating mechanism(s) involved in AIPT. Specifically, the role of free radicals in AIPT was examined. In addition, a preliminary investigation of the mitochondrion as a target organelle of AIPT was conducted. An understanding of the underlying mechanism(s) of AIPT will facilitate the development of therapeutics to prevent/counteract the clinical toxicities of AM and/or the development of antidysrhythmic agents of similar efficacy without pulmonary toxicity.

1.2 HISTORY AND THERAPEUTIC USE OF AMIODARONE

AM (2-N-butyl-3(4'-diethylaminoethoxy-3',5'-diiodobenzoyl-benzofuran), an iodinated benzofuran derivative (Fig. 1.1) was first synthesized in Belgium in 1961, for

A

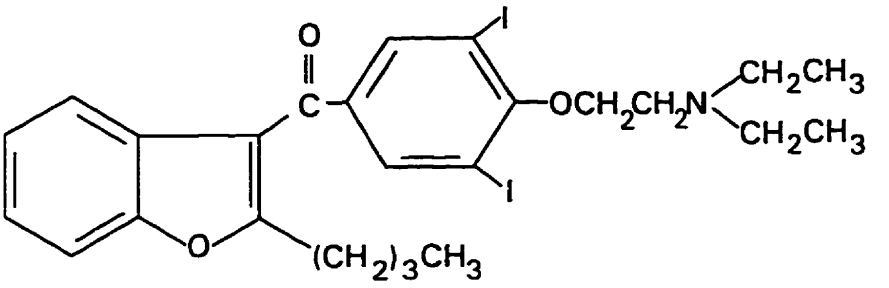

B

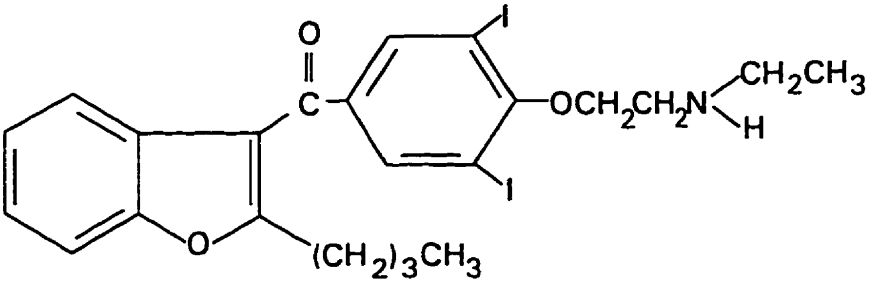

Fig. 1.1 The chemical structures of A) amiodarone (2-N-butyl-3(4'-diethylaminoethoxy-3',5'-diiodobenzoyl-benzofuran) and B) desethylamiodarone, a major metabolite of AM.

use as a coronary vasodilator (Charlier *et al.*, 1962). In 1967, it was marketed in Europe as an antianginal agent and was subsequently discovered to possess antidysrhythmic properties (Charlier *et al.*, 1969; VanSchepdael and Solvay, 1970). Oral AM was approved for the treatment of life threatening ventricular and supraventricular dysrhythmias resistant to other pharmacotherapy in the United States in 1985, and then in Canada, in 1986. Intravenous AM has recently received approval for the emergency treatment of these dysrhythmias in both Canada and the United States.

Currently, AM is considered to be the most effective agent in the control of ventricular tachycardia and fibrillation, and in maintaining sinus rhythm in patients with atrial fibrillation and flutter (Singh, 1996). However, due to its serious adverse effects (discussed in section 1.5), its use has been restricted for the treatment of sustained or severe dysrhythmias that are resistant to other treatments and thus has been referred to as a "last resort" therapy (Gill *et al.*, 1992). In spite of limited indications for AM therapy, Wyeth-Ayerst reported that oral Cordarone® was the number one selling antidysrhythmic agent in the United States in 1995 (American Home Products Corporation 1995 Annual Report) and in Canada in 1996 (C. McPhee of IMS Canada, personal communication).

Within this past decade, numerous clinical trials have been conducted to evaluate the prophylactic use of AM in post-myocardial infarction patients who are at high risk for developing dysrhythmias. The recent release of the results of the large multicenter Canadian Amiodarone Myocardial Infarction Arrhythmia Trial (CAMIAT)

and European Myocardial Infarction Amiodarone Trial (EMIAT) demonstrated that low dose AM (200 mg/day) can reduce the occurrence of dysrhythmic death in the two year period following a heart attack by nearly 50% and 35% respectively (Cairns *et al.*, 1991; Cairns *et al.*, 1997; Julian *et al.*, 1997). Although there was a trend toward a reduction in total mortality by AM, it was not significant. The prophylactic use of AM following post-myocardial infarction has been criticized because neither of these studies demonstrated a significant reduction in total mortality by AM, believed by some investigators to be the only important outcome (Gottlieb, 1997).

Thus, although AM is indicated in patients experiencing dysrhythmias, its benefit as a prophylactic therapy in post-myocardial infarction patients has not been unequivocally established.

1.3 PHARMACODYNAMICS OF AMIODARONE

AM is technically classified as a Class III antidysrhythmic agent. However, it has been found to possess characteristics of all four Vaughan-Williams antidysrhythmic classes. AM decreases the rate of onset of action potential by Na^+ channel blockade (class I); antagonizes α- and β-adrenergic receptors in a non-competitive manner (class II); increases action potential duration, thereby prolonging repolarization and refractoriness (class III); and blocks Ca^{2+} channels (class IV) (Rothenberg *et al.*, 1994).

AM's most important direct electrophysiological effect is its ability to lengthen action potential duration in all cardiac tissues. This action is thought to be attributed to

K^+ channel blockade and results in a reduction in membrane excitability which represents the antifibrillatory action of AM (Podrid, 1995). Unlike that of other Class III agents, the prolongation of action potential by AM persists at higher heart rates, which makes it especially effective in the treatment of tachycardias (Anderson *et al.*, 1989). However, Class III activity alone cannot account for AM's antidysrhythmic efficacy (Nattel and Talajic, 1988; Podrid, 1995).

AM is also a weak Na^+ channel blocker, which results in slowing of the upstroke velocity of the action potential and thus the rate of membrane depolarization and impulse conduction (Mason *et al.*, 1983). In contrast to other Na^+ channel blockers, AM selectively blocks inactivated Na^+ channels. Therefore, AM is more effective in depolarized tissue (as in myocardial ischemia), tissue with a brief diastole (as during tachycardia), and tissue with prolonged repolarization (Mason, 1987). Na^+ channel blockers are generally used to treat ventricular dysrhythmias (Nattel and Talajic, 1988).

AM directly depresses the automaticity of the sinus and atrioventricular (AV) nodes, and increases conduction time and refractoriness of the AV node. These increases are partially due to α- and β-adrenergic receptor and Ca^{2+} channel blockade (Podrid, 1995). Ca^{2+} channel blocking effects are beneficial for the treatment of re-entrant dysrhythmias involving the AV node, in controlling ventricular response to atrial fibrillation and flutter, and in dysrhythmias arising from early and delayed after-depolarizations (Singh, 1996).

AM also possesses antianginal properties which may be attributed to its non-

competitive α- and β-adrenergic blockade, in addition to Ca^{2+} channel blockade. These actions are responsible for the dilation of coronary and systemic arteries, which results in an increased coronary blood supply and reductions in systemic blood pressure and afterload (Singh and Vaughan-Williams, 1970). AM has mild direct negatively ionotropic actions, which reduces the force of myocardial contraction and myocardial oxygen consumption (Schwartz *et al.*, 1983).

AM interferes with thyroid hormone metabolism (Rao *et al.*, 1986) and antagonizes thyroid effects in the heart (Nademanee *et al.*, 1986), effects which are believed to contribute to the drug's antidysrhythmic action.

Mono-N-desethylamiodarone (DEA; Fig. 1.1), a major metabolite of AM, is also electrophysiologically active. Although DEA possesses a similar qualitative pharmacodynamic profile to AM, it appears to be more potent (Singh *et al.*, 1989).

1.4 PHARMACOKINETICS OF AMIODARONE

Knowledge of the unique and complex pharmacokinetics of AM is necessary to facilitate an understanding of the clinical toxicities produced by this agent. This pharmacokinetics section focuses primarily on clinical studies. However, the biotransformation section also includes a discussion of studies in experimental animals.

1.4.1 Physicochemical properties

AM is an amphiphilic molecule that contains both hydrophobic (benzofuran and di-iodinated benzene) and hydrophilic (tertiary amine) portions (Bonati *et al.*, 1983).

AM is therefore highly lipophilic and preferentially accumulates in the lipid rich regions of cells, particularly membranes (Chatelain and Laruel, 1985; Herbette *et al.*, 1988). Not suprisingly, AM has a great affinity for lipophilic tissues, has a large apparent volume of distribution (approximately 5000L) and extensively binds to plasma proteins (> 96 %) (Holt *et al.*, 1983).

1.4.2 Absorption

Large interindividual differences exist among all aspects of AM's pharmacokinetic spectrum, ranging from absorption to elimination (Gill *et al.*, 1992). AM is slowly absorbed following oral administration, and peak plasma levels are attained within 3 to 7 h (Roden, 1993). Oral AM bioavailability following a single dose is highly variable, ranging from 20-86% for comparable doses (Andreasen *et al.*, 1981; Riva *et al.*, 1982; Holt *et al.*, 1983; Latini *et al.*, 1984). This variability is thought to arise from AM's relatively low aqueous solubility and its extensive first pass metabolism (Holt *et al.*, 1983; Latini *et al.*, 1984).

1.4.3 Distribution

Analysis of autopsy samples from individuals who received chronic AM treatment has revealed that AM and DEA accumulate in a variety of tissues. In fact, tissue AM levels are usually 10 to 1000 times greater than plasma levels (Riva *et al.*, 1982; Plomp *et al.*, 1984). Generally, AM levels are highest in adipose tissue, lung or liver, followed in decreasing order by bone marrow, pancreas, spleen, heart, kidney,

skeletal muscle, thyroid and brain (Haffajee *et al.*, 1983; Holt *et al.*, 1983; Maggioni *et al.*, 1983; Canada *et al.*, 1980; Plomp *et al.*, 1984; Brien *et al.*, 1987). Lung AM levels are quite variable and range from 20 μg/g to 734 μg/g tissue following chronic AM therapy in humans (Haffajee *et al.*, 1983; Heger *et al.*, 1983; Holt *et al.*, 1983; Maggioni *et al.*, 1983; Plomp *et al.*, 1984; Brien *et al.*, 1987; Nalos *et al.*, 1987). With the exception of adipose and plasma, DEA levels are typically present in greater quantity in their respective tissues than are those of AM (Nalos *et al.*, 1987). This observation has been explained by a more favorable diffusion of DEA from plasma to tissues, due to decreased binding to plasma proteins and a different ionization state (pK_a) compared to AM (Plomp *et al.*, 1985).

Upon initiation of AM therapy, relatively less DEA compared to AM is present in plasma (Heger *et al.*, 1983). However, at steady state, plasma concentrations of DEA and AM are comparable (Holt *et al.*, 1983; Plomp *et al.*, 1984; Brien *et al.*, 1987). The therapeutic plasma AM concentration has been suggested to range from 1 to 2.5 μg/ml, with the risk of toxicity increasing beyond 2.5 μg/ml (Latini *et al.*, 1984; Rotmensch *et al.*, 1984). However, there is substantial interindividual variation between plasma AM concentration and therapeutic and toxic effects. Therefore, monitoring of plasma drug levels may be of limited predictive value (Greenberg *et al.*, 1987; Maling, 1988).

1.4.4 Biotransformation

The biotransformation of AM has not been completely characterized.

Nonetheless DEA, is recognized as a major metabolite of AM. As in humans, DEA is present in the blood and many tissues of experimental animals (Kannan *et al.*, 1985; Daniels *et al.*, 1990) following AM administration. Small quantities of N'N'-didesethylamiodarone have been observed in hamsters (Daniels *et al.*, 1989) and in dogs (Brien *et al.*, 1990), and a deiodinated metabolite has been detected in rats (Kannan *et al.*, 1989). Other unidentified metabolites were detected in serum from AM-treated patients (Stäubli *et al.*, 1985) and in *in vitro* incubations of AM with rabbit hepatic and gut microsomes (Young and Mehendale, 1986), and human hepatic microsomes (Trivier *et al.*, 1993).

DEA is believed to be produced mainly by hepatic cytochrome P-450 (CYP450) (Young and Mehendale, 1986; 1987; Rafeiro *et al.*, 1990; Blake and Reasor, 1995) and possibly to a much smaller extent by intestinal microsomal flavin containing monooxygenase (Young and Mehendale, 1987). Hepatic CYP450 3A was shown to play a major role in the production of DEA following treatment of rats with dexamethasone, an inducer of the CYP450 3A subfamily (Rafeiro *et al.*, 1990). Similarly, CYP450 3A4 and 1A1 were subsequently found to be particularly active in the biotransformation of AM to DEA in human hepatic microsomes (Ha *et al.*, 1992; Trivier *et al.*, 1993).

DEA production was not quantifiable in uninduced hamster and rat lung microsomes (Young and Mehendale, 1987; Rafeiro *et al.*, 1990; Blake and Reasor, 1995) and in isolated perfused rat lungs (Camus and Mehendale, 1986). DEA formation was slightly elevated in lung microsomes from rabbits treated with 3-

methylcholanthrene (a selective CYP450 1A1 inducer) and in rats treated with phenobarbital (an inducer of multiple forms of CYP450, particularly CYP2B1/2) (Young and Mehendale, 1987). Thus, although DEA accumulates in the lung, no significant metabolism of AM to DEA occurs in the lung.

Interestingly, Larrey and coworkers (1986) have shown that administration of AM to rats, mice and hamsters results in the *in vivo* formation of a biologically inactive CYP450-Fe(II)-AM metabolite complex in the liver. Indeed, AM has been shown to inhibit CYP450 and related enzyme activities. The inhibition of CYP450 mediated metabolism of certain drugs (ie., digoxin, warfarin) and accompanying increase in parent drug levels in the plasma (Grech-Bélanger, 1984; Staiger *et al.*, 1984) is believed to be responsible for the reported drug interactions associated with AM therapy (Grech-Bélanger, 1984; Duenas-Laita *et al.*, 1987; Padmavathy *et al.*, 1993).

1.4.5 Elimination

The elimination of AM from plasma after drug withdrawal is biphasic. There is a rapid short elimination phase followed by a protracted phase of slow elimination. This pattern is thought to be the result of initial rapid distribution of AM from its central compartment, followed by a much slower clearance from a poorly perfused peripheral compartment such as adipose (Holt *et al.*, 1983; Mason *et al.*, 1987). The plasma terminal elimination half-life of AM ranges from 3.2 to 79.7 h after single dose administration (Latini *et al*, 1984) and from 14-107 days following cessation of long-term AM therapy (McKenna *et al.*, 1983), with reports of plasma AM levels still

detectable for up to 9 months (Singh, 1996). The elimination half-life of DEA is even greater than that for AM and is thought to be a result of DEA's higher affinity for tissues (Holt *et al.*, 1983). Biliary and fecal excretion are the major routes of elimination for both AM and DEA. Renal excretion is negligible, with less than 1% of administered AM or DEA being recovered in the urine (Andreasen *et al.*, 1981; Anastasiou-Nana *et al.*, 1982; Riva *et al.*, 1982; Plomp et al., 1985).

Both AM and DEA have a great propensity to accumulate in tissues, and are slowly eliminated. Thus, their antidysrhythmic effects are maintained for a prolonged period following discontinuation of drug therapy (Plomp et al., 1984). More importantly, toxicity may be initiated or that which has been initiated, may progress (Martin, 1990).

1.5 CLINICAL TOXICITIES OF AMIODARONE

Amiodarone therapy is associated with a variety of adverse effects that affect a wide range of organs and tissues (Rothenberg *et al.*, 1994). The most common adverse effects (10 to 100% incidence) include corneal microdeposits, elevation of serum liver enzymes, gastrointestinal disturbances, skin photosensitivity, ataxia and fine hand tremors. Less frequent adverse effects (1-10% incidence) include hyperthyroidism, hypothyroidism, peripheral neuropathy and grey/blue skin discolouration (Gill *et al.*, 1992). These effects can all be abolished upon AM dose reduction or withdrawal of AM therapy (Vrobel *et al.*, 1989).

Adverse effects of greatest clinical concern are hepatitis (< 1% incidence)

(Marchlinski, 1987), exacerbation of cardiovascular disorders (ie., congestive heart failure, proarrhythmia, bradycardia) and pulmonary toxicity, due to their potential for mortality (Mason, 1987; Gill *et al.*, 1992). Since most patients requiring AM therapy have severe heart disease and dysrhythmias, it is difficult to distinguish between mortality attributable to the underlying illness or AM toxicity (Vrobel et al., 1989; Podrid, 1995). Consequently, it is the pulmonary toxicity produced by AM that limits its use and previously earned it the reputation of being a drug of last resort (Rakita *et al.*, 1983). It has been estimated that as many as 13% of patients receiving AM may develop AIPT, and that 10 to 23% of these may die as a result of complications (Mason, 1987; Vrobel *et al.*, 1989). In two recent multicentre trials (>2500 patients), only 2.4% of patients receiving low dose AM (200 mg/day) developed pulmonary toxicity. Nonetheless, pulmonary toxicity remains the adverse effect of greatest clinical concern (Cairns *et al.*, 1997; Julian *et al.*, 1997).

1.6 AMIODARONE-INDUCED PULMONARY TOXICITY (AIPT)

1.6.1 Clinical presentation and treatment of AIPT

Two types of clinical presentations of AIPT have been identified: an acute type and the more common subacute/chronic type which has an insidious onset of symptoms (Martin and Rosenow, 1988a; Fraire *et al.*, 1993). The subacute/chronic manifestation occurs in the majority of AIPT cases and rarely occurs prior to two months of therapy. It is associated with parenchymal infiltrates, primarily of a diffuse interstitial pattern. The acute type of presentation occurs in approximately one-third of affected patients

and is associated with a more rapid onset. A predominant alveolar pattern with a patchy distribution sometimes involving the peripheral lung is evident. This type of presentation is routinely associated with fever and may mimic an infectious pneumonitis.

Unfortunately the signs and symptoms of AIPT are not unique to the toxicity of AM. They normally include non-productive cough, pleuritic pain, dyspnea upon exertion and occasionally fever. Weakness and weight loss are also common symptoms (Martin and Rosenow, 1988a).

The risk of AIPT appears to increase with higher doses and the majority of patients with this complication have received AM maintenance doses of >400mg/day (Adams *et al.*, 1988). When AM is used in lower doses and not as a drug of last resort, toxicity appears to be much less a problem (Rakita and Mostow, 1988). However, there are reports that are inconsistent with these observations (Darmanata *et al.*, 1984; Pitcher, 1992). Cumulative drug dose and duration of therapy may be important determinants of the risk of AIPT (Suárez *et al.*, 1983; Joelson *et al.*, 1984). Preexisting lung disease may increase the risk of developing AIPT in patients receiving AM (Darmanata *et al.*, 1984; Kudenchuk *et al.*, 1984; Mason, 1987).

Reduction of AM dose or withdrawal of therapy with or without the administration of corticosteroids is used in the management of AIPT (Rakita *et al.*, 1983; Suárez *et al.*, 1983; Cazzadori *et al.*, 1986). Corticosteroid therapy is indicated when there is an immunological basis to pulmonary disease. In most cases, symptoms will begin to resolve. However, it may take months for complete recovery to occur

(Vrobel *et al.*, 1989). The benefit of corticosteroids is not certain as AIPT may resolve without their use (Suárez *et al.*, 1983; Gibb and Melendez, 1986).

1.6.2 Histopathology of AIPT

The histopathological features associated with AIPT may vary considerably among patients. The most common features include interstitial/alveolar thickening, cellular infiltration of the interstitium/alveoli consistent with pneumonitis, and/or fibrosis (Van Zandwijk *et al.*, 1983; Suárez *et al.*, 1983; Costa-Jussà *et al.*, 1984; Pollak and Sami, 1984; Brien *et al.*, 1987; Myers *et al.*, 1987; Nalos *et al.*, 1987). Pulmonary fibrosis is defined as the abnormal deposition of excess collagen in the lung (Reiser and Last, 1986). The pattern of damage may either be patchy or diffuse and may affect the alveoli, the interstitium, or both (Vrobel *et al.*, 1989; Dusman *et al.*, 1990).

Numerous "foamy" macrophages are located in the alveolar spaces as well as in the interstitium (Marchlinski *et al.*, 1982; Suárez *et al.*, 1983; Gefter *et al.*, 1983; Pollak and Sami, 1984; Dake *et al.*, 1985; Dean *et al.*, 1987; Myers *et al.*, 1987; Nalos *et al.*, 1987). Other pneumocytes (ie., endothelial, epithelial and interstitial) also possess a "foamy" appearance which is the result of the presence of cytoplasmic multilamellar phospholipid inclusion bodies. However, the presence of these foamy cells does not reliably predict AIPT as the lungs of individuals without AIPT may possess foamy cells (Fraire *et al.*,1993). Edema (Costa-Jussà *et al.*, 1984; Darmanta *et*

al., 1984) and intra-alveolar fibrin exudate (Dean *et al.*, 1987) sometimes accompanies the inflammatory response. Cellular infiltrates include macrophages, a variable number of lymphocytes, neutrophils and rarely eosinophils and plasma cells (Van Zandwijk *et al.*, 1983; Myers *et al.*, 1987). Alveolar wall thickening is caused by fibroblast proliferation and the production of excess collagen and elastin, which may progress to the more critical fibrosis observed in some patients (Gefter *et al.*, 1983; Van Zandwijk *et al.*, 1983; Cazzadori *et al.*, 1986; Dean *et al.*, 1987). Hyperplasia of alveolar type II cells may be evident, which is a normal reparative response to type I cell injury (Marchlinski *et al.*, 1982; Pollak and Sami, 1984; Brien *et al.*, 1987). Hyaline membrane formation may also be present (Sobol and Rakita, 1982; Cazzadori *et al.*, 1986; Brien *et al.*, 1987; Myers *et al.*, 1987; Kay *et al.*, 1988). Rarely, pleural thickening or pleural effusion may occur (Dusman *et al.*, 1990; McNeil *et al.*, 1992).

1.7 PROPOSED MECHANISMS OF AIPT

Although the etiology of AIPT is currently unknown, two types of toxic mechanisms have been proposed: 1) an indirect or immunologic mechanism and 2) a direct toxic mechanism (Fig. 1.2).

1.7.1 Indirect versus Direct Toxicity

Direct toxicity implies that AM and/or DEA are directly cytotoxic to lung cells. In contrast, the stimulation of an inflammatory or an immune response in the lung by

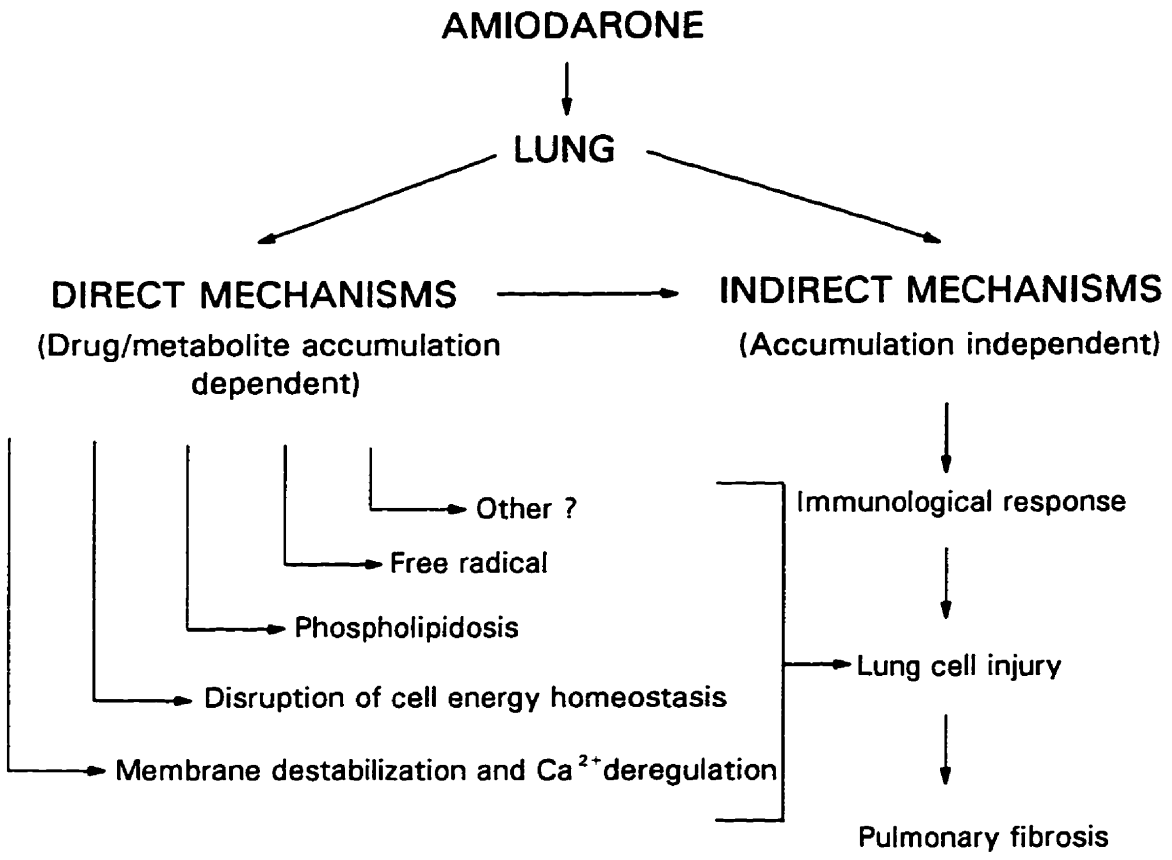

Fig. 1.2 Proposed mechanisms of AIPT. (modified from Massey *et al.*, 1995)

AM and/or DEA indicates an indirect mechanism of toxicity. It may be that AM mediates toxicity by more than one mechanism as AIPT occurs with varying clinical presentations (Fraire *et al.*, 1993). Thus, it has been suggested that the development of AIPT is multifactorial, and dependent upon individual patient characteristics, some of which may be genetically based (Martin, 1990; Reasor and Kacew, 1991; Pitcher, 1992). Likewise, other drugs (eg. nitrofurantoin, bleomycin) producing lung injury have been shown to exhibit features of both indirect and direct toxic mechanisms (Rosenow and Martin, 1990). However, differentiation between the initiating toxic event(s) and the events that follow as a result of the initiating event(s) is critical to the understanding of the etiology of AIPT.

1.8 INDIRECT TOXICITY (IMMUNOLOGIC MECHANISM)

The occurrence of AIPT is not always associated with AM dose (daily or cumulative) or blood levels and therefore has led to the proposal that the development of AIPT may have an immunological basis (Dunn and Glassroth, 1989).

Evidence for the role of a hypersensitivity mechanism in clinical studies of AIPT includes the following: 1) deposition of C3 fragment of complement in the lung (Joelson *et al.*, 1984; Manicardi *et al.*, 1989); 2) lymphocytosis in bronchoalveolar lavage fluid (BALF) (Akoun *et al.*, 1984; Venet *et al.*, 1984; Israël-Biet *et al.*, 1985); 3) an inverted ratio of helper/suppressor T lymphocytes in BALF in favour of suppressor (Akoun *et al.*, 1984; Venet *et al.*, 1984; Israël-Biet *et al.*, 1985; Manicardi *et al.*, 1989; Akoun *et al.*, 1991); 4) secretion of leukocyte inhibitory factor in the

presence of AM (Akoun *et al.*, 1984); 5) positive skin and basophil degranulation tests and lymphoblastic transformation tests in the presence of AM (Akoun *et al.*, 1984); 6) presence of serum anti-AM antibodies (Pichler *et al.*, 1988) which react with lung of patients with AIPT and with AM itself, but not with normal lung or fibrotic lung of patients not using AM (Fan *et al.*, 1987); 7) an increase in immunoglobulin levels in BALF of patients with AIPT (Sandron *et al.*, 1986); 8) an increase in BALF cellularity consisting of a variable increase in number of lymphocytes, neutrophils, eosinophils and mast cells (Venet *et al.*, 1984; Israël-Biet *et al.*, 1987; Akoun *et al.*, 1991; Coudert *et al.*, 1992); 9) alleviation of AIPT upon initiation of corticosteroid therapy with or without discontinuation of AM therapy (Venet *et al.*, 1984; Israël-Biet *et al.*, 1987; McNeil *et al.*, 1992). Some investigators have postulated that AM acts as a hapten by binding to a native lung tissue protein carrier *in vivo*, thereby eliciting a humoral antibody response (Fan *et al.*, 1987). However, immunoglobulins that are specific to patients with AIPT have not been found (Gefter *et al.*, 1983; Colgan *et al.*, 1984).

Evidence against an immunological basis for AIPT includes the following. Several clinical studies have failed to detect complement, immunoglobulins or lymphocytosis in patients with AIPT (Marchlinski *et al.*, 1982; Adams *et al.*, 1986; Ohar *et al.*, 1992) while others have found no difference in immune response between patients with AIPT and those without (Darmanata *et al.*, 1984; Liu *et al.*, 1986; Pichler *et al.*, 1988; Nicolet-Chatelain *et al.*, 1991; Coudert *et al.*, 1992). Additionally, upon resolution of pulmonary toxicity, rechallenge with AM does not

always result in reappearance of toxicity (Rakita *et al.*, 1983). The amelioration of AIPT upon cessation of AM treatment with or without the use of corticosteroid therapy (Gefter et al., 1983; Leech *et al.*, 1984) as well as the lack of improvement of AIPT with corticosteroids (Cooper *et al.*, 1986) further challenges an immunological mechanism.

Some investigators have suggested that the immune response may be a secondary response to direct drug toxicity (Israël-Biet *et al.*, 1987; Nicolet-Chatelain *et al.*, 1991). In various animal models of AIPT, increases in lung natural killer cell activity, lymphocytosis, neutrophilia and eosinophilia have been demonstrated (Cantor *et al.*, 1984; Karpel *et al.*, 1991; Blake and Reasor, 1995; 1996). However, these inflammatory cells did not appear sufficiently early to be considered initiating factors in the development of AIPT. It is possible that the immunological reaction may contribute to or amplify AIPT, and more importantly, pulmonary fibrosis. It is well known that the recruitment and/or activation of inflammatory cells leads to the release of inflammatory mediators which play an important role in the activation and proliferation of fibroblastic cells involved in the fibrotic process (Crystal *et al.*, 1991). The secretion of cytokines by rat and mouse alveolar macrophages in response to AM treatment has been shown to be variable (Zhitnik *et al.*, 1992; Wilson and Lippmann, 1993; Futamura, 1995; 1996; Reasor *et al.*, 1996b).

As described in section 1.6.1, in approximately one-third of patients with AIPT, pulmonary toxicity has a rapid onset and is characterized by an increase in inflammatory cells suggesting the involvement of an immunological mechanism (Martin

and Rosenow, 1988a). However, conclusive evidence for the involvement of an immunological mechanism in the initation of AIPT has not yet been provided.

1.9 DIRECT TOXICITY

Although a direct dose response relationship between AM and pulmonary toxicity is not clearly established, there does seem to be an increase in pulmonary toxicity with AM doses greater than 400 mg/day (Marchlinski *et al.*, 1982; Rakita *et al.*, 1983; Martin and Rosenow, 1988a). In addition, the development of AIPT appears to be related to accumulation of AM/DEA in the lungs (Reasor and Kacew, 1996) since the signs of greatest toxicity are usually evident in lungs, organs with the highest concentrations of AM and DEA (Plomp ., 1984; Brien *et al.*, 1987).

The direct toxicity of a pulmonary toxicant can be assessed *in vitro*, wherein blood borne inflammatory or immune responses are separated from lung cell responses (Martin, 1990). AM has been shown to be directly cytotoxic to isolated perfused lungs (Kennedy *et al.*, 1988) and a variety of pulmonary cell types such as alveolar macrophages (Ogle and Reasor, 1990; Leeder *et al.*, 1996), cultured bovine and human pulmonary artery endothelial cells (Martin and Howard, 1985; Kachel *et al.*, 1990) and rabbit lung fibroblasts (Wilson and Lippmann, 1990). AM is also directly cytotoxic to non-pulmonary cells such as human umbilical cord vein endothelial cells (Baudin *et al.*, 1996), human thyrocytes (Beddows *et al.*, 1989) and rat hepatocytes (Ruch *et al.*, 1991). DEA is somewhat more potent cytotoxicant than AM and therefore likely has a role to play in the development of AIPT (Ogle and Reasor, 1990).

Evidence for direct AM toxicity is also obtained from these *in vitro* studies whereby increases in various indices of cytotoxicity (eg. ^{51}Cr release, lactate dehydrogenase (LDH) release) were correlated with increases in AM or DEA concentration.

Several mechanisms have been proposed for initiation of AIPT, and are thought to occur as a result of direct toxicity by AM and/or DEA. These include: i) phospholipidosis; ii) alterations in membrane stability and intracellular calcium regulation; iii) free radical production and iv) disruption of cell energy homeostasis.

1.9.1 Phospholipidosis

Phospholipidosis is characterized by the excessive intracytoplasmic deposition of lysosomally derived phospholipids in the form of lamellar and/or granular inclusion bodies (Reasor, 1989). AM produces phospholipidosis in a variety of lung cells (Marchlinski *et al.*, 1982; Colgan *et al.*, 1984; Heath *et al.*, 1985; Riva *et al.*, 1987). However, alveolar macrophages are the principal targets of phospholipidosis and they exhibit a "foamy" appearance attributable to phospholipid accumulation (Costa-Jussà *et al.*, 1984; Heath et al., 1985; Hostetler et al., 1986; Reasor *et al.*, 1988; Padmavathy *et al.*, 1993).

AM-induced phospholipidosis also occurs in non-pulmonary tissues in which AM produces cytotoxicity (eg., liver, cornea, skin, peripheral nerves) (Dudognon *et al.*, 1979; D'Amico *et al.*, 1981; Poucell *et al.*, 1984; Dake *et al.*, 1985; Honegger *et al.*, 1995) as well as cells not showing toxicity, such as polymorphonuclear leukocytes

(PMNs) (Somani *et al.*, 1986).

AM can produce phospholipidosis following varying routes of administration (ie., oral, ip, it, iv) and in different animal models (hamster, rat, mouse, dog) (Mazue *et al.*, 1984; Riva *et al.*, 1987; Reasor *et al.*, 1988; Wilson *et al.*, 1991; Wang *et al.*, 1992). Development of phospholipidosis is time and dose dependent (Reasor *et al.*, 1988) and is reversible upon cessation of drug administration (Mazue *et al.*, 1984; Reasor *et al.*, 1988; Antonini *et al.*, 1994).

AM increases total phospholipids and the proportion of phosphatidylcholine (Chatelain and Brotelle, 1985; Heath *et al.*, 1985; Reasor *et al.*, 1988; Reasor *et al.*, 1989). AM may induce phospholipidosis either by the inhibition of phospholipases (enzymes involved in the degradation of phospholipids) and/or by the formation of non-degradable AM-phospholipid complexes (Joshi *et al.*, 1988). Indeed, AM is a potent inhibitor of lysosomal phospholipases A_1 and A_2 (Heath *et al.*, 1985; Hostetler *et al.*, 1986, 1988; Reasor *et al.*, 1996a) as well as phospholipase C (Kodavanti and Mehendale, 1991).

DEA is a more potent inhibitor of phospholipases and inducer of phospholipidosis (Hostetler *et al.*, 1988; Kannan *et al.*, 1990), is more cytotoxic to cells *in vitro* (Ogle and Reasor, 1990) and is more fibrogenic to hamsters *in vivo* (Daniels et al., 1989), compared with AM. DEA also accumulates in cells to a greater extent than does AM (Camus and Mehendale, 1986; Reasor *et al.*, 1988).

A causal relationship between phospholipidosis and fibrosis was implied upon attenuation of AM-induced phospholipidosis and pulmonary fibrosis in hamsters treated

with taurine and niacin (Wang *et al.*, 1992). However, Blake and Reasor (1996), found a dissociation between pulmonary fibrosis and phospholipidosis in hamsters treated with AM by oral versus intratracheal administration. Substantial AM, DEA, and phospholipid accumulation occurred in the lungs of orally treated hamsters with no signs of fibrosis. In contrast, minimal AM, DEA, and phospholipid accumulation occurred in the lungs of intratracheally treated hamsters that developed pulmonary fibrosis. Moreover, other cationic amphiphilic amines (eg. chlorphentermine, imipramine) do not produce the pulmonary fibrosis observed with AM, even though they cause pulmonary phospholipid accumulation (Lüllmann *et al.*, 1978).

Clinically, the development of AM-induced phospholipidosis in alveolar macrophages is more common than AIPT (Liu *et al.*, 1986). Thus, phospholipidosis may be an innocuous marker of AM exposure, or perhaps a threshold of phospholipid accumulation dictates the production of toxicity. Alterations in phospholipid composition and accumulation of toxic levels of phospholipids (eg. lysophosphatidylcholine) affect membrane fluidity and may also have detergent-like actions on membranes (Martin and Rosenow, 1988b; Honegger *et al.*, 1993). Furthermore, the increase in cell volume due to phospholipidosis may decrease efficient gas exchange in the lung (Kudenchuk *et al.*, 1984). Thus, it is likely that phospholipidosis contributes to cytotoxicity. However, its role as a causative factor in AIPT remains unknown.

1.9.2 Alterations in membrane stability and intracellular Ca^{2+} regulation

Due to AM's amphiphilic nature, both hydrophobic and electrostatic forces occur during its interaction with membranes (Sautereau *et al.*, 1992; Antunes-Madeira *et al.*, 1995). Thus AM may interact with lipophilic membrane-bound proteins and lipids (Chatelain *et al.*, 1986; Sautereau *et al.*, 1992; Dzimiri and Almotrefi, 1993). As well, electrostatic interactions may occur between the charged tertiary amine of AM and phospholipid phosphate groups or anionic groups of particular membrane receptors (Dzimiri and Almotrefi, 1993; Antunes-Madeira *et al.*, 1995). These interactions are believed to produce alterations in membrane fluidity (Honegger *et al.*, 1993; Antunes-Madeira *et al.*, 1995) and membrane water permeability (Federico *et al.*, 1996). The resultant alterations in membrane stability are likely responsible for the dose-dependent increases in cell volume observed in human erythrocytes and in rat liver and heart mitochondria (Guerreiro *et al.*, 1986b; Federico *et al.*, 1996), as well as the osmotic fragility of human erythrocytes treated with AM *in vitro* (Hasan *et al.*, 1984). In addition, AM selectively inhibits rat lung Na^+/K^+-ATPase activity, a marker of membrane function (Reasor *et al.*, 1989).

AM-induced effects on the aforementioned membrane properties likely contribute to intracellular ion deregulation. For example, although Ca^{2+} is a critical mediator of a variety of important physiological functions, it is also involved in many toxicological processes. Sustained elevations in cytosolic Ca^{2+} levels can lead to overstimulation of Ca^{2+}-dependent degradative enzymes (eg. endonucleases, proteases). Prolonged activation of these enzymes can result in the breakdown of cell constituents

and cell death (Nicotera *et al.*, 1992).

A sustained increase in intracellular Ca^{2+} due to the influx of extracellular Ca^{2+} in human pulmonary artery endothelial cells incubated with AM, coincided with cell toxicity (Powis *et al.*, 1990), suggesting that Ca^{2+} may be the ultimate intracellular mediator of cell injury and not necessarily the toxic initiating mechanism (Martin, 1990). Vitamin E prevented the increase in cytosolic Ca^{2+} (Martin *et al.*, 1989) and protected against AM-induced cytotoxicity, effects attributed to membrane stabilization (Kachel *et al.*, 1990; Ruch *et al.*, 1991).

Both AM and DEA interact with calmodulin to modify its Ca^{2+} binding properties, which may alter the regulation of calmodulin dependent metabolic pathways. AM inhibited calmodulin-dependent Ca^{2+}-ATPase activity, whereas DEA inhibited both Ca^{2+}-ATPase and phosphodiesterase activities (Vig *et al.*, 1991). Interestingly, AM activated G_i proteins (inhibitory guanyl-nucleotide-binding protein) and induced activation of nonselective cation channels with a resultant increase in cytosolic Ca^{2+} in the human leukemia cell line, HL-60 (Hageluken *et al.*, 1995). However, the contribution of G_i protein activation by AM to its therapeutic and/or toxic effects has not yet been addressed.

It is likely that AM produces alterations in the regulation of intracellular ions other than Ca^{2+}, as AM's antidysrhythmic efficacy is attributed to the blockade of several ion channels (ie., K^+, Na^+). However, AM's effects on membranes and ion regulation in the lung and their relationship to AIPT have not been adequately addressed and therefore are deserving of further investigation.

1.9.3 Free radicals

1.9.3.1 What is a free radical?

A free radical[1] is any chemical species capable of independent existence that contains one or more unpaired electrons occupying an outer atomic or molecular orbital(s) (Gutteridge, 1994). Free radicals are highly reactive species and are therefore short-lived. They have a tendency to attain stability by reacting rapidly with other molecules to pair their electron(s) (Reilly and Bulkley, 1990). A radical may donate its unpaired electron to a non-radical, abstract an electron from a non-radical, or may combine with a non-radical (Halliwell, 1991). In all of these potential interactions, the non-radical becomes a radical. Two radicals can also react with each other by combining their unpaired electrons to form a covalent bond (Halliwell, 1989).

The ubiquity of molecular oxygen in aerobic organisms and its ability to readily participate in electron transfer reactions to form reactive oxygen species (ROS), accounts for its mediation of many free radical reactions (Riley, 1994). ROS (also called oxyradicals or oxygen free radicals) collectively refers to O_2 radicals as well as O_2 derivatives that are not radicals but contain chemically reactive O_2. Biologically important ROS include superoxide ($O_2^{\bullet -}$), hydroxyl ($^{\bullet}OH$), hydroperoxyl ($HOO^{\bullet}$), peroxyl ($ROO^{\bullet}$), alkoxyl ($RO^{\bullet}$), nitric oxide ($NO^{\bullet}$) radicals as well as non-radicals (hydrogen peroxide (H_2O_2), singlet oxygen ($^1O_2$) and hypochlorous acid (HOCl)) (Kehrer, 1993; Halliwell and Cross, 1994). Free radicals (particularly $O_2^{\bullet -}$) as well as

---

[1] Free radical and radical are used synonymously in the current literature and in this thesis (Halliwell and Cross, 1994).

other ROS are continuously produced in biological systems (Halliwell and Chirico, 1993).

1.9.3.2 Antioxidant defense mechanisms

The lungs are especially vulnerable to ROS mediated toxicity or oxidative stress due to their intimate contact with the atmosphere and exposure to O_2 tensions higher than other tissues (Kinnula *et al.*, 1995). Oxidative stress has been defined as "a disturbance in the prooxidant-antioxidant balance in favor of the former, leading to potential damage" (Sies, 1991). Antioxidant defenses have evolved in the aerobic organism to protect against oxidative stress. Enzymatic defenses include catalase, superoxide dismutase (SOD), glutathione peroxidase, and indirectly, glutathione reductase. These enzymes may become induced in response to oxidative stress. SOD catalyzes $O_2^{\bullet-}$ dismutation into H_2O_2 and O_2. Selenium (Se) dependent glutathione peroxidase reduces H_2O_2 and organic hydroperoxides whereas the Se-independent enzyme reduces H_2O_2 only (Bast *et al.*, 1991). The activity of glutathione peroxidase depends on the availability of its substrate, glutathione (GSH), an abundant cellular nonprotein thiol that is oxidized to glutathione disulfide (GSSG). Regeneration of GSH from GSSG is catalyzed by glutathione reductase and requires NADPH as the electron donor species, which is supplied by the hexose monophosphate shunt (Southorn and Powis, 1988). Cells may avoid GSH depletion by depending on catalase for H_2O_2 degradation during increased rates of cellular H_2O_2 production. Catalase has a greater affinity for H_2O_2 at higher concentrations than does glutathione peroxidase (Cotgreave

et al., 1988).

Several non-enzymatic antioxidants including Vitamin E (α-tocopherol), vitamin C (ascorbate), vitamin A (β-carotene) and GSH directly scavenge ROS or products of their reactions by donating electrons required to complete O_2 reduction (Joyce, 1987; Bellomo, 1991). Some typical reactions of free radicals and interactions with antioxidant defenses are depicted in Fig. 1.3.

1.9.3.3 Free radical targets

When antioxidant defenses are overwhelmed by the production of free radicals, lipids, proteins, nucleic acids and carbohydrates may all be targets for attack leading to metabolic disturbances and potentially cell death (Davies, 1995). The oxidative deterioration of membrane cholesterol and polyunsaturated fatty acids (PUFAs) is initiated by the attack of free radicals ($R^{\bullet}$, $^{\bullet}OH$, $LOO^{\bullet}$, $ROO^{\bullet}$ and $HOO^{\bullet}$) on unsaturated bonds and is referred to as lipid peroxidation (LPO) (Brent and Rumack, 1993). LPO can result in loss of membrane structure and function. As well, cytotoxic byproducts of LPO including hydroperoxides, lipid alcohols and aldehydes can accumulate in the cell (Freeman and Crapo, 1982; Martínez-Cayuela, 1995).

Peptide fragmentation, cross-linking due to disulfide bond formation and amino acid modification (hydroxylation or oxidation) can also occur as a result of free radical attack on proteins (Freeman and Crapo, 1982; Ignatowicz and Rybczynska, 1994; Martínez-Cayuela, 1995). Nucleic acids may be damaged by deoxyribose sugar or base modification, cross linking or single and double strand breaks leading to chromosomal

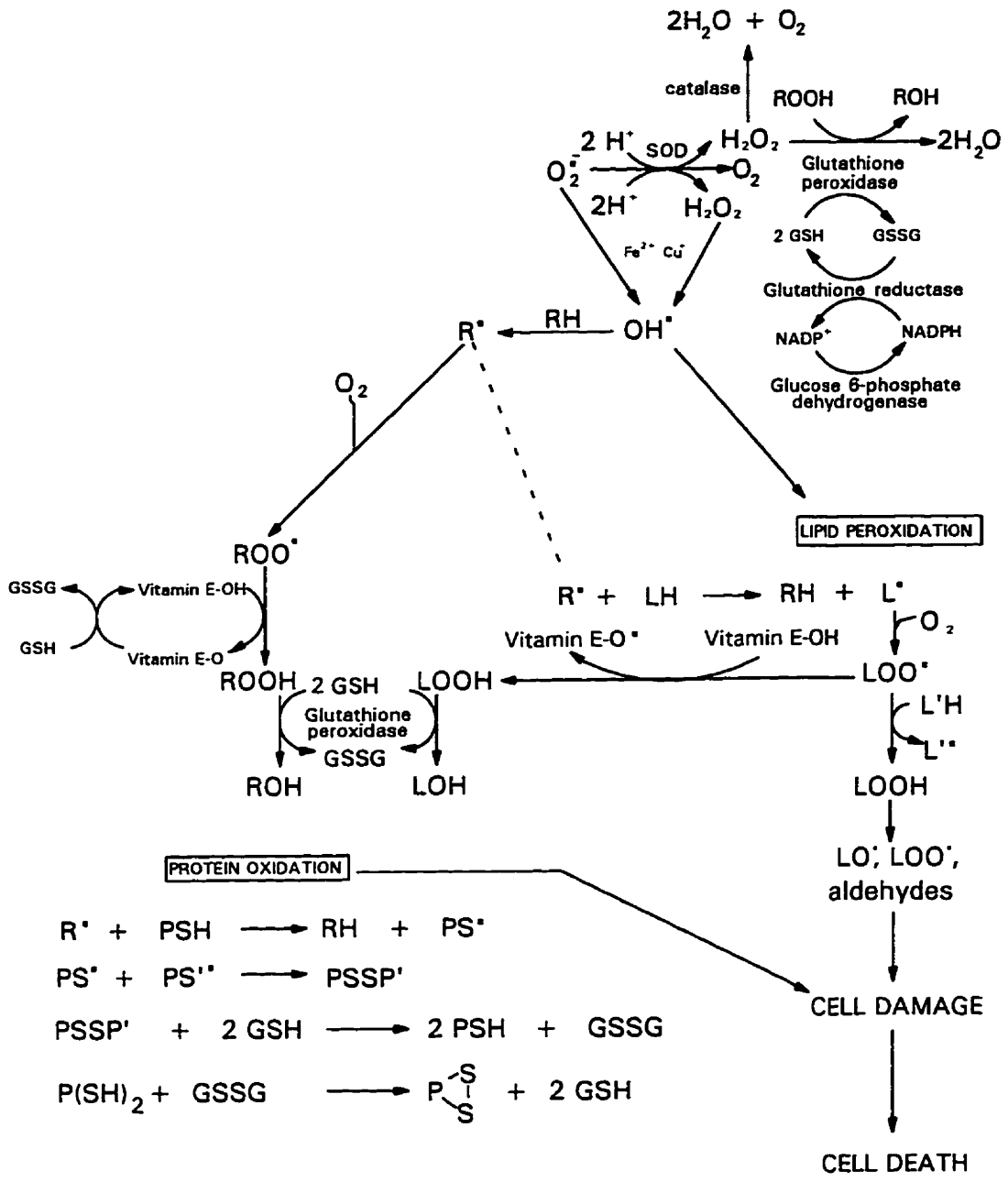

Fig. 1.3 Typical reactions of free radicals and interactions with antioxidant defenses. (L, L'= lipid, L•, L'•= lipid radical, LOO•=lipid peroxyl radical, LO•= lipid alkoxyl radical, LOOH=lipid hydroperoxide, LOH=lipid alcohol, PSH=thiol containing protein, PSSP'=oxidized protein (intermolecular), $P(SH)_2$= reduced protein (intramolecular), GSH=glutathione (reduced form), GSSG=oxidized glutathione, R•, =radical)

abberations causing cytotoxicity and/or carcinogenesis (Freeman and Crapo, 1982; Ignatowicz and Rybczyńska, 1994). Covalent binding of a free radical to a biomolecule (eg. protein, nucleic acid) can also result in impairment of its structure and/or function and cell death (Kehrer, 1993). Carbohydrates may also be oxidatively modified leading to their polymerization (Martínez-Cayuela, 1995). Enzymes are available to counteract the deleterious effects of free radicals by repairing DNA, degrading damaged proteins and metabolizing lipid hydroperoxides (Halliwell, 1991; Davies, 1995).

1.9.3.4 Free radical mediated toxicity

Many different types of free radicals can be involved in mediating toxicity in biological systems. Free radicals are generated as byproducts of normal metabolism, upon exposure to ionizing radiation or redox cycling drugs, by activated phagocytes and during drug metabolism (Freeman and Crapo, 1982; Aust *et al.*, 1993). The metabolism of xenobiotics can produce free radicals that mediate toxicity directly or indirectly by transferring electrons to O_2 to form ROS, which then act as mediators of toxicity (Freeman and Crapo, 1982). The destructive potential of a free radical is dependent upon its nature and its target site.

In free radical mediated toxicity, redox cycling agents that depend on quinoid groups or bound metals for activity are converted to free radicals and subsequently generate ROS via electron transfer reactions (Freeman and Crapo, 1982). For example, the herbicide paraquat (PQ^{2+}) can be reduced to a PQ cation radical ($PQ^{+\bullet}$)

by NADPH CYP450 reductases, with consequent depletion of cellular reducing equivalents (eg. NADPH). In the presence of O_2, $PQ^{+\bullet}$ transfers its electron to O_2 to produce $O_2^{\bullet-}$ and is reoxidized to PQ^{2+}. $O_2^{\bullet-}$ itself can be injurious to the cell or can lead to the production of other damaging ROS. This redox cycling mechanism is believed to be responsible for the pulmonary toxicity and fibrosis produced by PQ intoxication (Kehrer, 1993). In addition, a variety of xenobiotics (eg. benzo(a)pyrene-7,8-diol, bleomycin, procainamide) can be activated to reactive intermediates by various ROS that are generated by PMNs, or by organic free radicals (Trush et al., 1985). Therefore, the inflammatory process may contribute to chemical-induced toxicity (Kehrer *et al.*, 1988).

Other xenobiotics are metabolized to free radicals that participate in atom abstraction reactions. For example, carbon tetrachloride (CCl_4) is metabolized by CYP450 to highly reactive radical carbon centred trichloromethyl ($^{\bullet}CCl_3$). This radical can abstract a hydrogen atom from polyunsaturated fatty acids and initiate LPO, leading to hepatotoxicity (Slater, 1984).

A free radical may participate in radical addition reactions. For example, 3-methylindole, is a major tryptophan metabolite, is metabolized by CYP450 to electrophilic intermediates and free radicals which covalently bind to proteins and nucleic acids, and stimulate LPO. These reactions are believed to produce acute pulmonary edema and emphysema in ruminants (Bray and Kubow, 1985; Ruangyuttikarn *et al.*, 1992).

1.9.3.5 Detection of free radicals in biological processes

Since most free radicals are highly reactive, they are difficult to detect, identify and quantitate (Mason and Chignell, 1994). The existence of free radicals can be inferred from end product analysis or from the effects of antioxidants or antioxidant enzymes. Products of LPO such as volatile hydrocarbons (eg. ethane, pentane), thiobarbituric acid reactive substances and conjugated dienes can be measured using various techniques. However, these measurements lack specificity and may not be quantitative (Brent and Rumack, 1993). Modifications to proteins and nucleic acids can also be measured, but do not confirm the involvement of a free radical mediated event. In addition, chemiluminescence (eg. luminol) and fluorescent indicator (eg. dichlorofluorescin) methods are non-specific indicators of ROS and do not indicate the presence of other radicals (Hollán, 1995).

1.9.3.6 Electron spin resonance and spin trapping

Electron spin or paramagnetic resonance (ESR or EPR) is a spectroscopic technique that detects the unpaired electron present in a free radical and therefore is the only approach that can provide direct evidence for the presence of a free radical (Aust *et al.*, 1993; Knecht and Mason, 1993; Mason and Chignell, 1994). ESR involves the absorption of electromagnetic radiation by an unpaired electron in the presence of a static magnetic field (Wertz and Bolton, 1986). An unpaired electron possesses both spin angular momentum and orbital angular momentum. Spin angular momentum arises from an electron spinning frictionlessly on its own axis and orbital angular

momentum is due to its orbital motion. Magnetic dipole moments associated with electrons arise primarily from net spin angular momentum when free radicals are present in liquid or solid solution. For a single electron, the spin quantum number (S) is 1/2 such that an electron possesses two possible spin orientations, $M_S = +1/2$ and $M_S = -1/2$ (Wertz and Bolton, 1986).

In the presence of an external magnetic field, electrons with spin dipoles that align with the magnetic field (parallel) will move to a lower energy and electrons with spin dipoles that oppose the magnetic field (antiparallel) will move to a higher energy. In order for an electron to move from the low energy state to the high energy state, it must absorb the appropriate quantum of energy. For an unpaired electron, it is possible to induce spin reversal (resonance) by the application of electromagnetic radiation. The ESR signal would be observed as a single absorption line when the irradiating frequency corresponds to the energy difference between two energy states $(M_S - 1/2)$ and $(M_S + 1/2)$ (Fig. 1.4A). The ESR signal is displayed as the first derivative of net microwave power absorbed by the sample plotted against the strength of the external magnetic field (Borg, 1976) (Fig 1.4A). The first derivative is used to provide greater sensitivity as well as greater resolution of overlapping lines (Gordy,1979). For paired electrons, the net energy change is zero and no ESR spectrum is produced.

Since all radicals contain one or more atoms, some with magnetic nuclei, an unpaired electron in a radical fragment is inclined to interact with internal fields due to the nuclear magnetic dipole moments, as well as with the applied field. This

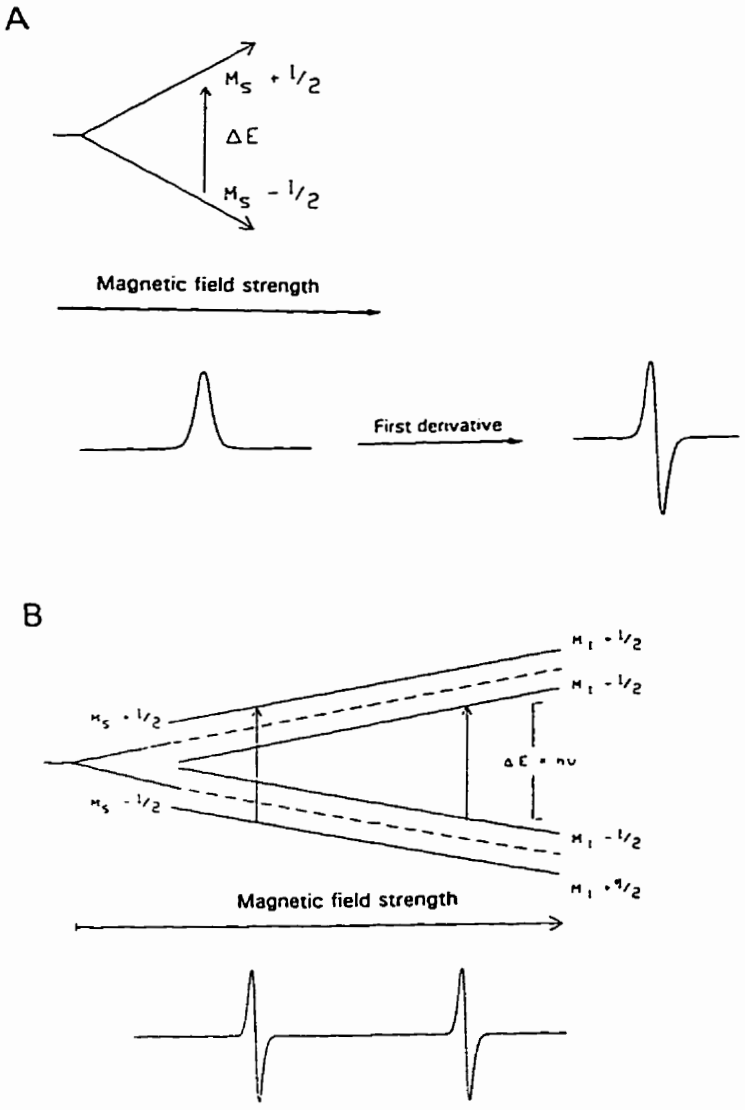

Fig. 1.4 A) ESR spectrum obtained due to the energy difference (ΔE) between two energy states M_S-1/2 and M_S+1/2 of an unpaired electron in the presence of an external magnetic field.
B) Influence of a magnetic nucleus (I=1/2) on the absorption of energy and the resultant ESR spectrum (1st derivative) by an unpaired electron in the presence of an external magnetic field. (from Jandrisits, 1988)

interaction with nuclear magnetic dipole moments is called the nuclear hyperfine interaction (Borg, 1976). Nuclear hyperfine interactions result in energy level splitting because the magnetic moment of the nucleus occupies discrete orientations in the magnetic field and subsequently can increase or decrease the net magnetic field sensed by the electron. For example, a nucleus with a spin of I=1/2 can occupy two possible orientations, M_I=+1/2 and M_I=-1/2. The difference in energy between the two M_S+1/2 and the two M_S-1/2 states is called the "hyperfine splitting" (Fig. 1.4B).

The pattern of splitting is determined by the spin of the nearby nucleus given by the value I (nuclear magnetic spin). The number of lines produced by a free radical is given by the equation 2nI + 1 where n is the number of equivalent nuclei and I is the spin of one nucleus. For example, for the hydrogen atom (I=1/2), the number of lines is 2. Other nuclei with spin include carbon-13 (I=1/2) and nitrogen-14 (I=1) while carbon-12 and oxygen-16 have no spin (ie., nuclei are not magnetic) and therefore do not influence the absorption of energy by an unpaired electron (Kubow, 1984).

Most reactive free radical species cannot be detected directly by ESR because of extremely low steady-state concentrations due to very short half-lives. Spin trapping was developed over 25 years ago (Janzen and Blackburn, 1969) and, in conjunction with ESR, is still considered the technique of choice for studying short-lived free radicals in biological systems. A spin trap is a diamagnetic (ie., having all electrons paired) compound with an unsaturated nitroso or nitrone (or nitronyl) function. Spin trapping involves the addition of the free radical across the double bond of a spin trap to form a relatively stable nitroxide (or aminoxyl) radical adduct or spin adduct (Fig.

1.5A) (McCay, 1987; Janzen, 1990; Knecht and Mason, 1993).

PBN (α-phenyl-N-t-butylnitrone) is an example of commonly used spin trap. The unpaired electron is delocalized by resonance between the nitrogen and oxygen atoms of the nitroxide free radical adduct (Fig. 1.5B). The spin of the nitrogen nucleus splits the single ESR resonance line produced by the unpaired electron, into three lines (Fig. 1.6). The hydrogen nucleus, which is two chemical bonds away from the nitroxyl group (ie., β to that group), splits each of these lines produced by the primary interaction of the electron with the nitrogen atom, to produce six lines. This is the effect of the β-hydrogen hyperfine splitting on the nitrogen splitting of the resonance signal from the unpaired electron (McCay, 1987). The use of PBN-*nitronyl*-^{13}C leads to further hyperfine splitting due to the presence of a ^{13}C nucleus in the α position to the nitroxide. The spacing between the peaks (a^x) for the interaction of a particular atom x with the unpaired electron is called the hyperfine splitting or coupling constant (hfsc) and is traditionally measured in Gauss, a unit of magnetic field strength[2] (Fig. 1.6). Additional splitting is possible with nuclei attached through three bonds (γ position) if these nuclei possess spin and are oriented in appropriate angles to the π-system of the nitroxyl function.

The nature of the R group in the original radical which reacted with the spin trap is reflected in the hfsc, which may be therefore used to determine the type of radical trapped (McCay, 1987; Janzen, 1990). Databases have been generated and

---

[2] A newer unit of magnetic field strength is the Tesla. One Tesla =10,000 G. Thus, 1 Gauss = 0.1 mTesla or 0.1 mT.

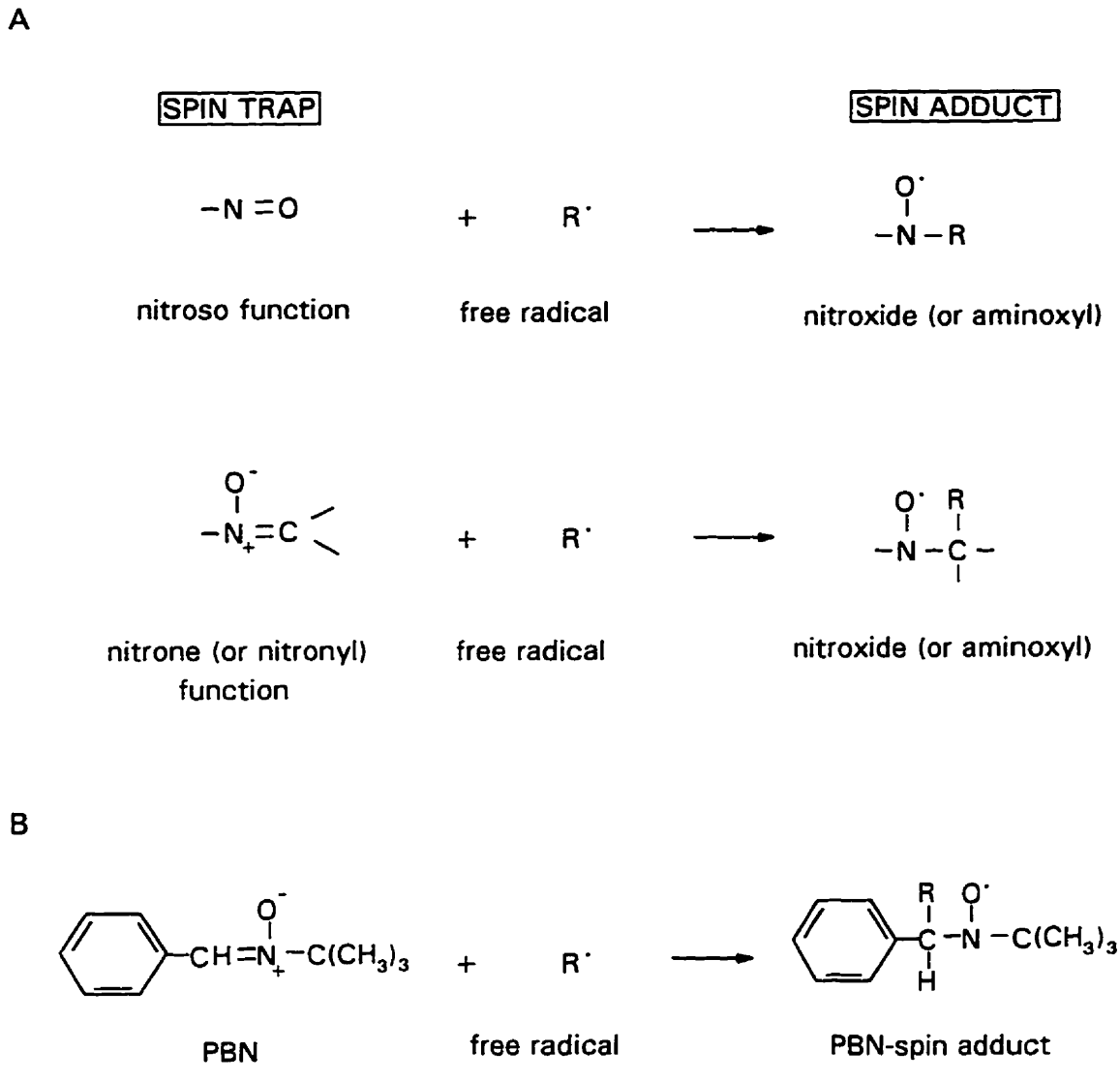

Fig. 1.5 A) Reaction of nitroso and nitronyl functional groups with a free radical to form a nitroxide radical adduct. B) Formation of a PBN-free radical adduct. (from McCay, 1987)

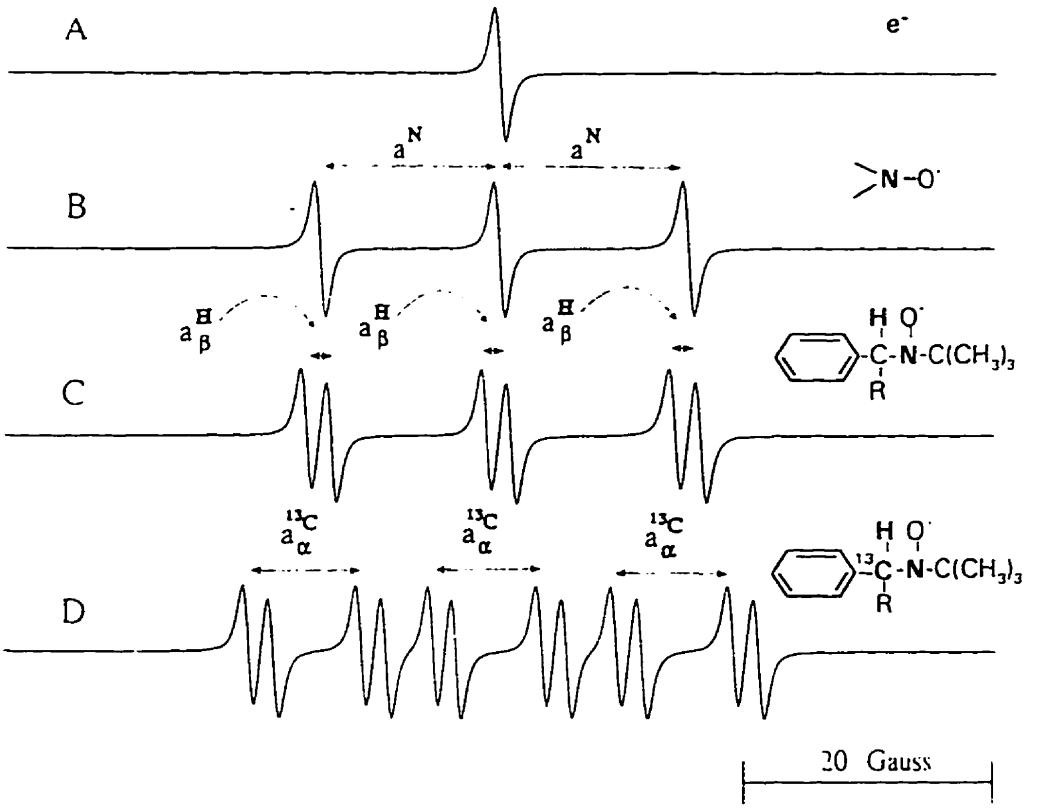

Fig. 1.6 First derivative ESR spectra. A) ESR spectrum of an unpaired electron (hypothetical). B) ESR spectrum of the interaction of an unpaired electron with ^{14}N nitroxide (hypothetical). C) ESR spectrum of the interaction of an unpaired electron, ^{14}N nucleus and H nucleus (hypothetical). D) ESR spectrum of the interaction of an unpaired electron, ^{14}N nucleus, H nucleus and ^{13}C nucleus (hypothetical). (adapted from Mason and Chignell, 1994)

published to allow identification of specific adducts in certain solvents since the solvent in which the spin adduct is analyzed by ESR may have a considerable effect on the magnitude of the hfsc (Janzen *et al.*, 1982).

1.9.3.7 Role of free radicals in AIPT

Free radicals have been implicated in the mechanism of AM-induced skin phototoxicity. ESR and absorption spectroscopy, oxygraph measurements and studies utilizing scavengers of ROS have demonstrated that $O_2^{\bullet-}$, H_2O_2, HOO• and $^1O_2$ are formed following UV irradiation of AM in the presence of air (Hasan *et al.*, 1984; Li and Chignell, 1987; Paillous and Verrier, 1988).

Under anaerobic conditions, a carbon centred aryl radical can be formed following photoionization and photodeiodination of AM (Li and Chignell, 1987; Paillous and Verrier, 1988). This radical is able to abstract a hydrogen atom from suitable donors (ie., ethanol, GSH, cysteine, linoleic acid). Similarly, Vereckei *et al.*, (1993) proposed that a highly reactive aryl radical was formed in a reducing environment upon stationary ^{60}Co-γ radiolysis and pulse radiolysis. Evidence for the formation of this radical was derived from the presence of deiodinated products.

Both AM and DEA are phototoxic to lymphocytes and sensitize red blood cells to hemolysis upon UV irradiation (Hasan *et al.*, 1984). Both agents provoked a higher rate of hemolysis after light irradiation than in the dark (Guerciolini *et al.*, 1984; Hasan *et al.*, 1984). Furthermore, hemolysis photosensitized by AM was partially O_2 dependent and was partially quenched by free radical scavengers (sodium azide,

mannitol, catalase and SOD). The presence of quenchers or deoxygenation did not affect AM-induced hemolysis in the dark. Based on the partial protection by free radical scavengers, it was suggested that oxidative species are generated by AM in the core of the membrane and may react preferentially with membrane components instead of diffusing into the aqueous solution to encounter H_2O soluble quenchers (Hasan *et al.*, 1984; Paillous and Fery-Forgues 1994). Indeed, vitamin E, a LPO chain terminating and lipid soluble antioxidant, has been shown to protect against AM-induced cytotoxicity in a number of *in vitro* studies, while a variety of other antioxidants have failed (Kachel *et al.*, 1990; Ruch *et al.*, 1991; Honegger *et al.*, 1995). AM has been shown to photosensitize phospholipid peroxidation (Sautereau *et al.*, 1992) and it is possible that vitamin E exerts its protective effect by prevention of LPO. Although AM has been shown to have the capacity to produce free radicals following UV irradiation, no relationship between this mechanism and that of AIPT has been shown.

The keto oxygen of AM has been postulated to be a focus for free radical formation which leads to cytotoxicity. DOAM, an AM derivative containing a methylene group in place of a keto oxygen group, lacked acute toxicity toward human lymphocytes and perfused rabbit lungs (Bennett *et al.*, 1987).

In support of an oxidant mechanism for AIPT, increases in lung $O_2^{\bullet-}$ and GSSG were observed in ventilated perfused rabbit lungs infused with AM (Kennedy *et al.*, 1988). In addition, hypoxia, pretreatment of rabbits with butylated hydroxyanisole, vitamin E or addition of N-acetylcysteine to the lung perfusate protected rabbit lungs

from AM-induced edema. Addition of SOD or SOD plus catalase to the perfusate, however, did not prevent edema. Although oxidant processes appear to produce edema in this system, their relationship to alveolitis and fibrosis in an *in vivo* system is unclear.

In an *in vivo* model of AIPT, a single intratracheal instillation of AM to the hamster resulted in the increased formation of GSSG in the lung 30 min and 2 h post-dosing. Elevations in lung SOD, glutathione peroxidase, glutathione reductase activities (at 3 and 7 days post-dosing) and lung MDA content (at 21 days), indicative of LPO were also evident (Wang *et al.*, 1992; Leeder *et al.*, 1994). However, it is possible that the increases in GSSG and antioxidant enzyme activities are derived from an influx of inflammatory cells into the lung that occurs following tissue injury.

Contrary to the oxidant stress hypothesis of AIPT, further studies using the hamster showed that GSSG formation was not exacerbated following inhibition of lung glutathione reductase activity with 1,2-bis(2-chloroethyl)-1-nitrosourea (BCNU). However, hamsters treated with both AM and BCNU showed enhanced AIPT at the light microscopic level, which was attributed to an additive effect, since BCNU is also fibrogenic (Leeder *et al.*, 1996). Furthermore, pretreatment of hamsters with several antioxidants (butylated hydroxyanisole, diallyl sulfide, N-acetylcysteine) did not prevent AM-induced pulmonary fibrosis (Leeder et al., 1994). However, dietary administration of taurine and/or niacin partially attenuated AM-induced lung fibrosis and phospholipidosis, and inhibited elevations in SOD and LPO at 21 days (Wang *et al.*, 1992). The partial protective actions of taurine were attributed to its antioxidant

and membrane stabilization properties whereas niacin may have protected against AIPT by the maintenance of lung levels of NAD and/or ATP (Nagai *et al.*, 1994; O'Neill and Giri, 1994).

Clinically, alterations in erythrocyte SOD activity in patients treated with AM suggested changes in the regulation of ROS (Pollak *et al.*, 1986; 1990). Patients undergoing AM therapy are at an increased risk for the development of postoperative adult respiratory distress syndrome (ARDS) following exposure to high concentrations of inspired O_2 during surgery (Wood *et al.*, 1985; Kay *et al.*, 1988; Greenspon *et al.*, 1991; Herndon *et al.*, 1992; Saussine *et al.*, 1992; Van Mieghem *et al.*, 1994). In the case of bleomycin, evidence for an ROS mediated mechanism of pulmonary toxicity was supported by oxygen exacerbation of toxicity (Giri and Wang, 1989).

Evidence against a free radical mechanism of AM toxicity was found in *in vitro* studies using cultured rat hepatocytes and pulmonary artery endothelial cells. These studies showed that a variety of antioxidants including SOD, catalase, butylated hydroxytoluene and N-acetylcysteine, as well as manipulation of ambient O_2 concentrations did not alter AM-induced cytotoxicity (Kachel *et al.*, 1990; Ruch *et al.*, 1991). Inhibition of lung alveolar macrophage glutathione reductase activity did not augment AM-induced cytotoxicity (Leeder *et al.*, 1996). In the same study, AM did not produce ROS in alveolar macrophages as measured by 2',7'-dichlorofluorescin. Similarly, Reasor and coworkers (1996b) found no alteration in luminol dependent chemiluminescence, indicative of ROS or excited state species, in phospholipidotic alveolar macrophages from AM treated rats. In contrast, Zitnik *et al.* (1992) suggested

that AM did not form ROS directly, but could prime rat alveolar macrophages stimulated with phorbol myristate acetate to release $O_2^{\bullet -}$.

The studies investigating the mechanism(s) of AM-induced phototoxicity indicate that AM is capable of forming ROS as well as a carbon centred free radical following UV irradiation. Although evidence exists for and against free radical involvement in the mechanism of AIPT, there is no direct evidence for the generation of an AM derived free radical in biological tissue. Therefore, the role of free radicals in the etiology of AIPT remains equivocal and requires further investigation.

1.9.4 Disruption of cellular energy homeostasis

AM accumulates in mouse liver mitochondria *in vitro* (Fromenty *et al.*, 1990b) and *in vivo* (Pirovino *et al.*, 1988), and in lung mitochondria from AM treated rats (Hostetler *et al.*, 1988).

At the ultrastructural level, incubation of isolated rat hepatocytes with AM or DEA (50 μg/ml) led to mitochondrial swelling prior to leakage of LDH through the plasma membrane (Gross *et al.*, 1989). Incubation of rat heart mitochondria with AM (95 nmol/mg protein) for 10 min led to rupturing of the inner mitochondrial membrane, extended cristae with enlargement of matrix volume and discharging of swollen vesicles into the external medium (Guerreiro *et al.*, 1986a). In contrast, alterations in mitochondrial morphology became evident long after other degenerative effects in hepatocytes (eg. autophagic vacuoles) from guinea pigs treated with AM for 16 weeks (30-50 mg/day) (Pirovino *et al.*, 1988).

Yasuda and coworkers (1996) showed that the mitochondrion was a target of AM toxicity in human lymphocytes. Mitochondria were extensively damaged and appeared as swollen electron-lucent bodies with disorganized cristae following incubation of cells with AM for 1 h; yet the plasma membrane was free of damage. They suggested that AM may have a direct toxic effect on mitochondria, beginning at $< 10\ \mu M$, with membrane damaging effects developing at higher drug concentrations. Interestingly, AM produced greater cell death (60 % vs. 5 %) in human lymphocytes than did the combination of tetracycline, rotenone and dinitrophenol, agents that together have uncoupling and inhibitory effects. They suggested that AM produces cytotoxicity by another mechanism, in addition to its effects on the mitochondria.

Glucose, a substrate that feeds into glycolysis, partially restored the AM-induced reduction in ATP content and accordingly partially protected against AM toxicity in human lymphocytes (Fromenty *et al.*, 1993). Similarly, niacin pretreatment of hamsters partially ameliorated AIPT (Wang *et al.*, 1992). Niacin, a precursor for NAD, was hypothesized to protect by stimulating ATP synthesis via glycolysis (O'Neill and Giri, 1994).

AM decreased mitochondrial membrane potential in mouse liver (Fromenty *et al.*, 1990b) and in rat heart (Guerreiro *et al.*, 1986b). AM also increased mitochondrial membrane permeability to K^+ and it was suggested that AM acts similarly to the K^+ ionophore, valinomycin (Guerreiro et al., 1986b).

AM inhibited the mitochondrial β-oxidation of fatty acids which was associated with the production of microvesicular steatosis in mouse liver (Fromenty *et al.*, 1990a).

AM also uncoupled oxidative phosphorylation, inhibited the tricarboxylic acid cycle and the respiratory chain, resulting in ATP depletion.

The inhibitory effects of AM may be due to a direct effect of AM itself or to an AM radical derived *in situ*. Mitochondria are major sites of electron transport processes, both via the mitochondrial CYP450 system and the respiratory chain, from which electron leakage can occur (Kubow *et al.*, 1985; Davies, 1995). Transfer of an electron to AM by either of these systems could lead to AM radical formation. The production of $^{\bullet}CCl_3$ from CCl_4 has been shown in rat liver mitochondria (Tomasi *et al.*, 1987). Free radical generation could result in the inhibition of respiratory enzymes or mitochondrial damage due to LPO followed by ATP depletion and cell death. Indeed, AM has been shown to inhibit mitochondrial ATPase activity in guinea pig heart (Dzimiri and Almotrefi, 1993).

The role of the mitochondrion as a target organelle in AIPT requires further investigation.

1.10 RATIONALE, HYPOTHESES AND OBJECTIVES

AM is an efficacious antidysrhythmic agent. Its use however, is limited due to its ability to produce AIPT. Elucidation of the mechanism(s) involved in the etiology of AIPT would be beneficial by facilitating: 1) the development of therapeutic strategies to ameliorate or prevent AIPT; 2) the development of novel and effective antidysrhythmic agents which do not produce pulmonary toxicity; 3) the assessment of risk factors for AIPT; 4) the diagnosis of AIPT; and 5) a better understanding of the pathogenesis of drug-induced pulmonary toxicity, including fibrosis.

Free radical generation has been suggested as a possible mechanism in the etiology of AIPT. The **main hypothesis** of this thesis research was that free radicals play a role in the etiology of AIPT. A second **minor hypothesis** was that the mitochondrion is a target organelle of AM toxicity.

In order to test these hypotheses, specific hypotheses and objectives were designed. The following studies have been divided into separate sections for clarity.

The role of the keto oxygen of AM in pulmonary toxicity.

The keto oxygen of AM has been suggested as a key site for free radical generation and the development of pulmonary toxicity (Bennett *et al.*, 1987). DOAM, a synthetic derivative of AM, possesses a methylene group in place of the keto group of AM. DOAM unlike AM, did not produce edema in perfused rabbit lungs or toxicity in human lymphocytes *in vitro* (Bennett *et al.*, 1987). However, the *in vivo* pulmonary toxicity of DOAM has not been examined.

Hypothesis 1

The keto oxygen of AM plays a key role in the production of AIPT.

Objective 1

To compare the *in vivo* pulmonary toxicities of DOAM and AM following intratracheal instillation to the hamster. Intratracheal administration of AM to the hamster results in the production of histopathological changes, including fibrosis, that are similar to those observed in humans with AIPT. Thus, the intratracheal route of administration in the hamster serves as a reliable *in vivo* model and has been used extensively for the study of AIPT including fibrosis (Cantor *et al.*, 1984; Daniels *et al.*, 1989; Wang *et al.*, 1992; Leeder *et al.*, 1996). Systemic administration of AM to rodents has not been shown to reliably produce pulmonary fibrosis (Wilson *et al.*, 1989; Daniels *et al.*, 1990; Reinhart *et al.*, 1996).

An ESR-spin trapping study of free radical generation by AM in hamster lung and liver microsomes.

Free radical generation has been proposed as an initiating mechanism in AM-induced pulmonary and hepatic toxicities. A highly reactive carbon centred radical was formed in a reducing environment upon stationary ^{60}Co-γ radiolysis and pulse radiolysis of AM *in vitro*. It was subsequently proposed that AM may be reduced to an AM free radical *in vivo* following the transfer of an electron (Vereckei *et al.*, 1993). Prior to this thesis research, however, there was no direct evidence for AM-induced generation of free radicals in biological tissues. Since the endoplasmic reticulum is one

of the major sites of electron transport, it may be a potential site of free radical generation (Freeman and Crapo, 1982).

Hypothesis 2

Free radicals are generated upon incubation of AM with hamster lung or liver microsomes.

Objective 2

To determine whether free radicals are generated by AM in pulmonary and hepatic microsomes, using ESR and spin trapping with PBN. Since both DEA and DOAM also produce pulmonary toxicity, their abilities to generate free radicals in this system were determined.

Cultured hamster lung slices as a model for the investigation of AIPT and oxidative stress.

The *in vivo* response of a variety of pulmonary toxicants has been mimicked in cultured adult peripheral hamster lung slices *in vitro* (Placke and Fisher, 1988). This system is devoid of the extrapulmonary factors that often complicate the study of the initiating mechanisms of a disease process. Thus, critical initiating events and events that follow as a result of initiating events in the development of toxicity may be more easily differentiated.

AM administration to the hamster has been shown to cause elevation of lung antioxidant enzymes (Wang *et al.*, 1992; Leeder et al., 1994), an effect consistent with an adaptive response to AM-induced oxidative stress. However, it was not possible to

distinguish between oxidative stress-related induction of lung antioxidant enzyme activities and elevations attributable to the influx of inflammatory cells occurring subsequent to lung injury.

Hypothesis 3a

Selective AM-induced cytotoxicity occurs in cultured lung slices.

Objective 3a

i) to assess the cytotoxic response of cultured lung slices to AM and to compare this response with other *in vitro* and *in vivo* models of AM toxicity

Hypothesis 3b

AM induces oxidative stress in cultured lung slices.

Objective 3b

i) to determine whether AM produces oxidative stress by measuring GSSG reductase activity, an antioxidant enzyme that is induced by oxidative stress.

ii) to compare the AM-induced response (cytotoxicity and oxidative stress) of cultured lung slices to that of paraquat (PQ), a pulmonary toxicant, believed to produce toxicity by an oxidant mechanism.

The effect of AM on lung mitochondrial oxygen consumption.

At present, pretreatment of hamsters with the combination of taurine and niacin has been the only successful *in vivo* treatment in the partial amelioration of AM-induced pulmonary fibrosis (Wang *et al.*, 1992). The maintenance of lung NAD and/or ATP was suggested as a likely mechanism for niacin's protective actions

(O'Neill and Giri, 1994). Furthermore, AM exerted several ATP depleting effects in lymphocytes (Yasuda *et al.*, 1996) and in isolated hepatic mitochondria, including the inhibition of respiration at the level of complexes I and II (Fromenty *et al.*, 1990b). The inhibitory effects of AM may be due to a direct effect of AM itself or to an AM radical generated *in situ*. Since AM accumulates in lung mitochondria (Hostetler *et al.*, 1988), this organelle may be a target for AIPT.

Hypothesis 4

AM exerts inhibitory effects on lung mitochondrial oxygen consumption.

Objective 4

To determine the *in vitro* effect of AM on lung mitochondrial oxygen consumption; specifically state 4 respiration, at the level of complexes I and II of the respiratory chain.

CHAPTER 2

COMPARISON OF THE *IN VIVO* PULMONARY TOXICITY OF AMIODARONE AND DES-OXO-AMIODARONE IN THE HAMSTER

2.1 INTRODUCTION

The keto oxygen of AM has been proposed as a key site for free radical formation in the generation of oxidative stress (Bennett *et al.*, 1987). It has been suggested that the extended π conjugation available to AM could facilitate free radical reactions by stabilizing the radical intermediates. This conjugation could be interrrupted by elimination of the oxygen of the bridging carbonyl group (Kabalka *et al.*, 1989), thus reducing pulmonary toxicity.

Des-oxo-amiodarone (DOAM, Fig. 2.1), a synthetic derivative of AM, possesses a methylene group in place of the keto group of AM. Unlike AM, DOAM did not produce edema in perfused rabbit lungs and was not acutely cytotoxic towards human lymphocytes *in vitro* (Bennett *et al.*, 1987). In terms of potential antidysrhythmic activity, DOAM possessed sodium, potassium and calcium channel blocking properties in guinea pig ventricular myocytes (Bennett *et al.*, 1987; Bennett *et al.*, 1989). Since DOAM appears to possess cardiac electrophysiological properties similar to AM and might be considered as a therapeutic alternative to AM, further characterization of its toxicity and potential for fibrogenicity *in vivo,* has potential clinical importance (Bennett *et al.*, 1987; Valenzuela and Bennett, 1991). However, the *in vivo* fibrogenicity of DOAM has not been studied.

A

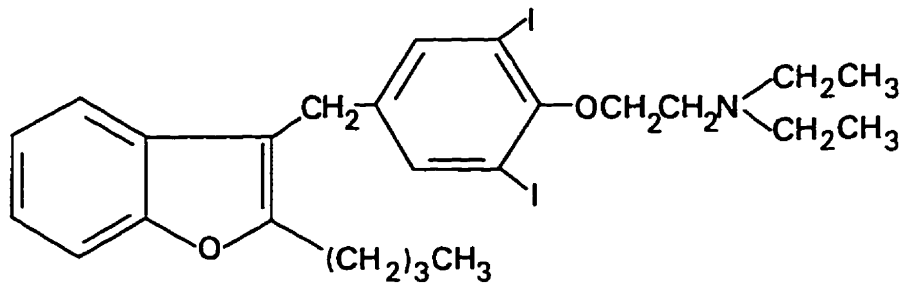

B

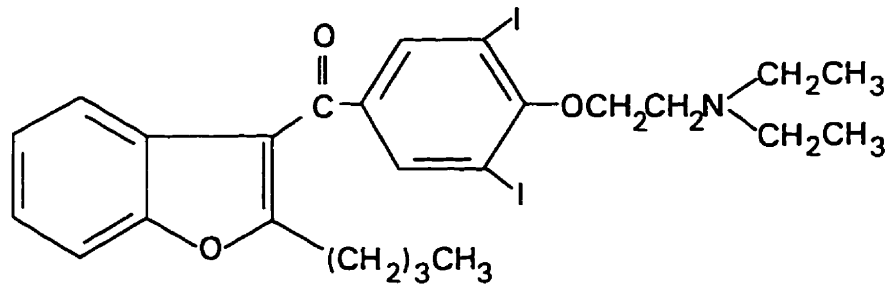

Fig. 2.1 Chemical structures of A) des-oxo-amiodarone and B) amiodarone.

The purpose of this study was to determine whether DOAM produces pulmonary toxicity following intratracheal administration to the hamster.

2.2 METHODS AND MATERIALS

2.2.1 Chemical Sources

AM HCl was obtained from Ceres Chemical Co. Inc., White Plains, NY, USA. DOAM HCl was a generous gift of Dr. Kabalka (University of Tennessee) and was synthesized and purified as described by Kabalka *et al.*(1989). Chloramine-T (N-chloro-*p*-toluenesulfonamide sodium salt), Ehrlich's reagent (*p*-dimethylaminobenzaldehyde), sodium thiosulfate, alanine and 10% neutral buffered formalin solution were obtained from Sigma Chemical Co., St. Louis, MO, USA. *Trans*-4-hydroxy-L-proline was obtained from Aldrich Chemical Co., Milwaukee, WI, USA. Sodium pentobarbital was from M.T.C. Pharmaceuticals, Mississauga, ON, Canada. Ketamine HCl was from Rogar/STB Inc., London, ON, Canada. Hematoxylin, eosin and HPLC grade acetonitrile and methanol were from BDH Chemicals, Toronto, ON, Canada. All other chemicals were of reagent grade and were obtained from common commercial suppliers.

2.2.2 Animal treatments

Male golden Syrian hamsters (145-165 g; Charles River Canada, Inc., St. Constant, PQ) were housed in group plastic cages containing hardwood shavings. They were maintained on a 12 h light/dark cycle and fed Purina Laboratory Rodent Chow

(No. 5001) and water *ad libitum*, and were allowed to acclimatize for at least one week prior to experimentation. Animals were cared for in accordance with the principles and guidelines of the Canadian Council on Animal Care.

AM and DOAM were dissolved in distilled water at 60°C and 90°C, respectively, and were allowed to cool to room temperature before instillation. Hamsters were anesthetized with ketamine HCl (80-100 mg/kg) injected intramuscularly into the hind leg, followed by a single dose of AM (1.83 μmol, 12.5 mg/ml), an equimolar amount of DOAM (12.2 mg/ml) or an equivalent volume of vehicle (0.1 ml H_20) by transoral intratracheal instillation using a 22-gauge stainless steel catheter (Daniels *et al.*, 1989). The instillation of drug or vehicle was followed by the rapid intratracheal injection of 0.6 ml air to facilitate deposition of drug or vehicle into the lungs.

2.2.3 Histological preparation of lung tissue

At 21 days post dosing, each hamster received a lethal dose of pentobarbital (approx. 300 mg/kg ip). Following thoracotomy, the trachea was exposed and cannulated. The right bronchus was then ligated, and the right lung was removed, weighed, frozen in liquid nitrogen, and stored at -20°C for analysis of hydroxyproline content within 4 weeks. Via the trachea, the left lung was inflated *in situ* with neutral buffered formalin to a pressure of 20 cm H_2O for 1 h. The trachea was ligated, and the left lung was removed and placed in formalin for 3 days.

For each hamster, two 2-mm thick sections from each of the upper and lower

lobes of the left lung were cut, dehydrated, embedded, sectioned (5 μm) and stained with hematoxylin and eosin for disease index determination or with Masson's trichrome for visualization of collagen.

Fixed lung slices were dehydrated (Fisher Tissuematon®) by the following sequential steps: 70% (v/v) aqueous ethanol, 1 h; 80% (v/v) aqueous ethanol, 1 h; 2 sequential series 95% (v/v) aqueous ethanol, 1 h each; 3 sequential series absolute ethanol, 1 h each; 1:1 (v/v) absolute ethanol: toluene, 1 h; 2 sequential series toluene, 1 h each; and 2 sequential series of paraffin wax (Paraplast® tissue embedding medium, Oxford Labware, St. Louis, MO), at 62°C, 1 h each.

Lung slices were then embedded in paraffin blocks using a Tissue Tek II® embedding centre, and the blocks were allowed to cool. Five micrometer sections were cut on a Spencer 820® microtome and placed on microscope slides. Tissue sections were subsequently deparaffinized and hydrated as follows: xylene, 5 min; xylene, 2 min; absolute ethanol, 2 min; 95% (v/v) aqueous ethanol, 1 min; 70% (v/v) aqueous ethanol, 1 min; 50% (v/v) aqueous ethanol, 1 min; distilled H_2O, 1 min. Tissues were then stained with hematoxylin solution (192 ml Harris' hematoxylin plus 8 ml glacial acetic acid, filtered immediately prior to use) for 2 min, rinsed with running tap H_2O for 20 min, and then counterstained with 1% (w/v) alcoholic eosin for 2 min. Tissues were then hydrated as follows: 50% (v/v) aqueous ethanol, 1 min; 70% (v/v) aqueous ethanol, 1 min; 95% (v/v) aqueous ethanol, 1 min; absolute ethanol, 1 min; and two changes in xylene, 2 min each. Following staining, coverslips were mounted on slides containing tissue sections with Permount® medium (Fisher Scientific, Nepean, ON).

2.2.4 Determination of disease index

A disease index was used to quantitate histological lung damage by an established procedure (Snider *et al.*, 1978; Cantor *et al.*, 1984; Daniels *et al.*, 1989) and was conducted in a blind manner. The identity of the drug treatment was concealed by an individual who was not involved in the determination of the disease index. An eye piece grid containing 100 equal sized squares was used to quantitate damage at a magnification of 200X. A square was considered diseased if it contained lung tissue exhibiting cellular infiltration of the alveolar space or interstitium, thickening of the interstitium, or fibrosis. Squares were not counted more than once if they contained more than one contributor to disease. Disease index was expressed as the percentage of tissue area showing damage. The number of squares examined per lung section was 5911 $\pm$ 1168 ($\bar{x} \pm$ SD), and the total number of squares examined per animal was 23643 $\pm$ 4674.

2.2.5 Lung hydroxyproline analysis

Hydroxyproline content, a biochemical index of collagen and hence fibrosis, was determined spectrophotometrically according to the method of Lindenschmidt and Witschi (1985). Following pulverization of the right lung in liquid nitrogen, it was hydrolyzed in 6.0 N HCl (5.0 ml) in tightly capped glass centrifuge tubes with teflon lined caps at 110°C for 72 h. Hydrolysates were neutralized with 10 N NaOH (2.75 ml) and the total volume was adjusted to 10 ml with distilled H_2O. The contents of tubes were allowed to cool, mixed (Fisher Vortex Genie 2®) and centrifuged

(Sorvall®RT6000) at 1000 x g for 5 min at room temperature. Triplicate aliquots (0.2 ml) were removed and added to 2.3 ml of borate-alanine buffer (1 part of 1:9 (v/v) aqueous dilution of alanine solution (0.112 M alanine in distilled H_2O, pH adjusted to 8.7 with 5 N KOH) plus 2 parts of a 1:9 (v/v) aqueous dilution of borate buffer (1M boric acid, 3M KCl in distilled H_2O, pH adjusted to 8.7 with KOH). Tube contents were saturated with excess solid KCl, mixed and then oxidized by addition of 0.6 ml freshly prepared 0.2 M chloramine T. Tube contents were mixed and allowed to stand for 30 min. The oxidation was stopped by addition of 2.0 ml 3.6 M sodium thiosulfate and tubes were mixed. Toluene (3.0 ml) was added, tubes were tightly capped and then placed in a boiling water bath for 30 min. Following cooling, tubes were shaken vigorously by hand (approx. 100 X) and centrifuged (1000 x g, 5 min). The toluene upper phase (1.5 ml) was removed and added to tubes containing 0.6 ml Ehrlich's reagent and mixed. Ehrlich's reagent was prepared by adding 13.7 ml concentrated sulfuric acid to 200 ml absolute ethanol on an ice bath. In another beaker, 130 g *p*-dimethylaminobenzaldehyde was added to 200 ml absolute ethanol followed by the slow addition of the acidified ethanol mixture while stirring. Thirty minutes later, the absorbance of the chromophore was measured at 560 nm (Beckman DU-7 spectrophotometer) against a blank. Blanks consisted of tubes treated as described above with the exception that 0.2 ml distilled H_2O was used in place of diluted neutralized hydrolysate. The standard curve was prepared by dilution of 0-16 μg trans 4-hydroxy-L-proline in 2.5 ml borate-alanine buffer prior to tissue analysis. The amount of hydroxyproline was expressed as μg hydroxyproline/right lung.

2.2.6 Pulmonary disposition of AM and DOAM

Hamsters were killed by pentobarbital overdose 1 or 5 h following intratracheal instillation of AM or DOAM. Each animal's thoracic cavity was exposed, and the lungs were removed and lavaged twice with 5 ml of 0.9% (w/v) NaCl. Following centrifugation (500 x g, 10 min at 4°C) of the bronchoalveolar lavage fluid (BALF), the supernatant and cell pellet were separated and stored tightly sealed at 4°C until quantitative analysis of AM or DOAM by a modification of a high performance liquid chromatographic (HPLC) assay (Brien et al., 1987). Extraneous tissue was removed, and lavaged lungs were stored at -20°C. On the day of HPLC analysis, 1.0 ml of mobile phase was added to the BALF cell pellet, and the sample was mixed vigorously and centrifuged at 16,250 x g (IEC Micromax®) for 3 min. The BALF supernatant was also centrifuged at 16,250 x g. The BALF cell pellet and supernatant samples were analyzed for AM or DOAM.

Each lavaged lung was blotted, weighed and pulverized in liquid nitrogen. Mobile phase (2.0 ml) was added to pulverized lung (0.15-0.20 g), which was homogenized with a ground-glass tube and pestle and then centrifuged (800 x g, 10 min, 4°C). The resulting supernatant was removed and centrifuged again (16,250 x g, 3 min). The supernatant from the latter centrifugation was analyzed for AM or DOAM by HPLC (Brien *et al.*, 1987).

The HPLC system consisted of a Waters 501 pump set at 2.0 ml/min, a Waters Lambda-Max Model 481 LC spectrophotometer operated at 254 nm and a Shimadzu C-RGA Chromatopac recorder. AM and DOAM were separated on a reverse phase

column (μBondapak®-C_{18}, 10 μm particle size, 300 mm length x 3.9 mm I.D.). Authentic standards (0-100 μg/ml) were prepared daily by dissolving AM and DOAM in mobile phase. The mobile phase consisted of acetonitrile:5% acetic acid (80:20 v/v) adjusted to pH 5.9 with ammonium hydroxide and was vacuum filtered prior to use (0.45 μm Magnanylon® filter, Micron Separations Inc.). The lower limit of quantitative sensitivity was 7.0 ng on the column. The within and between day coefficients of variation did not exceed 4% for either AM or DOAM.

2.2.7 Blood concentrations of AM and DOAM

Analysis of AM or DOAM concentrations was performed by a modification of the method of Brien *et al.* (1987). Blood was obtained by cardiac puncture using heparinized syringes (5 ml). A 500 μl aliquot of blood was mixed with an equal volume of ethanol. The mixture was allowed to stand for 15 min, and then centrifuged at 16,250 x g for 10 min. The supernatant (500 μl) was adjusted to pH 6.0 with 1.2 M HCl, centrifuged again, and the supernatant analyzed by HPLC. The lower limit of quantitative sensitivity was 0.20 μg/ml. The mobile phase (methanol:H_2O:ammonium hydroxide (94.8:5.1:0.1 v/v/v) was pumped at a flow rate of 1.5 ml/min.

2.2.8 Statistical Analysis

The results were expressed as $\bar{x} \pm$ standard deviation (SD). Statistical analysis for data comparing two groups was performed by an unpaired Student's t-test, whereas comparison of three or more groups was performed using a randomized one way

analysis of variance (ANOVA) followed by a Newman Keuls test. Data was considered significant when p was less than 0.05 ($p<0.05$). Percentage data underwent an arcsine transformation prior to statistical analysis.

2.3 RESULTS

2.3.1 Lung weight and hydroxyproline content

Twenty-one days post dosing, right lung wet weight was elevated to 116% and 113% of control for AM and DOAM treatment, respectively, whereas there was no significant difference in lung weight between the AM- and DOAM-treated hamsters (Table 2.1). A 23% and 13% increase in lung hydroxyproline content for AM and DOAM treatment, respectively, was observed compared with control (Table 2.1). There was no significant difference in hydroxyproline content between the AM- and DOAM-treated hamsters. Positive trichrome staining of lung sections confirmed the increased deposition of collagen in the interstitium of lungs from animals that received AM or DOAM (results not shown).

2.3.2 Histopathology

Quantitation of histopathological changes 21 days post dosing revealed a significantly greater disease index for lungs of hamsters that had received AM ($36.5 \pm 5.8\%$) or DOAM ($31.0 \pm 5.6\%$) compared with vehicle ($14.1 \pm 2.4\%$) (Fig 2.2). Furthermore, lung disease index values of AM-treated animals were modestly, albeit significantly higher than those of DOAM-treated hamsters.

Table 2.1 Effect of amiodarone or des-oxo-amiodarone treatment on right lung wet weight and hydroxyproline content of hamsters 21 days post dosing[a].

Treatment	Right lung wet weight (g)	Hydroxyproline content (μg/right lung)
Control	0.402 $\pm$ 0.051 (8)	499 $\pm$ 64 (8)
AM	0.466 $\pm$ 0.038* (8)	614 $\pm$ 44* (8)
DOAM	0.455 $\pm$ 0.027* (8)	565 $\pm$ 15* (5)

[a] Hamsters received a single intratracheal instillation of AM (1.83 μmol), DOAM (1.83 μmol), or 0.1 ml H_2O. Numbers in parentheses indicate number of animals per group.

* significant difference from control, randomized one way ANOVA followed by Newman-Keuls test ($p < 0.05$).

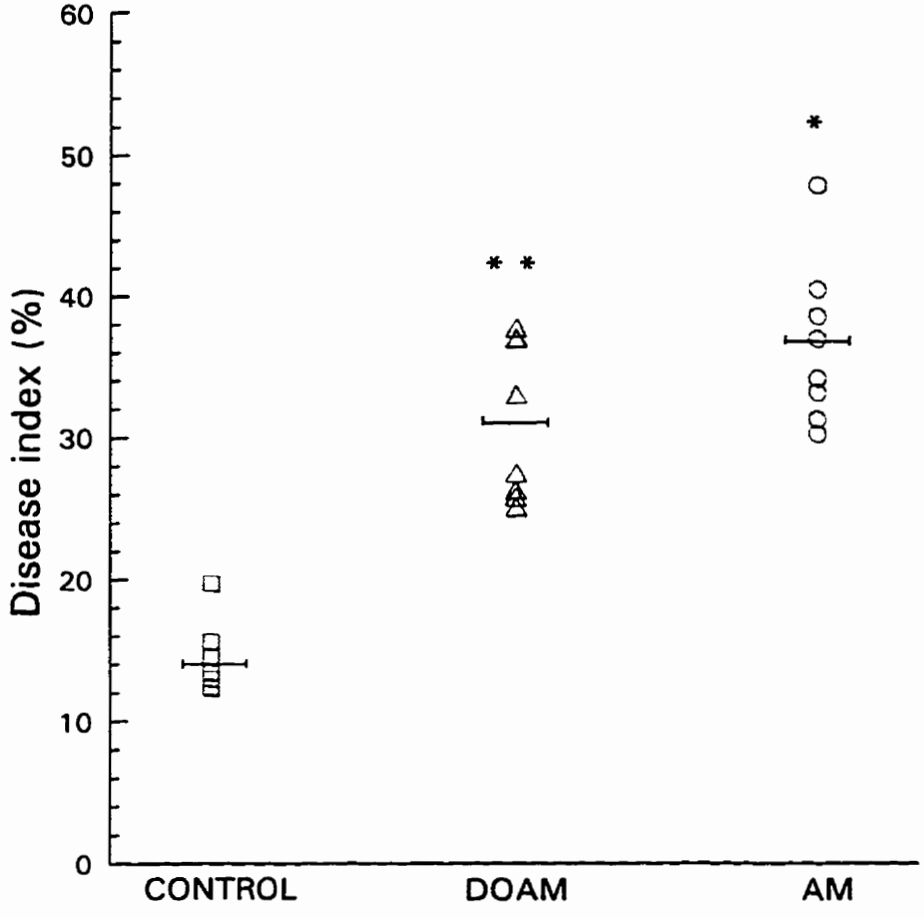

Fig. 2.2 Disease index of hamster lungs 21 days post dosing. Bars represent $\bar{x}$, (n=8 for each treatment group). * and **significant difference ($p < 0.05$) from control, from control and AM treatment, respectively, (arcsine transformation of percentage data followed by a randomized-design, one-way ANOVA plus Newman-Keuls test).

Lungs from hamsters treated with AM or DOAM demonstrated influx of inflammatory cells into the alveoli. These cells were mostly macrophages, with some polymorphonuclear leukocytes (Figs.2.3A and B). Hyperplasia of Type II pneumocytes was also evident in AM and DOAM treated lungs. In six out of eight animals treated with AM, areas of marked alveolar infiltration by large foamy macrophages were observed (Fig. 2.3A). This degree of infiltration was not observed in lungs from DOAM-treated animals, and thus contributed to the difference in disease index values between AM and DOAM treatment. In addition, both AM and DOAM treatments caused marked septal thickening and patchy, as well as diffuse, fibrosis (Figs. 2.3A and B). Fibrosis and cellular infiltration of the alveoli appeared to be located most frequently near blood vessels and airways. Lungs of hamsters treated with vehicle exhibited sparse areas of alveolar septal thickening and modest cell infiltration of the alveoli, but did not display any signs of fibrosis (Fig. 2.3C).

2.3.3 Pulmonary disposition of AM and DOAM

AM and DOAM were resolved with the HPLC system employed (Fig. 2.4). Approximately 50% and 41% of the administered DOAM dose was recovered in the lung (including BALF contents) at 1 h and 5 h respectively while for AM, 16% and 5% of the dose was recovered at 1h and 5 h respectively. DOAM was present in much greater amount than AM in BALF cell pellet and supernatant fractions, as well as in the lung, at both 1 and 5 h post dosing, with the exception that there was no significant difference between the amounts of AM and DOAM in the 1 h BALF supernatant

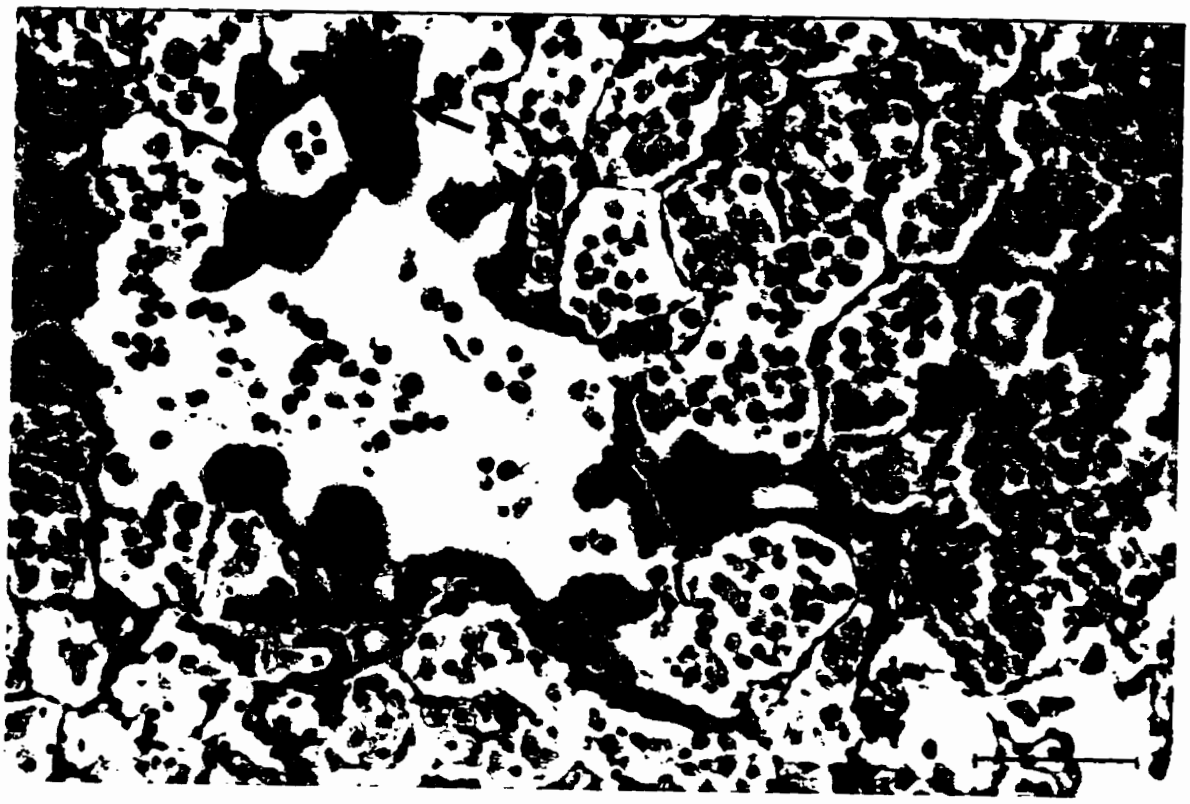

Fig. 2.3A Light photomicrograph of hamster lungs 21 days following a single intratracheal instillation of AM. Fibrosis (arrow) as well as massive cellular infiltration of alveolar spaces and interstitium are observed. (H&E stain, bar represents 100 μm in all cases).

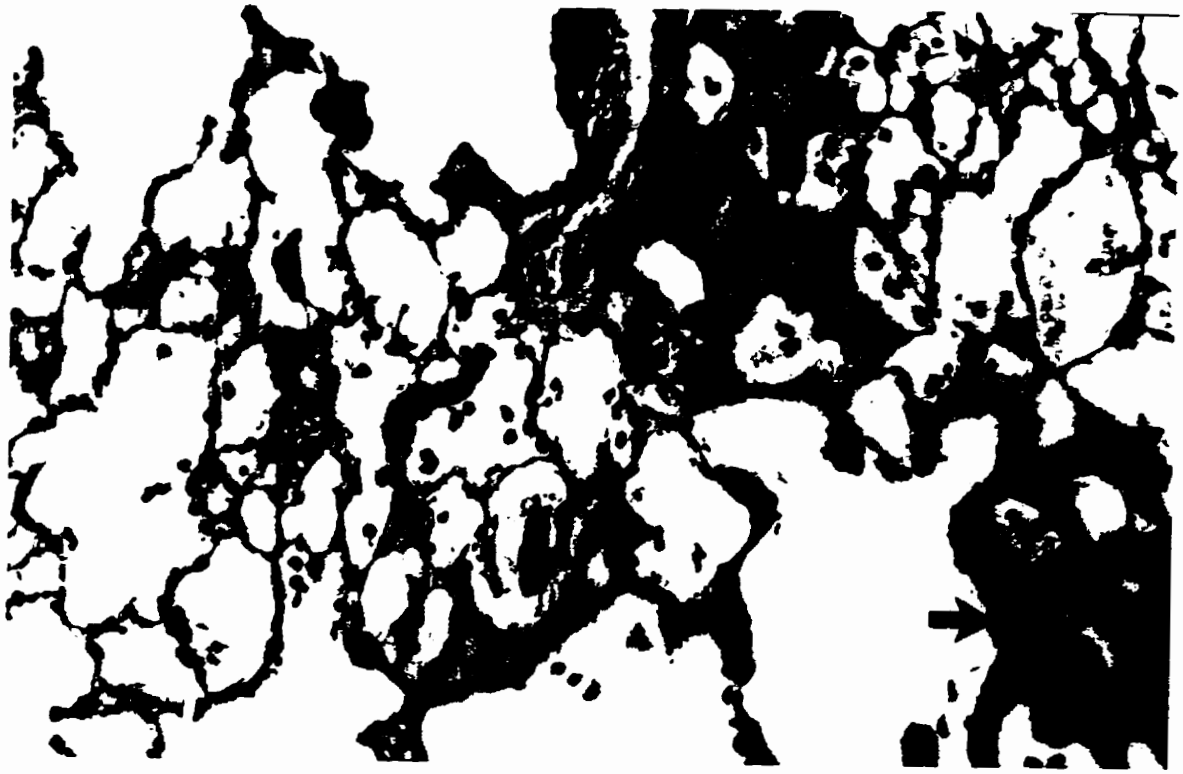

Fig. 2.3B Light photomicrograph of hamster lungs 21 days following a single intratracheal instillation of DOAM. Fibrosis (arrow) and cellular infiltration of alveolar spaces and interstitium are evident.

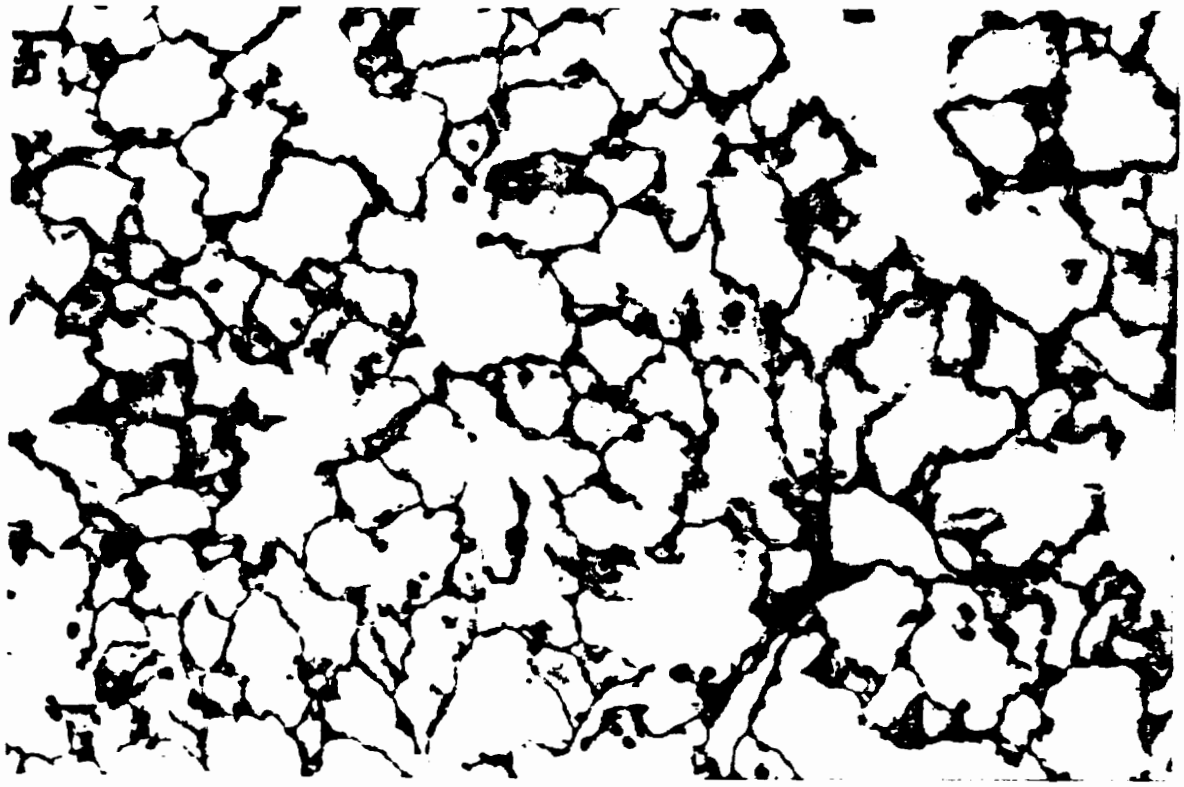

Fig. 2.3C Light photomicrograph of hamster lungs 21 days following a single intratracheal instillation of vehicle (H_2O). Lung architecture is normal.

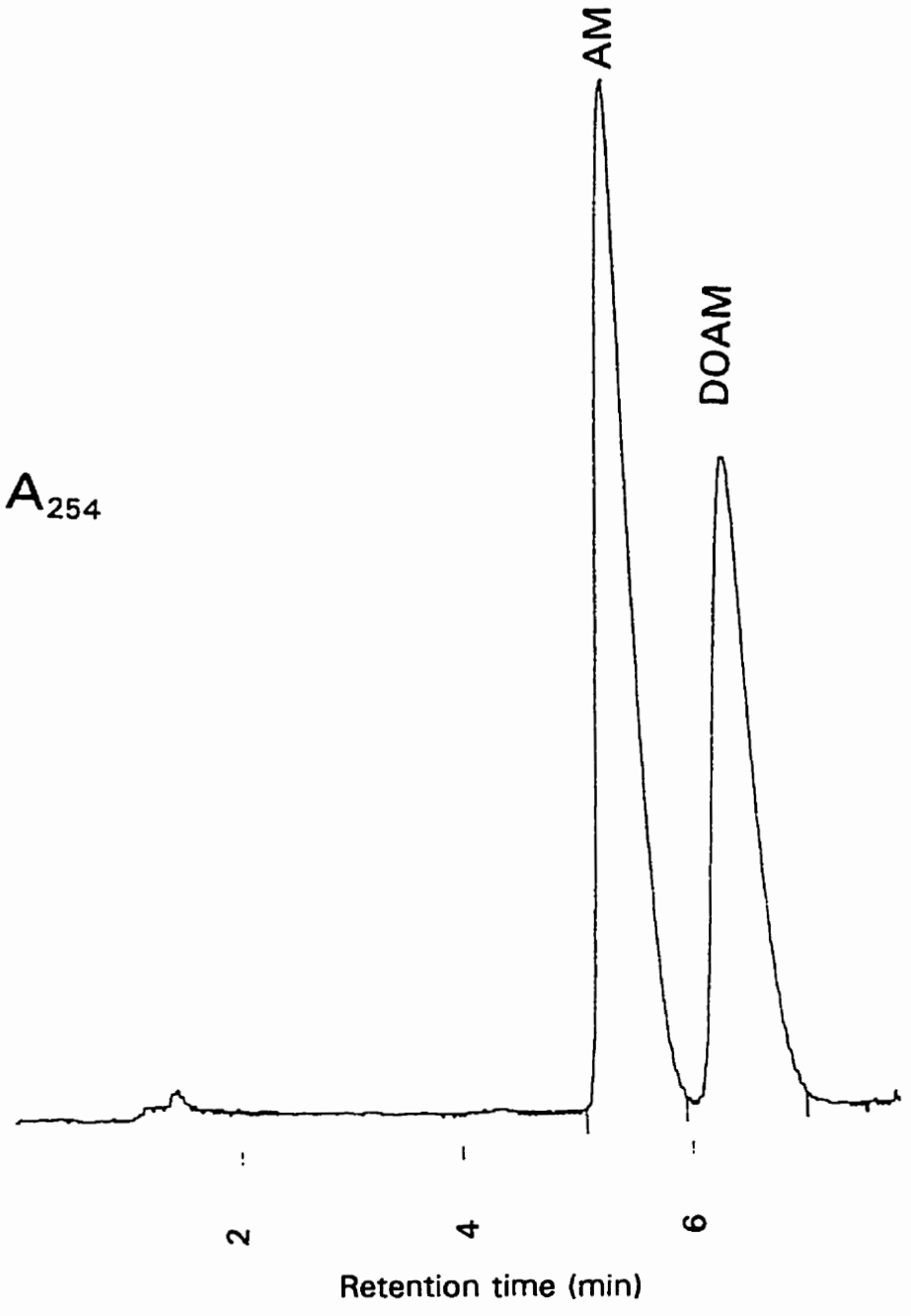

Fig. 2.4 HPLC chromatogram from analysis of AM and DOAM standards. The retention times for AM and DOAM were 5.4 min and 6.4 min respectively.

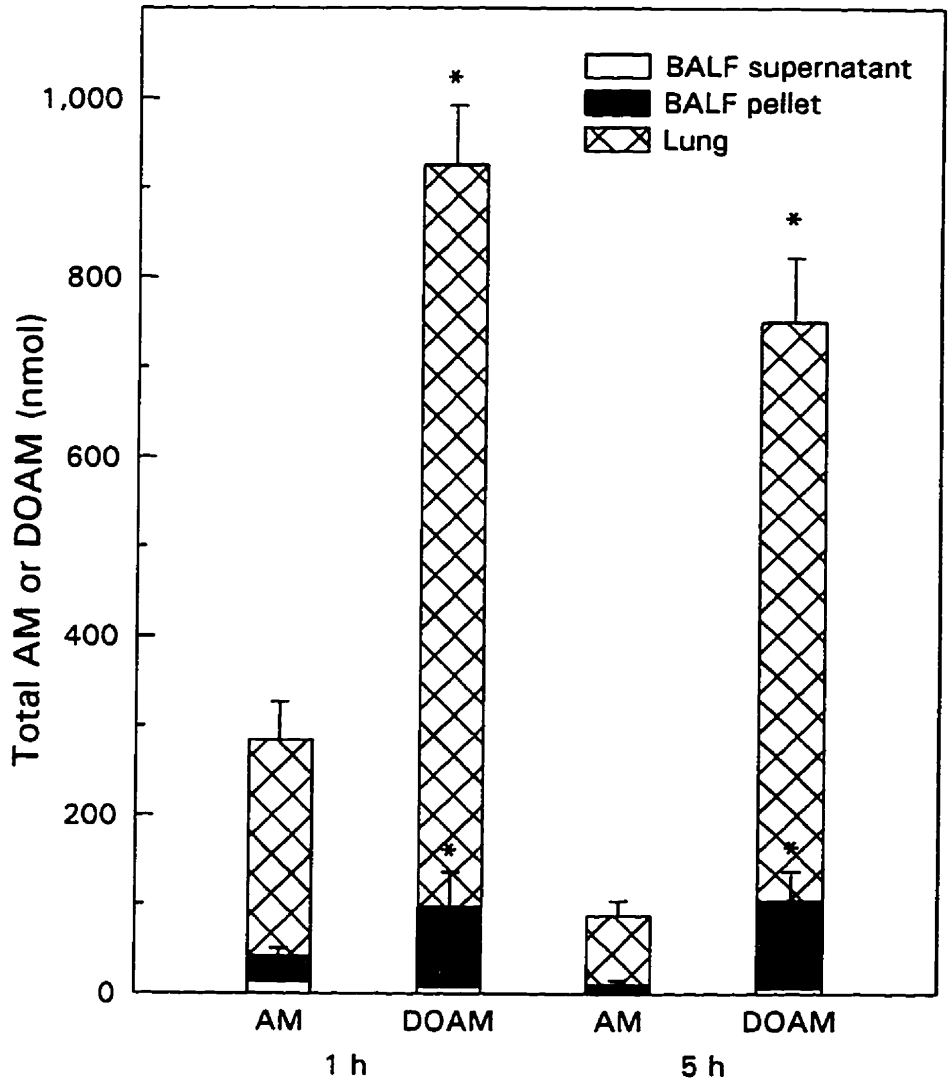

Fig. 2.5 Pulmonary disposition of AM and DOAM. Comparison of total amount of AM with the amount of DOAM in BALF supernatant, BALF pellet, or lung tissue at 1 and 5 h following intratracheal administration. Bars represent $\bar{x} \pm$ SD, (n=8 for each treatment group). * significant difference ($p < 0.05$) between DOAM and AM (unpaired Student's t-test).

fraction (Fig. 2.5). This, however, represents a small proportion of the total amount of drug. There was a 3 to 4 fold higher amount of AM in lung and BALF at 1 h compared with 5 h. In contrast, the amount of DOAM in lung and BALF was relatively constant from 1 to 5 h. There was no measurable AM or DOAM in blood at 1 or 5 h post dosing.

2.4 DISCUSSION

The hamster was used in our study because it has been shown to be susceptible to pulmonary toxicity following intratracheal instillation of AM (Cantor et al., 1984; Daniels *et al.*, 1989), and the histopathological features are similar to those observed clinically in AIPT (Cantor et al., 1984). Histopathological analysis was conducted 21 days post dosing, since AM-induced morphological changes are most prominent at this time (Cantor *et al.*, 1984; Daniels et al., 1989).

A single intratracheal instillation of DOAM into the hamster produced histopathological changes that were qualitatively similar to those observed with AM treatment 21 days post dosing. However, AM treatment resulted in a greater degree of alveolar infiltration, which was characterized by an abundance of large foamy macrophages. The cytoplasms of some adjacent macrophages appeared to fuse, and their nuclei had undergone lysis. The presence of foamy alveolar macrophages is a feature also commonly observed clinically in patients treated with AM (Costa-Jussà *et al.*, 1984). Alveolar macrophages from rats treated with chlorphentermine, which like AM is a cationic amphiphilic drug, exhibit similar alterations (Heath et al., 1973).

Cationic amphiphilic drugs have been shown to inhibit the catabolism of phospholipids (Hostetler and Matsuzawa, 1981), possibly by the formation of drug-phospholipid complexes, which inhibit the action of lysosomal phospholipases (Lüllmann *et al.*, 1978). It is possible that AM is a more potent inducer of phospholipidosis than is DOAM. Desethylamiodarone, a major metabolite of AM, is a more potent *in vivo* inducer of phospholipidosis than the parent drug in rats (Kannan et al., 1990), and has been shown to produce greater toxicity in various cell types (Gross *et al.*, 1989; Somani et al., 1990; Ogle and Reasor, 1990) as well as greater fibrosis (Daniels *et al.*, 1989). The increase in lung wet weight observed for AM and DOAM treatments is attributable to the influx of inflammatory cells and the accompanying edema.

An examination of the pulmonary disposition of AM and DOAM following instillation led to some interesting observations. Alveolar macrophages, which comprise the majority of cells in the BALF pellet fraction, were able to retain an appreciable proportion (approx. 10%) of the total AM and DOAM in the BALF plus lung. This confirms results of other studies showing that rat alveolar macrophages accumulate AM to a considerable extent following oral administration (150 mg/kg, for 2 days) (Reasor et al., 1990). The observation of considerably higher amounts of DOAM than AM in BALF and lung after instillation indicates that DOAM was retained in the lung to a greater extent than was AM. Although AM treatment produced greater overall pulmonary toxicity as indicated by the disease index, DOAM was present in greater quantity in the lung and it produced fibrosis to a similar extent as AM. Thus DOAM appears to be a less potent inducer of pulmonary toxicity.

In contrast to AM, DOAM reportedly lacks acute toxicity in human lymphocytes, and does not produce pulmonary edema in the perfused rabbit lung (Bennett *et al.*, 1987). However, in the present *in vivo* study, DOAM was not innocuous, thus confirming the importance of *in vivo* factors in DOAM-induced pulmonary toxicity. Inflammatory cells and the mediators they release are critical participants in the development of inflammation and pulmonary fibrosis (Crystal *et al.*, 1991). Matrix components may also contribute to inflammatory and fibrotic processes by acting as chemoattractants. Thus, fibrosis is a complex and progressive process, which cannot be mimicked in cultured cells or in acute studies in perfused lung.

Hasan and coworkers have suggested that the keto group of AM can abstract an allylic hydrogen from lipid, and thus may have a role to play in AM-induced phototoxicity (Hasan *et al.*, 1984). However, other investigators have proposed that an aryl radical is produced by deiodination of AM *in vitro* (Li and Chignell, 1987; Vereckei *et al.*, 1993). Thus, chemical groups other than the keto group may be the foci for free radical formation. If oxidative stress is involved in AIPT, these chemical groups may participate in free radical production and the ensuing pulmonary toxicity.

In conclusion, the keto oxygen of AM is apparently not a key determinant of AM-induced pulmonary fibrosis in the hamster, since DOAM, which lacks a keto group, also produced pulmonary toxicity and fibrosis.

CHAPTER 3

AN ELECTRON SPIN RESONANCE AND SPIN TRAPPING STUDY OF FREE RADICAL PRODUCTION BY AMIODARONE *IN VITRO*

3.1 INTRODUCTION

In vivo studies have suggested that AM may be producing pulmonary toxicity by a free radical mechanism(s). Elevations in lung antioxidant enzymes, GSSG and malondialdehyde (a LPO product) content have all been observed following intratracheal AM administration to hamsters (Wang *et al.*, 1992; Leeder *et al.*, 1994). AM also produced elevated levels of $O_2^{\bullet-}$ and GSSG in isolated perfused rabbit lungs, indicative of oxidative stress (Kennedy *et al.*, 1988). However, the failure of various antioxidants and antioxidant enzymes to provide protection against AIPT does not support the involvement of a free radical mediated mechanism. In *in vivo* studies, taurine and niacin partially protected against AIPT (Wang *et al.*, 1992), while several antioxidants were ineffective (Vereckei *et al.*, 1993; Leeder *et al.*, 1994). With the exception of vitamin E, several antioxidants did not protect against AM toxicity in hepatocytes, pulmonary artery endothelial cells and alveolar macrophages (Kachel *et al.*, 1990; Ruch *et al.*, 1991; Leeder *et al.*, 1996; Reasor *et al.*, 1996a). Clearly, the role of free radicals in the production of AIPT requires further investigation.

AM is capable of forming ROS as well as a highly reactive carbon centred aryl radical following UV irradiation (Li and Chignell, 1987; Paillous and Verrier, 1988). Vereckei *et al.* (1993) also proposed that a highly reactive aryl radical was formed following ^{60}Co-γ and pulse radiolysis. They further speculated that this highly reactive

aryl AM radical could be formed upon reduction of AM by a hydrated electron, or an organic radical concomitantly releasing an iodide ion *in vitro* (Vereckei *et al.*, 1993). The AM radical may then abstract hydrogen atoms from neighbouring organic molecules, thereby initiating LPO and other free radical reactions. Thus, the possibility exists that AM radical formation occurs in subcellular compartments active in electron transport (Vereckei *et al.*, 1993). Mitochondria and endoplasmic reticulum are two potential sites (Freeman and Crapo, 1982).

Hepatic and pulmonary toxicity are important adverse effects associated with AM therapy due to their potential for causing mortality. Free radical generation has been proposed as a possible mechanism in AM-induced skin photosensitivity (Hasan *et al.*, 1984; Li and Chignell, 1987), hepatotoxicity (Vereckei *et al.*, 1993) and pulmonary toxicity (Bennett *et al.*, 1987). However, there is currently no direct evidence for the formation of free radicals derived from AM in biological tissues. The objective of this study was to determine whether free radicals are generated by AM in pulmonary and hepatic microsomes, using electron spin resonance (ESR) spectroscopy and spin trapping with α-phenyl-N-t-butylnitrone (PBN). In addition, the abilities of desethylamiodarone (DEA) and des-oxo-amiodarone (DOAM) to produce free radicals were investigated (Figs. 1.1 and 2.1). Both DOAM, a structural analogue of AM, and DEA, a major metabolite of AM, have been shown to produce pulmonary fibrosis in the hamster following single intratracheal administration (Daniels *et al.*, 1989, Chapter 2).

3.2 MATERIALS AND METHODS

3.2.1 Chemical sources

Chemicals were obtained as follows: Chelex 100 from Bio-Rad Laboratories (Mississauga, ON); α-phenyl-N-t-butylnitrone (PBN) from Aldrich Chemical Co. (Milwaukee, WI) and Sigma Chemical Co. (St. Louis, MO); PBN-*nitronyl*-^{13}C (99% pure) from the Oklahoma Medical Research Foundation Spin Trap Source; β-NADPH (tetrasodium salt, chemically reduced) from Sigma Chemical Co. Desethylamiodarone HCl (DEA) was obtained from Ayerst Laboratories, Montreal, PQ. All organic solvents were of HPLC grade and were obtained from Fisher Scientific (Nepean, ON, Canada). All other chemicals were of reagent grade and obtained from common commercial suppliers.

3.2.2 Animal treatments

Male Golden Syrian hamsters (140-180g; Charles River Canada Inc. St. Constant, PQ) were housed and cared for as described in Section 2.2.2.

3.2.3 Lung and liver microsome preparation

Lung and liver microsomes were prepared by differential centrifugation (Mazel, 1971) as follows. Male Golden Syrian hamsters were killed by pentobarbital injection (300 mg/kg, ip). Lungs and livers were perfused *in situ* with 0.01 M K-phosphate buffer (pH 7.4) plus 1.15% KCl via pulmonary artery and inferior vena cava respectively. Lungs and livers were removed, rinsed in ice cold 0.01 M K-

phosphate buffer plus 1.15% KCl, blotted dry and tissue weights recorded. Tissues were minced and homogenized in buffer (4.0 ml/g tissue, wet weight) using a Potter-Elvehjem® teflon pestle-glass tube homogenizer. Homogenates were centrifuged at 10 000 x g for 20 min. The microsomal fractions were collected as 100 000 x g pellets by further centrifugation of 10 000 x g supernatants for 60 min. Lung and liver microsomal pellets were pooled (8-12 hamsters) separately and resuspended in 0.025M K-phosphate buffer plus 1.15% KCl (pH 7.4) to yield protein concentrations of 15-25 mg/ml and 25-35 mg/ml respectively (Lowry *et al.*, 1951). Approximately 2 mg lung microsomal protein and 120 mg liver microsomal protein was obtained from one hamster. Microsomes were frozen in liquid nitrogen and stored at -80°C.

All K-phosphate buffers were stirred overnight in Chelex 100® chelating ion exchange resin (5g/100 ml) to remove trace metal ion impurities and then were filtered through a 0.45 μm nylon membrane (Micron Separations Inc.) to remove Chelex 100 prior to use.

3.2.4 Microsomal incubations

Reaction mixtures consisted of liver or lung microsomes (1-16 mg protein), 50 or 100 mM PBN and 0.3 mM NADPH in a total volume of 2.0 ml 0.01 M K-phosphate buffer (pH 7.4) plus 1.15% KCl (Kubow *et al.*, 1984). Mixtures were incubated (Precision® Mechanical Convection Incubator Model 6LM) in capped glass centrifuge tubes (10 ml) at 37°C for 0.5, 1.0 or 1.5 h. Incubations contained either AM, DOAM, DEA in varying concentrations (1-20 mM) or an equivalent volume (20-

400 μl) of vehicle (dH_2O). Incubations not containing AM were maintained at pH 5.7 to account for the alteration in pH produced by AM which occurs during its dissolution in isotonic buffer. For incubations containing boiled microsomes, microsomes were heated in a 100°C waterbath for 10 min and then cooled to room temperature.

Reactions were terminated by addition of ice-cold chloroform (2 mL). PBN-spin adducts formed in the incubation mixtures were extracted twice with chloroform (2 x 2 mL) by centrifugation (2000 rpm, 10 min, IEC Centra MP4). Chloroform was evaporated to dryness using a stream of N_2 gas and residues containing PBN spin adducts were reconstituted in 0.4 mL benzene.

3.2.5 ESR analysis

Benzene extracts were transferred to an ESR round cell. The cell was sealed with a rubber septum (8-9 mm fitting, Aldrich) through which a needle was inserted. N_2 gas was bubbled (approx. 5 min) into the sample via the needle to eliminate oxygen. The sample was placed in a ST-ESR cavity and subjected to analysis by ESR spectroscopy at room temperature. ESR spectra were obtained using a Bruker EPR ER-200D X-band spectrometer. The instrument settings were: microwave power 20.5 mW, modulation amplitude 1 G, scan range 100 G, time constant 50 ms, sweep width 100, centre field 3480 G.

3.2.6 Measurement of hyperfine splitting constants (hfsc's)

To calculate the magnitude of the hyperfine splitting constants (hfsc's) a^N, a_β^H,

and $a_{\alpha}^{^{13}C}$, spectra line separations were measured for each constant as indicated by the arrows in Figure 3.1. The nitrogen hyperfine splitting was measured eight times and averaged (four times for each of the maxima and minima) and the β-hydrogen hyperfine splitting was measured six times and averaged (three times for each of the maxima and minima). The α-^{13}-carbon hyperfine splitting was measured twelve times and averaged (six times for each of the maxima and minima). The averages of hyperfine splittings for each atom were divided by the length of the scan and then converted to units of magnetic field strength (Gauss) and the hfsc obtained (Janzen, 1984). Hfsc's were expressed as $\bar{x} \pm SD$, with n=1 represented by an ESR spectrum obtained on a different experimental day.

Signal intensity was calculated by measuring the height of each peak in mm, from maxima to minima (six times) and obtaining averages. ESR signal intensity is represented by peak height and the peak height was normalized for gain. Signal intensity is directly related to the number of free radicals in the sample (Borg, 1976).

3.2.7 Isolation of PBN-radical adduct

Liver microsomes were incubated in quadruplicate as described in section 3.2.4 (10 mM AM, 16 mg microsomal protein, 0.3 mM NADPH, 50 mM PBN) for 30 min. Reactions were terminated by addition of ice-cold chloroform and the PBN-radical adduct was extracted as described in section 3.2.4. Following detection of a PBN-free radical adduct by ESR analysis, samples were pooled and benzene was evaporated to a final volume of 0.8 ml. The benzene extract containing the PBN-free radical adduct

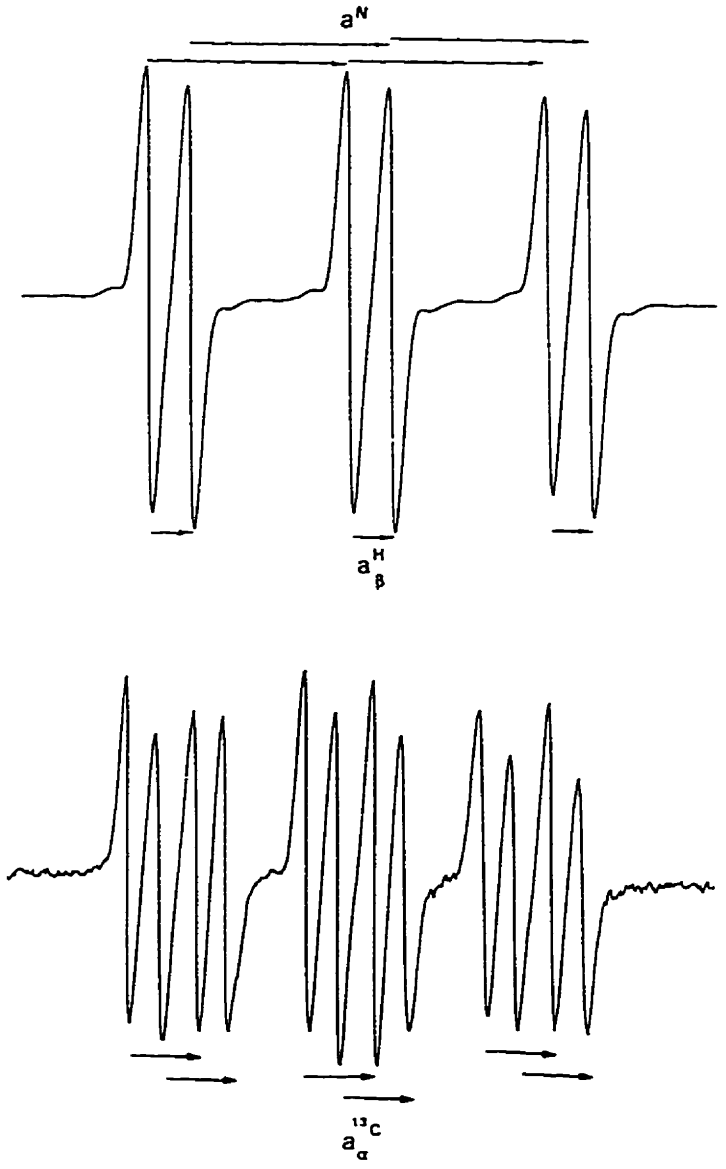

Fig. 3.1 Sample ESR spectra indicating measurement of hyperfine splitting constants (hfsc's).

was cooled to -80°C immediately following ESR analysis. This frozen sample was thawed on the following day, benzene was evaporated under a stream of N_2, and the residue containing the PBN-free radical adduct was reconstituted with 0.5 ml hexane. This sample was filtered (Cameo 3N syringe filter, nylon, 0.22 μm, Micron Separations Inc.) prior to HPLC.

The HPLC system consisted of a chart recorder (Fisher Recordall Series 5000), a solvent pump (Hewlett Packard Series 1050), a UV detector (Hewlett Packard Series 1050) and a normal phase column (Bondclone™ 10μ Silica column 300 X 3.9 mm, Phenomenex, Torrance, CA). The mobile phase consisted of hexane:isopropanol (97:3 v/v) and was pumped at a flow rate of 1.0 ml/min. The PBN-free radical adduct was measured at 254 nm. HPLC eluate corresponding to chromatographic peaks was collected manually. This was performed for three consecutive injections (25 μl) and fractions corresponding to the same retention times were pooled. Mobile phase was evaporated using a stream of N_2 gas and residues were reconstituted in 0.4 ml benzene. Collected chromatographic fractions (6) were subjected to ESR analysis.

3.2.8 The use of PBN-*nitronyl*-^{13}C for further analysis of PBN-spin adduct identity

PBN-*nitronyl*-^{13}C was used to gain more information about the identity of the trapped radical. The ^{13}C nucleus has a nuclear spin of 1/2 and therefore can contribute another hfsc $a_{\alpha}^{^{13}C}$.

Liver microsomes were incubated with 10 mM AM, 16 mg protein, 0.3 mM NADPH and 50 mM PBN-*nitronyl*-^{13}C for 30 min. The incubation mixture was

terminated, extracted and then subjected to ESR analysis as described previously in sections 3.2.4 and 3.2.5.

3.2.9 Determination of the effect of ambient laboratory fluorescent light on signal production

In order to determine whether photoactivation was involved in ESR signal production observed in non-microsomal incubates, experiments were conducted in ambient laboratory fluorescent light and away from direct ambient light. In experiments performed away from direct light, laboratory lighting was reduced to a minimum and incubation tubes were sheltered from light by wrapping them with aluminum foil.

3.3 RESULTS

3.3.1 Spin trapping experiments

3.3.1.1 Generation of a PBN-radical adduct

A PBN radical adduct was formed upon incubation of AM with hamster lung and liver microsomes. PBN radical adducts formed in both lung and liver microsomal incubations produced identical spectra. A triplet of doublets pattern and hyperfine splitting constants (hfsc's) in liver ($a^N = 14.4 \pm 0.1$ G, $a_\beta^H = 2.6 \pm 0.1$ G; n=5) and lung ($a^N = 14.4 \pm 0.1$ G, $a_\beta^H = 2.6 \pm 0.1$ G, n=5) were obtained (Fig. 3.2). An ESR signal was not observed when PBN was excluded. The hfsc's for the PBN-*nitronyl*-^{13}C spin adduct were $a^N = 14.3$ G, $a_\beta^H = 2.5$ G and $a_\alpha^{C13} = 5.5$ G (Fig. 3.3).

Fig. 3.2 ESR spectra from hamster lung and liver microsomes incubated with AM. ESR spectra of incubates containing microsomal protein (4 mg), 5 mM AM, 50 mM PBN and 0.03 mM NADPH. A) liver, hfsc's: a^N= 14.4 G, a^H_β= 2.6 G and B) lung, hfsc: a^N= 14.4 G, a^H_β= 2.6 G (gain 2.5 x 10^5)

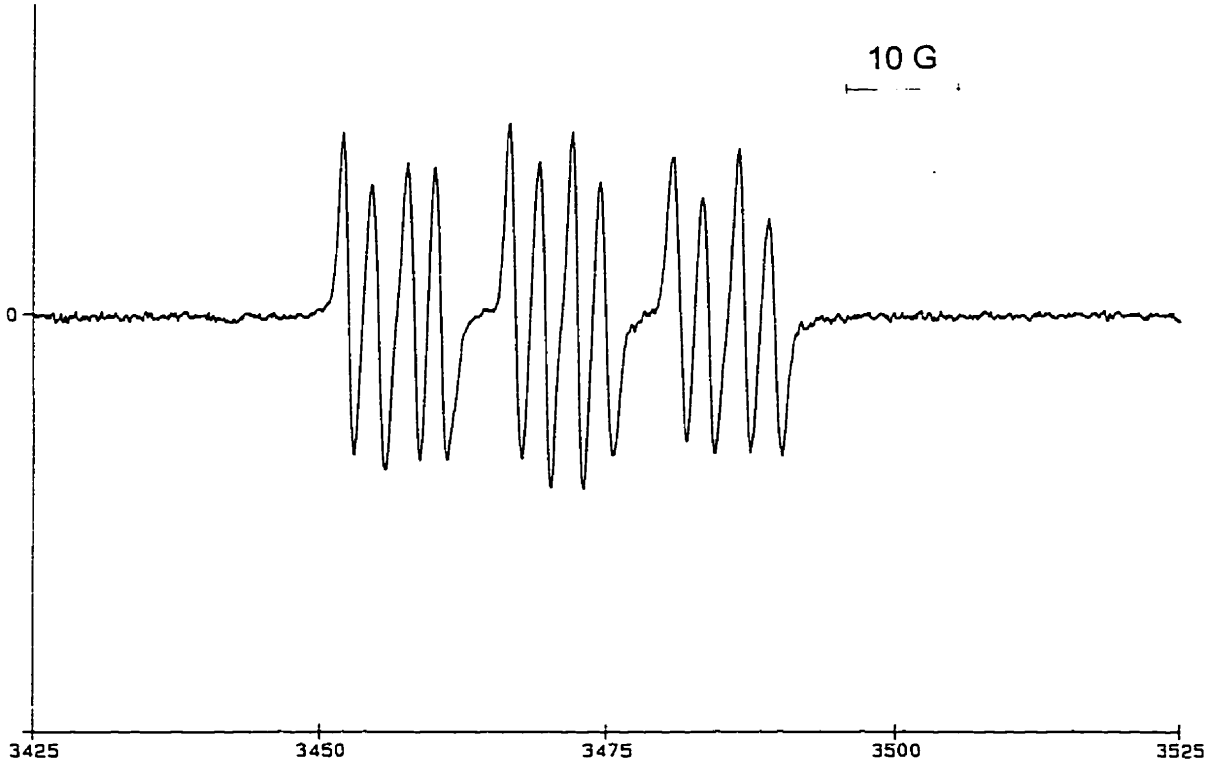

Fig 3.3 ESR spectrum of a benzene extract from liver microsomes incubated with AM and ^{13}C-PBN. Incubates contain microsomal protein (16 mg), 10 mM AM, 50 mM ^{13}C-PBN and 0.3 mM NADPH. hfsc's: a^{N}= 14.3 G, a^{H}_{β}= 2.5 G and $^{13}a^{C}_{\alpha}$= 5.5 G (gain 2.5 X 10^{5})

3.3.1.2 Production of a PBN-radical adduct

It was difficult to establish a relationship between AM concentration and intensity of the PBN-free radical adduct signal. There was no increase in signal intensity with an increase in AM concentration beyond 5 mM AM (Fig. 3.4). The effect of AM concentration on PBN radical adduct production was not examined in lung microsomes due to the large amounts of protein and therefore large numbers of hamsters required to determine a concentration response relationship.

An increase in signal strength was observed with increasing lung microsomal protein concentration (1.0-12 mg) (Fig 3.5). In contrast, a relationship between liver microsomal protein concentration and ESR signal strength could not be determined. A relationship between NADPH concentration and ESR signal strength for both lung and liver microsomal incubations could not be determined.

In the absence of microsomes, an ESR signal was observed with various concentrations of AM (2-20 mM). The characteristics (hfsc's: $a^N = 14.3$ G, $a_\beta^H \approx 2.5$ G) of this signal were identical to those of the signal obtained in the presence of microsomes (Fig. 3.6). An ESR signal was also observed in incubates containing AM, PBN, NADPH and boiled lung microsomes. However, this signal's magnitude was similar to that obtained with AM-containing incubates devoid of microsomes, indicating that it was not attributable to heat-resistant activity in boiled microsomes.

Incubation times of 0.5, 1 and 1.5 h produced ESR signals of similar intensity (results not shown).

A PBN radical adduct (hfsc's: $a^N = 14.6$ G, $a_\beta^H = 2.9$ G) was also formed in

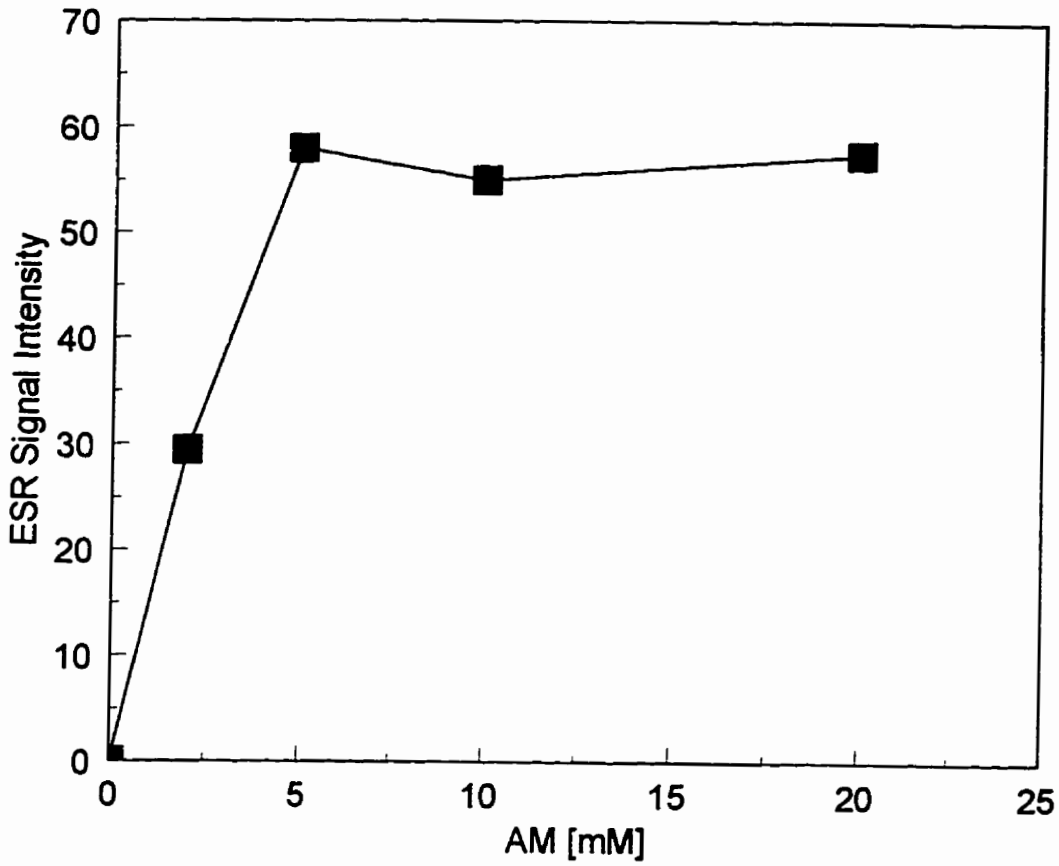

Fig. 3.4 Effect of AM concentration on ESR signal intensity in hamster liver microsomes. Incubates contained microsomal protein (4 mg), 50 mM PBN and 30 μM NADPH. Data points represent means of n=2 separate experiments.

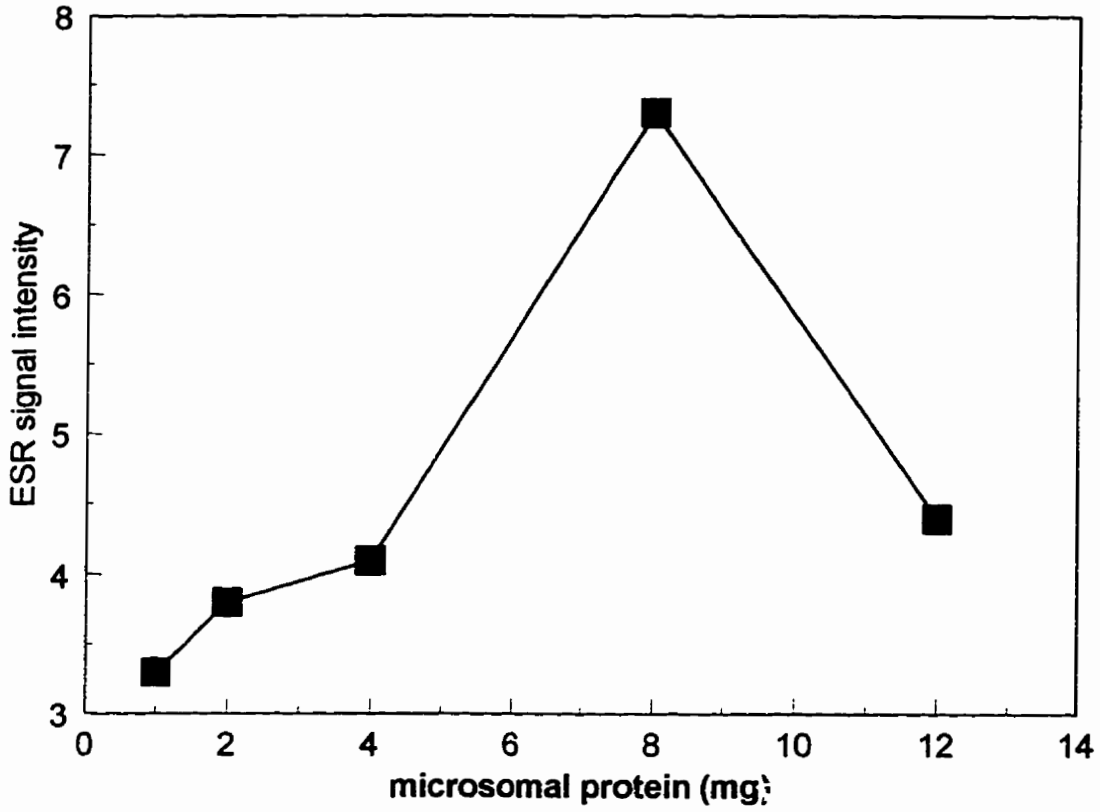

Fig. 3.5 Effect of hamster lung microsomal protein concentration on ESR signal intensity. Incubates contained microsomal protein (1-12 mg), 5 mM AM and 50 mM PBN and 30 μM NADPH. Data points represent means of n=2-4 separate experiments.

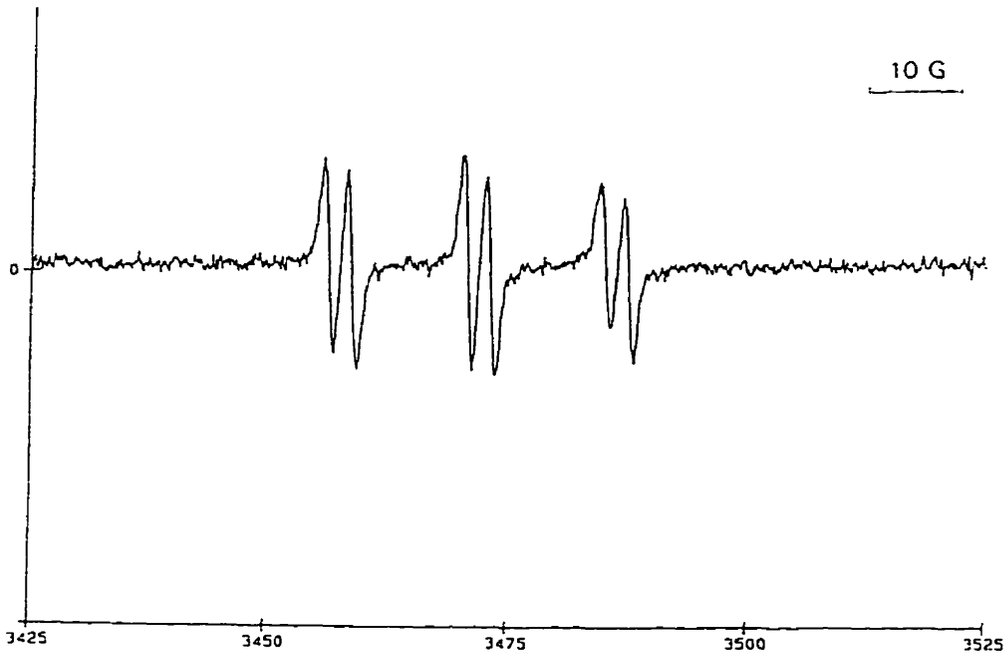

Fig. 3.6 ESR spectrum obtained from an AM containing incubation in the absence of microsomes. Incubate contained 10 mM AM, 50 mM PBN and 0.3 mM NADPH. hfsc's: a^N=14.3 G, a_β^H=2.5 G (gain 5.0 X 10^5)

liver microsomes incubated with DEA, a major metabolite of AM (Fig 3.7). Incubation of DOAM with lung (Fig. 3.8) or liver microsomes resulted in the generation of a PBN-radical adduct which had similar hfsc's ($a^N = 14.5 \pm 0.1$ G, $a_\beta^H =$ 2.5 G, n=3) to the PBN radical adduct derived from the respective microsomal incubation of AM.

A two-fold increase in PBN concentration (50 mM vs 100 mM) produced ESR signals of similar strength. However, a decrease in signal strength was observed with 10 mM PBN (Fig. 3.9).

Upon incubation of microsomes in isotonic buffer (pH 5.7) and PBN, the absence of an ESR signal indicated that the low pH did not stimulate free radical production and LPO in microsomes (Fig. 3.10). Rarely, an ESR signal was obtained from incubation of PBN with H_2O alone or isotonic buffer (pH 5.7) alone. However, this ESR signal was attributed to PBN decomposition which is believed to occur following its repetitive exposure to air and/or light (Chamulitrat *et al.*, 1993). Upon decomposition, a PBN free radical adduct of relatively small intensity was generated with hfsc's similar to the free radical adduct derived from incubations containing AM. Thus, it is important to ensure the purity of PBN prior to conducting spin trapping experiments.

Experimentation with minimal laboratory fluorescent light exposure resulted in a PBN radical adduct signal with hfsc's and intensity similar to those produced in direct light. However, additional peaks indicative of PBN decomposition were observed in a few samples implying that experimentation is preferable away from direct light.

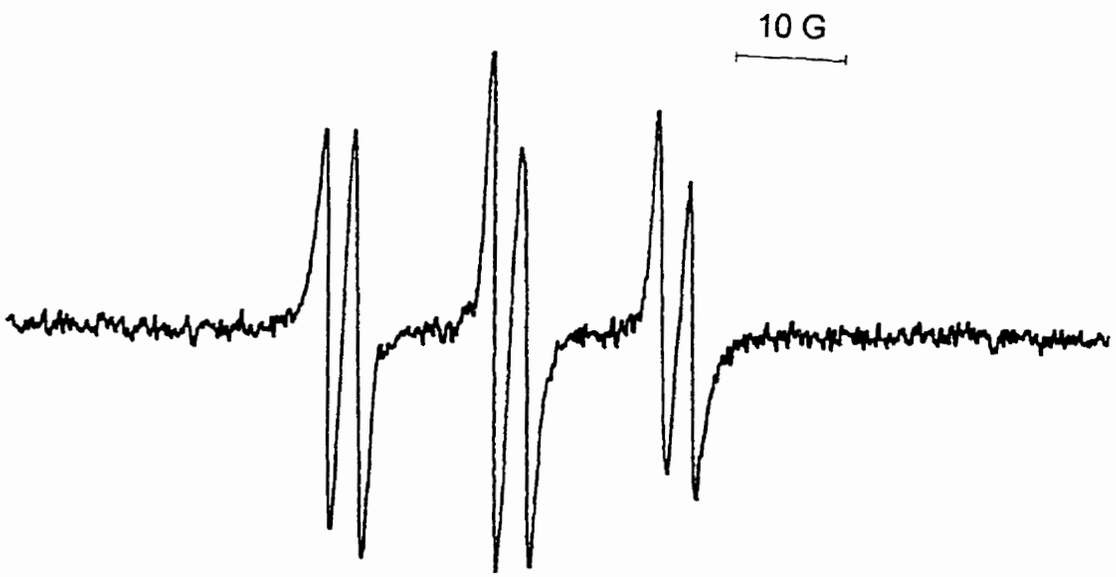

Fig. 3.7 Effect of DEA on free radical (PBN-spin adduct) formation. ESR spectrum obtained from liver microsomal incubate containing 16 mg protein, 10 mM DEA, 0.1 M PBN and 0.3 mM NADPH. hfsc's: a^N= 14.6 G, a^H_β= 2.6 G (gain 1.6 X 10^5)

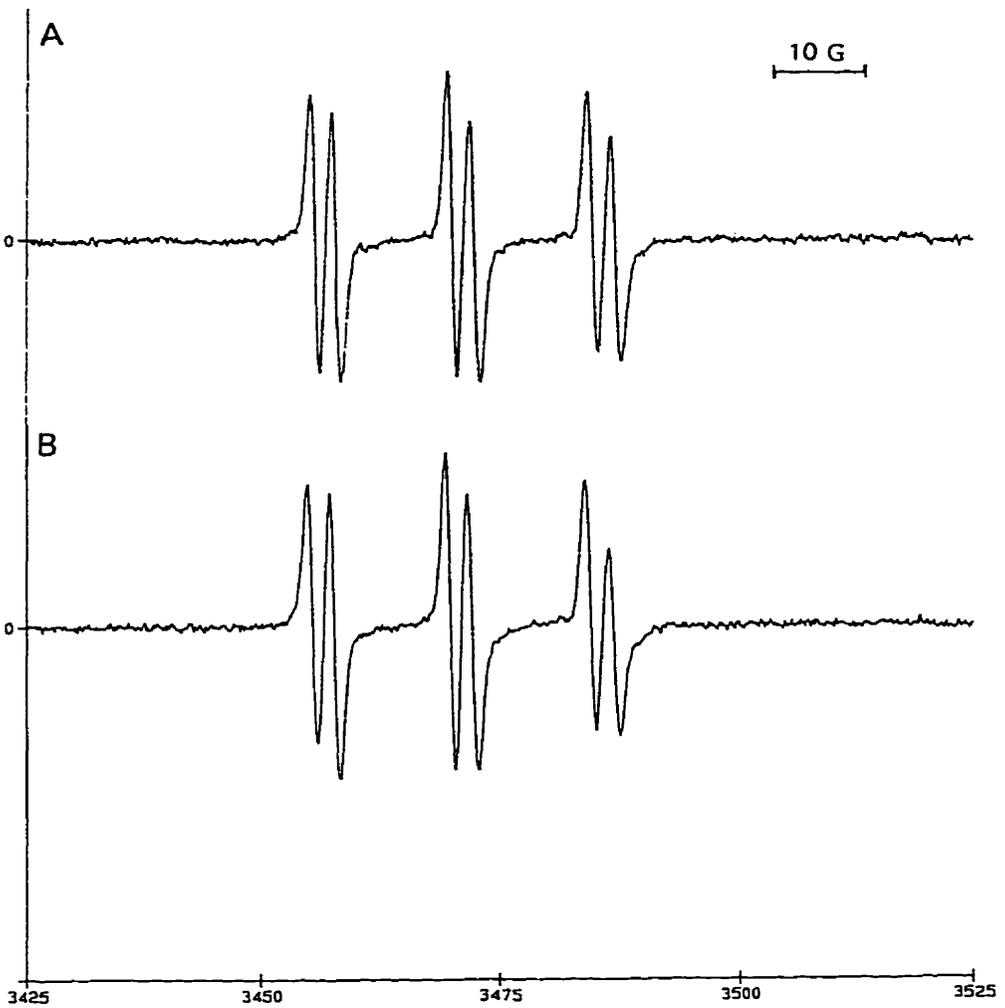

Fig. 3.8 Comparison of effects of DOAM and AM on free radical (PBN-spin adduct) formation. ESR spectrum obtained from liver microsomal incubates containing microsomal protein (16 mg), 50 mM PBN and 0.3 mM NADPH. A) 10 mM DOAM; B) 10 mM AM; hfsc's: $a^N = 14.4$ G, $a_\beta^H = 2.5$ G (gain 2.5 X 10^5)

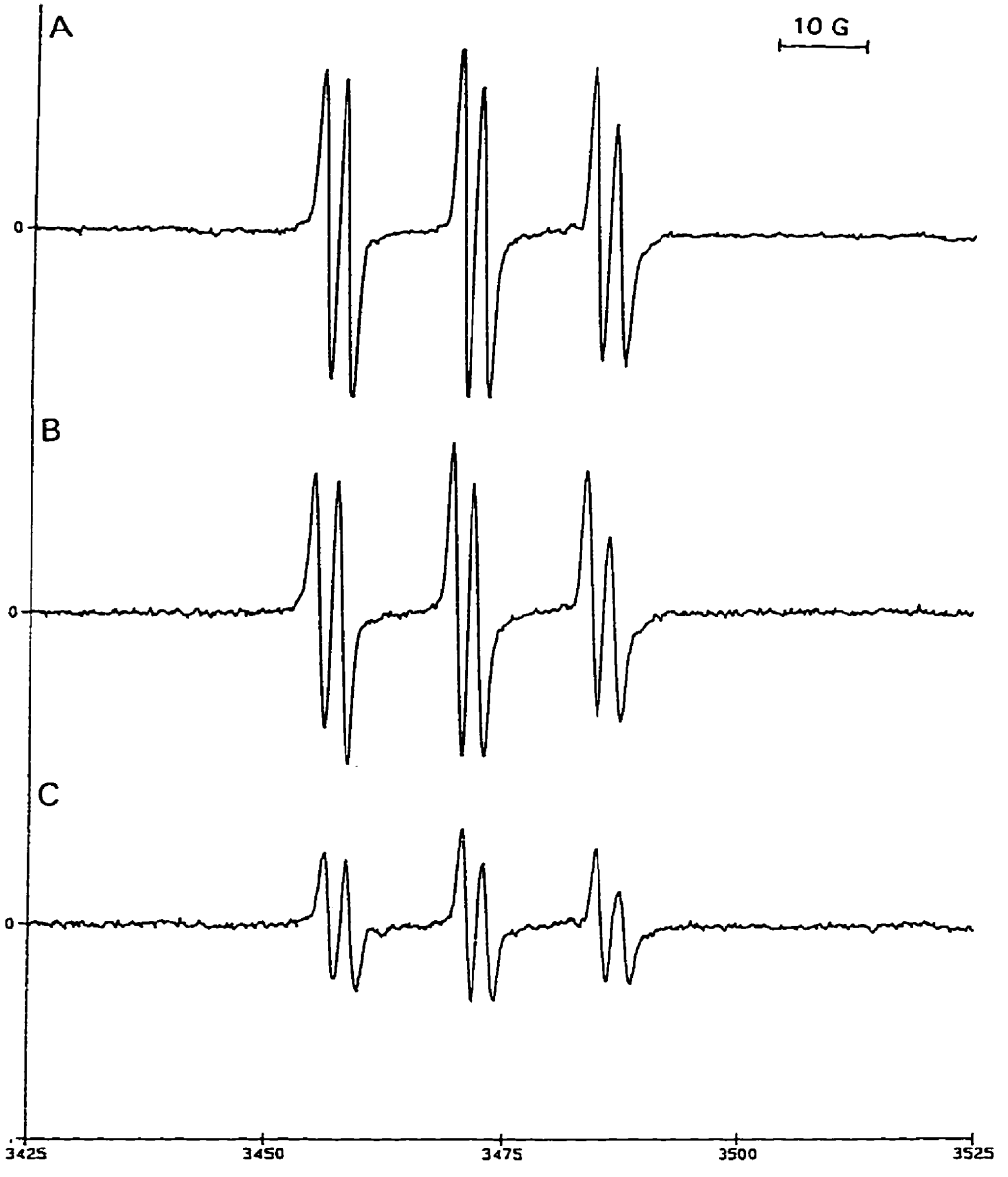

Fig. 3.9 Effect of varying PBN concentrations on free radical (PBN spin adduct) formation by AM. ESR spectra of incubates contained microsomal protein (16 mg), 10 mM AM and 0.3 mM NADPH. A) 100 mM PBN; B) 50 mM PBN; C) 10 mM PBN. (gain 2.5 X 10^5)

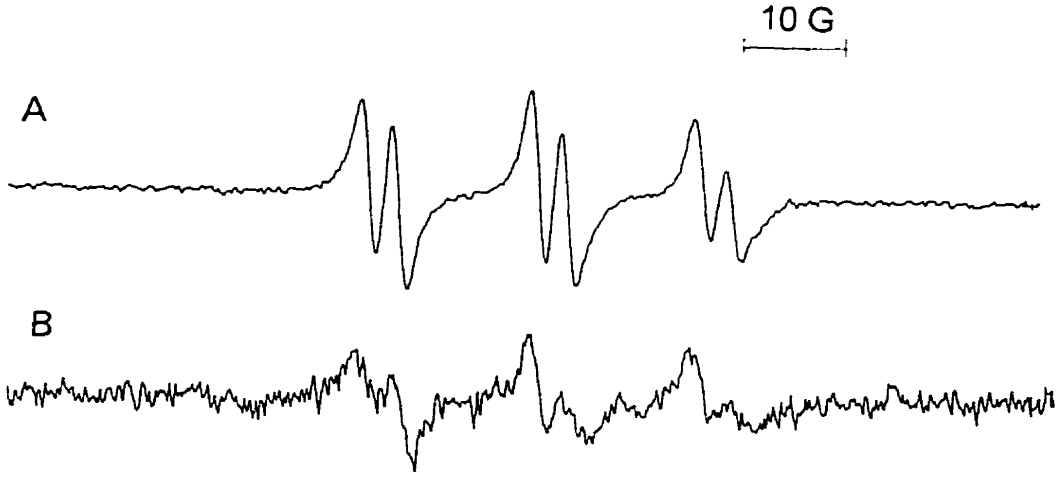

Fig. 3.10 Effect of 0.01 M K-phosphate buffer plus 1.15% KCl (pH 5.7) on free radical formation (PBN spin adduct) in liver microsomes. ESR spectra of incubates containing A) 50 mM AM, 16 mg microsomal protein, 0.1 M PBN, 0.3 mM NADPH and B) no AM, same as A in buffer pH 5.7 (gain A=1.25 X 10^5, B=5 X 10^5)

3.3.2 HPLC separation of PBN-radical adduct

Upon analysis of HPLC fractions by ESR, only fraction A produced a signal consistent with the presence of a PBN spin adduct (Fig. 3.11). The PBN-free radical active peak was determined to have a retention time of 4.04 min and was the first peak to elute from the column (Fig. 3.12). The resultant ESR signal had the same hfsc's as the original sample prior to HPLC separation. Fraction B contained a small ESR signal that resembled that of Fraction A (Fig. 3.12) and was attributed to contamination by Fraction A, since the two peaks eluted from the column very closely and were not completely resolved. PBN spin adducts were not present in other fractions (results not shown).

A similar, albeit less intense ESR signal indicative of a PBN-spin adduct, was obtained following the storage (-80°C) of a benzene extract. This extract originated from a microsomal incubation in which an ESR signal was observed prior to storage.

3.3.3 PBN-spin adduct assignments

These results strongly suggested that the trapped free radical (hfsc's: a^N= 14.3 G, a_β^H= 2.5 G and a_α^{13C}= 5.5 G) was similar (hfsc's in benzene) to the PBN-phenyl radical (a^N= 14.37 G, a_β^H= 2.18 G and a_α^{13C} = 5.53 G) and to the PBN-toluyl radical adduct (a^N= 14.45 G, a_β^H= 2.54 G and a_α^{13C} = 5.68 G) as shown in Table 3.1. However, based on the structure of AM (ie. lack of toluyl group), the trapped radical is most likely more similar to a phenyl radical.

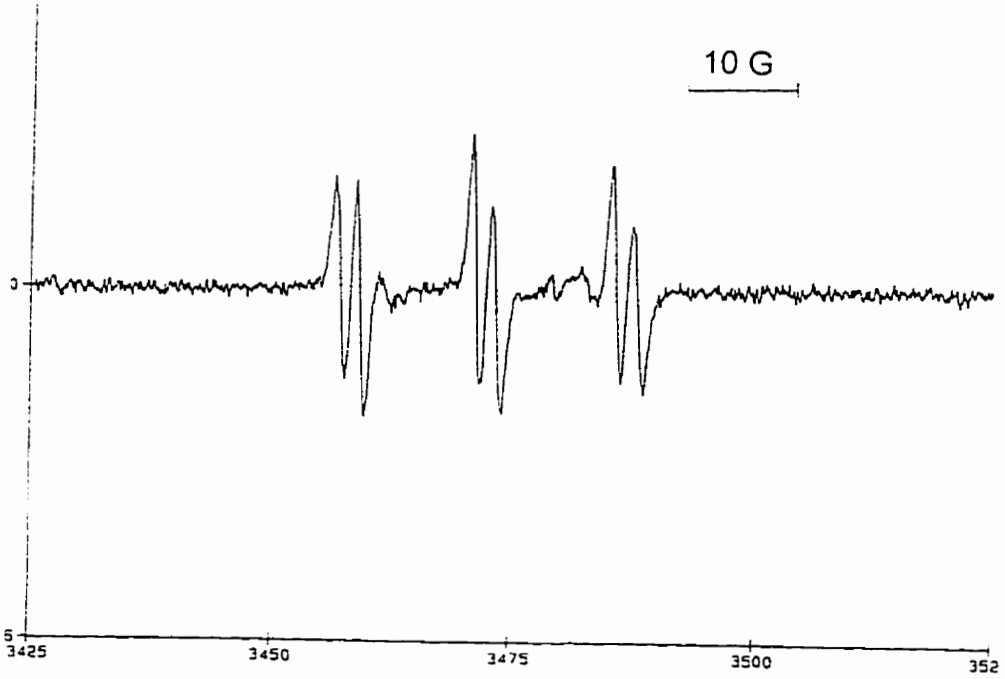

Fig. 3.11 ESR spectrum of PBN-spin adduct eluted from HPLC fraction A in figure 3.12. (gain 5 X 10^5)

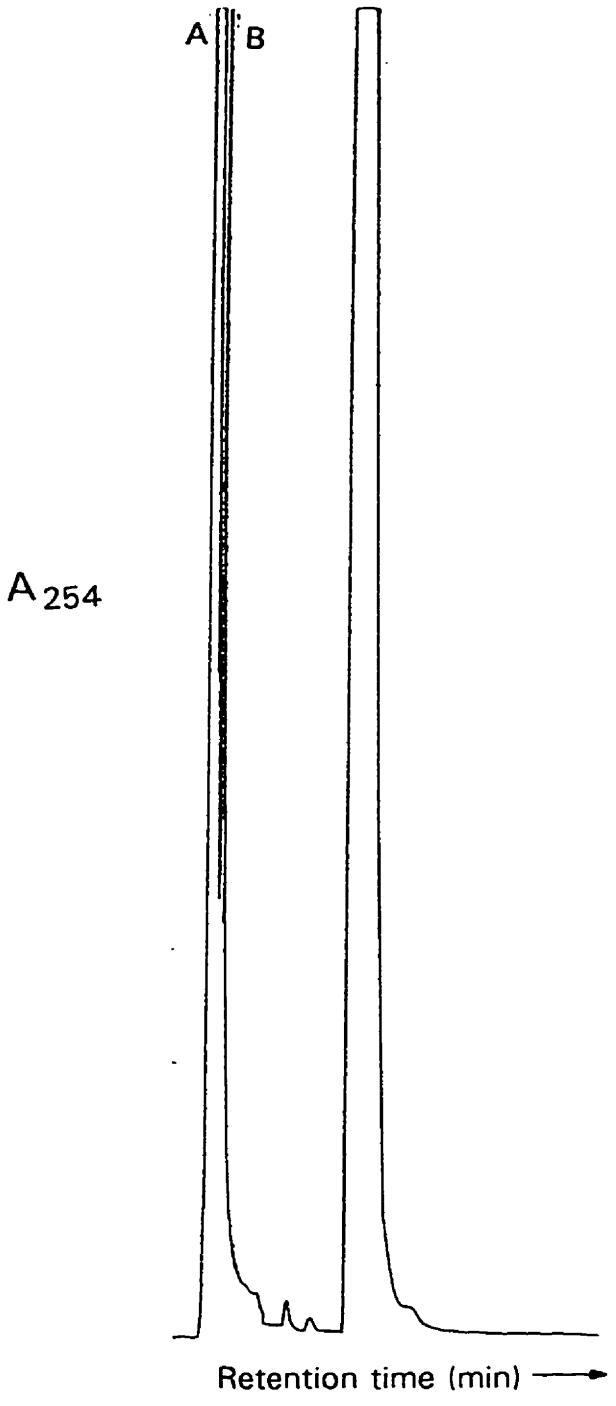

Fig. 3.12 Normal phase HPLC chromatogram of PBN spin adduct in hexane.

Table 3.1 EPR Hyperfine Splittings for Radical Adducts of PBN-*nitronyl*-^{13}C in Benzene. (from Haire et al., 1988)

radical addend	a^N	a_β^H	a_α^{13C}
$Si(C_2H_5)_3$	14.67	6.00	5.14
$Ge(C_6H_5)_3$	14.66	6.27	5.40
CH_3	14.85	3.53	5.29
$C(CH_3)_3$	14.66	2.32	5.49
H	14.87	7.41	5.38
$C(CH_3)_2CN$	14.28	3.29	5.78
$CH(CH_3)_2$	14.67	2.59	5.30
$CH_2CH=CH_2$	14.64	3.27	5.38
$CH_2C_6H_5$	14.45	2.54	5.68
$CHOHCH_3$	15.1 15.1	4.7 5.4	5.4 5.8
CH_2OH	14.88	6.51	5.74
$CH=CH_2$	14.85	2.68	5.31
C_6H_5	14.37	2.18	5.53
$C(O)C_2H_5$	14.27	3.14	5.90
$C(O)C_6H_5$	14.30	4.54	5.79
CCl_3	14.01	1.77	5.82
CF_3	13.97	1.85	5.92
$NC_{12}H_8$	14.65	4.64	4.64
N_3	13.95	1.92	3.47
OCH_3	13.59	1.84	4.55
$OCH_2CH(CH_3)_2$	13.72	1.97	4.56
$OC(CH_3)_2CN$	13.93	2.16	4.70
$OC(CH_3)_3$	14.28	2.03	4.91
$OOC(CH_3)_3$	13.25	1.15	4.65
$OC(O)C_6H_5$	13.29	1.48	3.17
$P(C\text{-}C_6H_{11})_2$	14.39	3.35	6.33
$P(O)(OC_2H_5)_2$	14.65	3.06	6.16
SCH_2CH_3	13.80	2.00	4.90
CN	14.84	1.76	3.4

3.4 DISCUSSION

This ESR study has shown that AM is capable of generating a PBN-trappable free radical in lung and liver microsomes. The lack of an ESR signal in the absence of PBN suggests that the free radical produced is too short-lived to accumulate to sufficient concentrations to be measured without spin trapping. Spin trapping extends the detection limits of ESR to very low concentrations of free radicals normally undetectable by direct ESR methods (Janzen and Haire, 1990). The nitrogen hfsc for the PBN radical adduct obtained in this study was consistent with the radical being carbon- or oxygen-centered. The ranges of nitrogen hfsc's for carbon- and oxygen-centered radical adducts overlap and are 14.0-14.8 and 13.3-14.2 G respectively (Haire *et al.*, 1988). The magnitude of the nitrogen hfsc depends on the spin density on the nitrogen atom and the geometry about the aminoxyl function. The β-hydrogen hfsc is predisposed to radical addend conformational alterations that may result from steric or intramolecular interactions between the radical addend and the aminoxyl function (Janzen *et al.*, 1982). Thus, in principle, each free radical adduct should have a unique ESR spectrum.

The use of PBN-*nitronyl*-^{13}C allows discrimination between carbon- and oxygen-centered radicals by providing an extra hfsc, a_{α}^{C}. In general, the α-^{13}C hfsc is usually greater than 5 G (ie. 5.3-5.9) for a carbon-centered radical adduct whereas oxygen-centered radical adducts possess values below 5 G (ie. 3.2-4.9) in benzene (Haire *et al.*, 1988). The ESR spectrum derived from the PBN-*nitronyl*-^{13}C incubation and all three hfsc's (a^{N}= 14.3 G, a_{β}^{H}= 2.5 G and a_{α}^{C}= 5.5 G) are consistent with a carbon-

centred radical. Furthermore, the hfsc's of this radical are comparable to those reported for the PBN-*nitronyl*^{13}C-phenyl radical adduct in benzene (Table 3.1). Indeed, the magnitude of the hfsc's is routinely used as the spectroscopic criterion for corroboration of the identities of an experimentally obtained PBN-spin adduct of unknown identity with those of known PBN-radical adducts.

It is likely that the free radical detected in this study was derived from AM since it is very similar to a phenyl radical. Other investigators have reported formation of a carbon-centered radical from AM following UV irradiation (Li and Chignell, 1987), or radiolysis by ^{60}Co-γ and electron pulse (Vereckei *et al.*, 1993). Li and Chignell (1987) demonstrated that the aryl radical derived from AM was able to abstract a hydrogen atom from various donors (eg. cysteine, glutathione, ethanol) as well as from linoleic acid, to form the corresponding dienyl radical. Similarly, Vereckei *et al.* (1993) proposed that AM formed a radical which abstracted hydrogen atoms in aqueous solutions of different alcohols. Based on the formation of partially and fully deiodinated AM molecules as measured by thin layer chromatography and HPLC, they speculated that the radical formed by radiolysis was a highly reactive aryl radical capable of abstracting hydrogen atoms and initiating LPO and other free radical reactions in biological systems. The free radical was proposed to be formed by the reduction of AM by a hydrated electron or an organic radical *in vitro* and was accompanied by the release of iodide ion (Vereckei *et al.*, 1993). Indeed, the C-I bond of the benzofuran moiety of the AM molecule may be a likely site since it has a relatively low bond dissociation energy (Sharma and Kharasch, 1968). In addition,

aromatic iodine derivatives are known to photodissociate in solution via a free radical mechanism (Levy *et al.*, 1973). Free iodide ion has been detected in UV and γ-irradiated solutions of AM (Li and Chignell, 1987; Paillous and Verrier, 1988; Vereckei *et al.*, 1993), and monodeiodinated DEA has also been detected in the serum of rats treated with AM (Kannan *et al.*, 1989).

Free radical formation upon exposure of other halogenated compounds (eg., carbon tetrachloride (CCl_4), bromotrichloromethane) to light has been observed (McCay *et al.*, 1980). Photoactivation with resultant free radical production was thought to be a possible explanation for the observed PBN radical adduct in AM-containing solutions devoid of microsomes in this study. However, ESR signals with the same hfsc's were obtained after performing experiments away from a direct ambient fluorescent light source. Thus, photoactivation was unlikely to be responsible for the observed ESR signals in samples devoid of microsomes.

The PBN radical adducts derived from UV irradiated solutions of 3-methylindole (3-MI), CCl_4 and bromotrichloromethane have been shown to be identical to the PBN radical adducts derived from their respective microsomal incubations (McCay *et al.*, 1980; Kubow *et al.*, 1984). Li and Chignell (1987) trapped a PBN carbon-centered radical adduct following the UV irradiation of an AM solution; however, a comparison between the hfsc's of their PBN radical adduct and the radical generated in this study cannot be made as different solvents (acetonitrile vs. benzene) were used for ESR analysis. The magnitudes of both nitrogen and β-hydrogen hfsc's are altered by solvent polarity (Janzen *et al.*, 1982).

Although AM accumulates in target tissues of toxicity in low millimolar concentrations (Brien *et al.*, 1987), the concentrations used in these experiments were necessarily higher (5 mM) for the detection of a readily measurable amount of PBN-radical adduct. AM concentrations greater than 5 mM did not result in a significant increase in signal. Similarly, no increase in signal was achieved with CCl_4 concentrations beyond 10 mM (Janzen *et al.*, 1994). Generally, much larger concentrations of the free radical precursor of interest are used in ESR studies than would be present in pathophysiological systems (Kubow *et al.*, 1984; Janzen *et al.*, 1987).

The ESR signal produced by lung and liver microsomes possessed the same characteristics (ie. hfsc's) but was greater in intensity than the signal produced in the absence of microsomes suggesting that microsomes increased the production of this radical. It is possible, as suggested by Vereckei and coworkers (1993), that AM meets its reductive environment during its metabolism in the liver by the CYP450 enzyme system with an electron being transferred directly to AM by NADPH-CYP450 reductase. Numerous xenobiotics (eg., CCl_4, halothane, chloroform, adriamycin, *t*-butylhydroperoxide) are substrates for CYP450 xenobiotic reductase (Goeptar *et al.*, 1995). Interestingly, benzyl halides, xenobiotics that are structurally similar to AM, are reduced by rat liver microsomal CYP450. However, during their reduction, electron transfer may lead to the formation of a free radical with the release of a halide ion. The intermediate free radical may be released from the active site and react with microsomal proteins and unsaturated lipids or it may bind to CYP450 leading to a

CYP450-metabolite complex (Mansuy and Fontecave, 1983). AM too, forms a biologically inactive CYP450Fe(II)-metabolite complex in hepatic microsomes following administration to rats, mice and hamsters and *in vitro* (Larrey *et al.*, 1986).

The possibility of CYP450 mediated reductive metabolism of AM in the liver where varying oxygen tensions exist in different zones is more plausible than in the lung. *In vivo*, AM free radical production may occur in the lung and the liver, but by different mechanisms resulting in the formation of the same radical. In this *in vitro* study, both microsomal systems were capable of producing the same free radical under similar conditions. However, the nature of microsomal activity responsible for free radical production is not clear at present as an NADPH concentration dependence was not established.

In the mitochondrion, electron leakage may occur from the electron transport chain (Freeman and Crapo, 1982). For example, CCl_4, an agent known to produce hepatotoxicity via LPO, was reduced to the trichloromethyl radical ($^{\bullet}CCl_3$) by isolated rat liver mitochondria incubated under hypoxic conditions with succinate and ADP (Tomasi *et al.*, 1987). Conceivably, electrons may be transferred directly to AM to produce an AM radical which may then abstract a hydrogen atom from unsaturated lipids and initiate LPO. The free radical trapped in microsomal preparations may initiate LPO, but is not an LPO product itself because the hfsc's were similar to those for the free radical trapped in an AM-buffer solution devoid of microsomes. In addition, the results with PBN-*nitronyl*-^{13}C were consistent with the free radical being very similar to a phenyl radical. The production of LPO by AM has been investigated

in a variety of systems and has yielded variable results (Grech-Bélanger, 1984; Rekka *et al.*, 1990; Ruch *et al.*, 1991; Wang *et al.*, 1992; Vereckei *et al.*, 1993).

The goal of a study by Janzen and coworkers (1994) was to determine the reproducibility of the ESR signal intensity of the trichloromethyl adduct of PBN. It was found that at least eight repeat experiments were required under identical conditions to attain an average value with an error of $\pm 10\%$. In the current study, the NADPH concentration dependence of ESR signal intensity could not be established. A concentration-response relationship may be difficult to obtain for a variety of reasons. Firstly, PBN has shown a Type I binding spectrum with CYP450 indicating an interaction with the CYP450 substrate binding site which could interfere with CYP450 mediated radical production. Secondly, PBN inhibits a variety of CYP450 dependent enzyme activities such as aminopyrine N-demethylation, aniline *p*-hydroxylation and ethoxycoumarin O-deethylation (Cheeseman *et al.*, 1985). Thirdly, the formation of an unidentified PBN metabolite was modified by CYP450 inducers and inhibitors *in vivo* (Chen *et al.*, 1991). Finally, nitroxides may be reduced to non-ESR active hydroxylamines by NADPH CYP450 reductase or CYP450 (Janzen, 1984; Swartz, 1990). All of these factors contribute to the difficulty in determining a linear relationship between experimental variables. Nonetheless, qualitative results can be very informative. For example, compounds known to modulate free radical scavenging defense systems (eg. GSH, cysteine, vitamin E, diethylmaleate) alter the production of 3-MI derived free radicals (Kubow *et al.*, 1984; Kubow *et al.*, 1985; Kubow and Bray, 1988). Modulator induced qualitative changes in free radical production and

production and corresponding changes in the production of a toxic response can be used as evidence for free radical involvement in the mechanism of a particular drug induced toxicity (Aust *et al.* 1993).

AM, DEA and DOAM have previously been shown to produce pulmonary toxicity in the hamster *in vivo* (Daniels *et al.*, 1989; Leeder *et al.*, 1994; Chapter 2). In this ESR study, all three compounds were capable of generating free radicals in lung and liver microsomes. All three PBN spin adducts possessed similar hfsc's suggesting that a similar free radical can be produced from all three compounds. This is not suprising, since all three compounds have related chemical structures. Thus, free radical production must be considered as a possible mechanism for AM-, DEA- and DOAM-induced pulmonary toxicities.

In a number of studies, antioxidants failed to provide protection against AM toxicity. However, in these studies, antioxidant enzymes were not conjugated with polyethylene glycol or encapsulated by liposomes and thus would not be able to effectively penetrate the cell membrane to exert their protective effects. In addition, some of these antioxidants were H_2O soluble, and thus may not have had access to the lipid soluble site of radical generation or LPO propagation sites. Lipid soluble vitamin E, however, protected against AM-induced cytotoxicity (Kachel *et al.*, 1990; Ruch *et al.*, 1991). Furthermore, in *in vivo* studies, measurement of antioxidant concentration in target tissues was not performed and thus failure of antioxidant protection may have been due to insufficent antioxidant concentrations at sites of free radical generation (Vereckei *et al.*, 1993; Leeder *et al.*, 1994).

In conclusion, this is the first study to directly demonstrate the formation of an AM derived free radical in biological tissue. Secondly, by the use of three parameter ESR spin trapping techniques, the trapped radical could be assigned to a phenyl type of radical with some confidence. However, further studies are required to determine the structural identity as well as the mechanism of formation of this radical. Most importantly, it must be determined whether this radical has a role to play in AIPT and in other toxicities associated with AM use.

CHAPTER 4

AN INVESTIGATION OF AIPT IN CULTURED ADULT PERIPHERAL HAMSTER LUNG SLICES

4.1 INTRODUCTION

The heterogeneous cell composition of the lung coupled with extrapulmonary factors complicates the investigation of the mechanisms of action of pulmonary toxicants *in vivo*. These interacting variables may interfere with identification of initiating events responsible for pulmonary tissue damage (Placke and Fisher, 1987a). *In vitro* systems lack systemic influences, and therefore may provide information regarding the initiating events involved in the mechanisms of toxicity. Cultured lung slices offer an advantage over isolated cell culture systems because the heterogeneous cell composition of the lung, and important cell-cell and cell-matrix interactions are maintained (Stefaniak *et al.*, 1992; Fisher *et al.*, 1994; Kinnard *et al.*, 1994; Sawyer *et al.*, 1995).

For over 20 years, cultured fetal and neonatal lung slices have been successfully employed in the study of morphogenesis and maturation (Adamson and Bowden, 1975; Gross *et al.*, 1978; Gross *et al.*, 1980). However, adult peripheral lung culture systems are associated with problems such as atelectasis (alveolar collapse) and subsequent necrosis which occur shortly after explantation (Stoner *et al.*, 1978). Instillation of alveolar spaces with agarose provides a diffusible matrix for internal support, thus preventing alveolar collapse and promoting long term viability (Placke and Fisher, 1987a). Cultured adult peripheral lung slices have been shown to mimic

the *in vivo* response to various pulmonary toxicants such as paraquat, bleomycin, silica, asbestos (Fisher and Placke, 1987; Placke and Fisher, 1987b), sulfur mustard (Wilde and Upshall, 1994; Sawyer *et al.*, 1995), and hyperoxia (Shapiro *et al.*, 1994).

Induction of antioxidant enzyme activities is a compensatory response in tissues exposed to oxidative stress (Crawford and Davies, 1994). A single intratracheal instillation of AM to the hamster has been shown to increase lung antioxidant enzyme activities such as superoxide dismutase, glutathione peroxidase and glutathione reductase (Wang *et al.*, 1992; Leeder *et al.*, 1994). In addition, this dosing regimen increased lung GSSG production 30 min and 2 h following dosing (Leeder *et al.*, 1994), effects suggestive of oxidative stress. However, the increase in total tissue antioxidant enzyme activities could also be attributable to enzymes' presence in inflammatory cells which invade the lung in response to cell damage. Thus, *in vivo*, it is difficult to differentiate between the induction of lung antioxidant enzyme activity, and elevations due to influx of inflammatory cells following injury.

The purpose of this study was to assess the utility of cultured adult peripheral hamster lung slices as a model system for the investigation of amiodarone-induced pulmonary toxicity (AIPT). The objectives of this study were: 1) to assess the cytotoxic response of cultured lung slices to AM and to compare this response with other *in vitro* and *in vivo* models of AM toxicity; 2) to determine whether AM produces oxidative stress. Specifically, glutathione reductase, an antioxidant enzyme, was measured without the confounding influx of inflammatory cells; 3) to compare the AM-induced response (cytotoxicity and oxidative stress) of cultured lung slices to that of

paraquat (PQ), a pneumotoxic herbicide believed to produce oxidative stress by a redox cycling mechanism (Boyd, 1984).

4.2 METHODS AND MATERIALS

4.2.1 Chemical sources

Chemicals were obtained as follows: agarose (Type VII: low gelling temperature), medium M199, insulin (crystalline, from bovine pancreas), hydrocortisone 21-hemisuccinate, retinyl acetate (all *trans*), gentamicin sulfate, antibiotic antimycotic (10 000 units penicillin, 10 mg streptomycin, 25 μg amphotericin B per ml solution), MTT tetrazolium (3-[4,5-dimethylthiazol-2-yl]-2,5-diphenyl-tetrazolium bromide), MTT formazan (1-[4,5-dimethylthiazol-2-yl]-3,5-diphenyl-formazan), 8% glutaraldehyde (Grade I), paraquat (1,1'-dimethyl-4-,4'-bipyridylium dichloride, methyl viologen), GSSG (99% purity), NADPH (chemically reduced, tetrasodium salt) and glutathione reductase (Type IV, from Bakers yeast) from Sigma Chemical Co., St. Louis, MO, USA; nystatin from ICN Pharmaceuticals, Montreal, PQ, Canada; bovine serum albumin (BSA, Fraction V) from Boehringer Mannheim Biochemicals, Laval, PQ, Canada. All other chemicals were of reagent grade and were obtained from common commercial suppliers.

4.2.2 Animals

Male golden Syrian hamsters were obtained and cared for as described in Section 2.2.2.

4.2.3 Preparation of cultured lung slices

Cultured lung slices were prepared according to the methods of Placke and Fisher (1987a) and Sawyer *et al.* (1995). Hamsters were killed with an overdose of sodium pentobarbital (300 mg/kg ip). Abdominal and thoracic surfaces were disinfected with 70% ethanol and a midline incision was cut to expose the thorax. Lungs were perfused via the pulmonary artery with sterile phosphate-buffered saline (PBS, pH 7.3) to remove blood. The trachea was exposed, cannulated *in situ* with polyethylene tubing (PE 160; 1.14 mm I.D., 1.57 mm O.D.) and the cannula ligated. Lungs and trachea were removed from the thoracic cavity intact, transferred to a beaker containing sterile PBS (37°C) and held to avoid submersion of the trachea in PBS. The tracheal cannula was attached to a gravity perfusion apparatus and the lungs were infused at a constant hydrostatic pressure of 20 cm H_2O with warm (40°C) 0.5% (w/v) agarose dissolved in sterile supplemented medium M199 (0.1 μg/ml retinyl acetate, 1 μg/ml bovine insulin, 0.1 μg/ml hydrocortisone hemisuccinate, 10 μg/ml gentamicin sulphate, 2 μg/ml nystatin and 1% antibiotic antimycotic). Following inflation of the lungs, the cannula was clamped and the lungs were placed in ice-cold sterile PBS containing 1% antibiotic antimycotic). The agarose was allowed to solidify for 45-60 min. The heart, trachea and fascia were removed, and the lungs were separated into lobes. Complete serial transverse sections (1mm thick) were sliced from each lobe using a McIlwain® tissue chopper (Mickle Laboratory Engineering Co. Ltd. Surrey, UK). Lung slices were gently separated from one another using fine tipped forceps and randomly distributed on sterile Gelfoam® absorbable gelatin sponges (size 4, 20 x 20 x

3 mm, Upjohn Co. of Canada, Don Mills, ON) in 6-well (35 mm) Corning® culture plates. Each well contained one sponge and each sponge contained enough lung slices to cover it without overlapping lung slices. Supplemented M199 (1.0 ml) with or without toxicants was added to saturate the sponge and cover the bottom of each cell well, but was not permitted to submerge the gelatin sponge. Lung slices were incubated in a tissue culture incubator (National, Weinicke Co.) at 37°C in a humidified atmosphere of 95% air (3-4 L/min) and 5% CO_2 (0.10-0.15 L/min). Medium was replaced every 48 h with fresh supplemented M199 (0.8 ml) containing the appropriate toxicant concentration.

4.2.4 Determination of AM content in cultured lung slices

AM content in lung slices was quantitated by the HPLC method described in Section 2.2.6. Slices were incubated in supplemented M199 containing AM or vehicle (H_2O) for 3 days. Slices (2-3, in duplicate) were removed from culture plates, rinsed with supplemented M199, blotted dry and weighed. Slices were then transferred to microcentrifuge tubes (1.5 ml) containing 500 μl of mobile phase (section 2.2.6). The slice/mobile phase mixture was sonicated (Insonator Model 1000, Savant Instruments, Hicksville, NY) for 10 sec while tubes were kept on ice. Contents were then centrifuged at 16 250 x g for 2 min (IEC Micromax®). Supernatants were removed, filtered (0.22 μm nylon syringe filter, Micron Separations Inc.) and kept on ice until HPLC analysis. AM content was expressed as μg AM/g lung slice.

4.2.5 Measurement of glutathione reductase activity in cultured lung slices

Lung slices (6-7, in duplicate) were removed from each treatment, pooled, blotted dry and homogenized in ice-cold 0.05 M K-phosphate buffer (pH 7.4, 600 μl) using a glass homogenization tube and teflon pestle (1 ml, Reacti-Ware , Pierce Chemical Co.). The homogenate was centrifuged at 10 000 x g for 10 min at 4°C. The resultant supernatant and pellet were separated and stored at -80°C until the day of GSSG reductase activity and cytosolic protein content measurements respectively.

GSSG reductase activity was measured according to a modification of the method of Smith and Boyd (1984). Briefly, NADPH (0.36 μmol), EDTA (0.3 μmol), BSA (2.4 mg) and 10 000 X g supernatant (25-150 μg protein) were made up to a total volume of 1.2 ml with 0.05 M K-phosphate buffer (pH 7.6). The rate of disappearance of NADPH (NADPH oxidation) was monitored spectrophotometrically at 340 nm for 2 min. This represented either non-GSSG reductase activity and GSSG reductase activity attributed to GSSG present in the 10,000 x g supernatant, and thus served as background activity for each sample. GSSG (0.11 μmol) was then added to the same sample and the disappearance of NADPH was monitored again. Background activity was subtracted to obtain GSSG reductase specific activity. Protein concentration was determined by the method of Lowry *et al.* (1951) following dilution (1 to 20) of sample. GSSG reductase activity was expressed as nmol NADPH oxidized/min/mg protein, based on an NADPH standard curve (0-0.18 μmol/ml).

4.2.6 Assessment of cultured lung slice viability

An attempt was made to use the LDH leakage assay (Moldéus *et al.*, 1978) for the assessment of cell viability. However, this assay produced highly variable leakage and unreliable results in cultured lung slices (data not shown).

The MTT cytotoxicity assay is based on the ability of mitochondrial succinic dehydrogenase in viable cells to reduce soluble yellow MTT tetrazolium to MTT formazan, an insoluble blue product (Altman, 1976). This assay was adapted for use in lung slices by Sawyer and coworkers (1995).

In order to establish the appropriate conditions for MTT cytotoxicity assessment in this cultured lung slice system, slices were incubated with varying concentrations of MTT tetrazolium in supplemented M199 (25,50,75,100 μg/ml) for various time periods (5,20,40,60,90,120 min) (Sawyer *et al.*, 1995).

Lung slices were incubated with MTT tetrazolium solution (75 μg/ml supplemented M199) for 1 h in a gently shaking waterbath (Grant, Cambridge, England) at 37°C. Slices were removed and MTT formazan extracted into 1.0 ml isopropanol. Formazan production was quantitated spectrophotometrically by measuring absorbance at 570 nm and lung slice formazan was expressed as μg MTT formazan/mg protein by using an MTT formazan standard curve (0-200 μg/ml isopropanol). The viability of lung slices from each treatment group was expressed as a percent of control viability.

Lung slices were air dried in test tubes to remove residual isopropanol and then each lung slice was transferred to a test tube containing 1.0 ml 1N NaOH. Lung slices

were stored in NaOH in the refrigerator for at least 2 days. On the day of protein concentration measurement, lung slices were incubated at 50°C for 1 h for further digestion of protein. An aliquot of digested lung slice solution was diluted (1 in 4) and protein concentration determined by method of Lowry *et al.* (1951), using BSA as the standard.

4.2.7 Electron microscopy

Lung slices were removed from incubation (2, 4, 8 and 14 days), cut into smaller pieces using a scalpel blade and were fixed with 2% (v/v) glutaraldehyde in 0.1 M K-phosphate buffer (pH 7.4) for 2 h. Slices were then transferred to cryovials containing 0.1 M K-phosphate buffer (pH 7.4) and stored at 4°C until processing for electron microscopy (Appendix I). Electron microscopy was performed by Dr. R.M. Walker at Parke-Davis Research Institute, Mississauga, ON.

4.2.8 Statistical Analysis

Results are expressed as $\bar{x} \pm$ SD. A repeated measures one-way ANOVA followed by a Newman-Keuls test was used to compare treatment groups. MTT cytotoxicity results were presented as a percent of control for each treatment group, however, statistical analysis was performed on MTT formazan produced ($\bar{x} \pm$ SD) for each treatment group. Differences were considered to be statistically significant when $p<0.05$.

4.3 RESULTS

Accumulation of AM in lung slices was maximal at 200 μM AM, so this concentration was used in toxicity experiments (Fig. 4.1).

Incubation of lung slices with 75 μg/ml MTT tetrazolium for 60 min was considered suitable for the determination of lung slice viability as this concentration produced sufficient formazan for a decrease in production to be quantifiable. As well, MTT formazan production was linear for 60 min at 25, 50 and 75 μg/ml MTT tetrazolium (Fig. 4.2). Incubation of lung slices with 250 μg/ml or 500 μg/ml MTT tetrazolium resulted in the production of MTT formazan exceeding the linear range of the MTT formazan standard curve (data not shown).

Cell viability of control lung slices was maintained throughout the 8 day incubation period as MTT formazan production varied only 9.1% from 0 to 8 days. This was confirmed by electron micrographs showing preservation of alveolar cells and architecture at 8 days (Fig. 4.4). Cells appear to possess normal amounts of mitochondria. Lamellar bodies, while present, did not appear to be very numerous in type II cells. There was some evidence of a loss in endothelial cells. Following 2 weeks of incubation, electron microscopy revealed the presence of numerous cytoplasmic vacuoles in the alveolar cells, as well as spreading of Type II epithelial cells on some surfaces of the alveoli (Fig. 4.5). Type II cell spreading refers to flattening of the cell as it assumes the appearance of a type I cell (Simon, 1992).

Significant toxicity was not detected following incubation of lung slices with

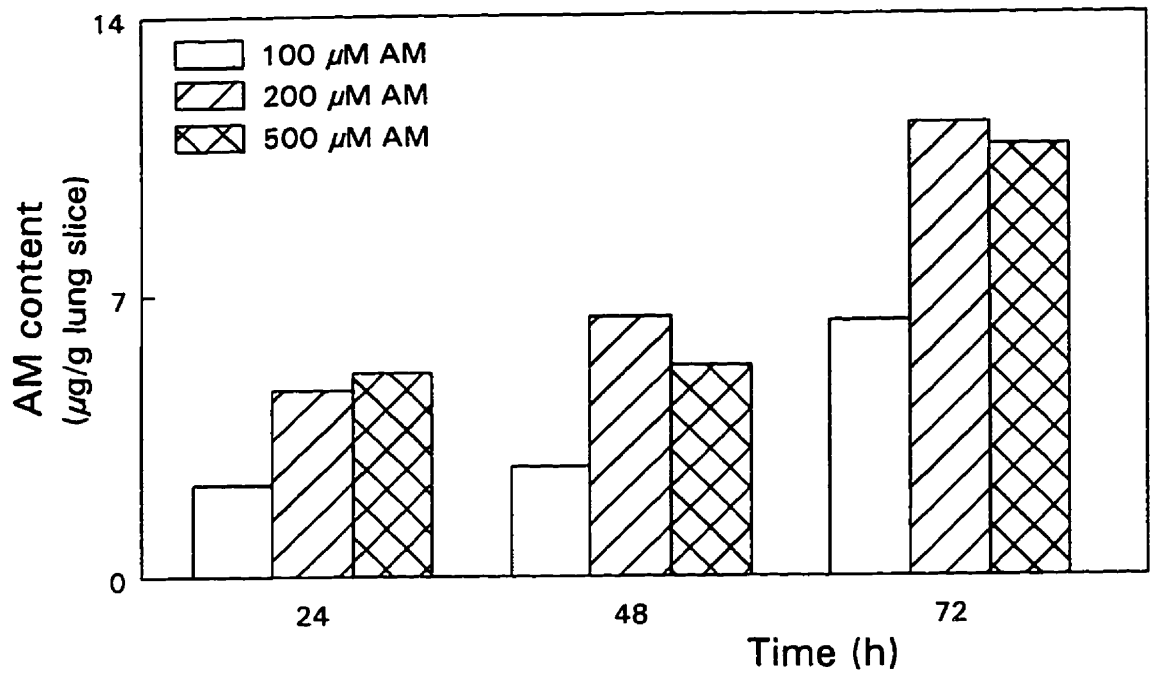

Fig. 4.1 Relationship between AM content in cultured lung slices and AM concentration in the medium. Lung slices were incubated with 100, 200 and 500 μM AM for up to 72 h; mean of n=2 separate experiments shown.

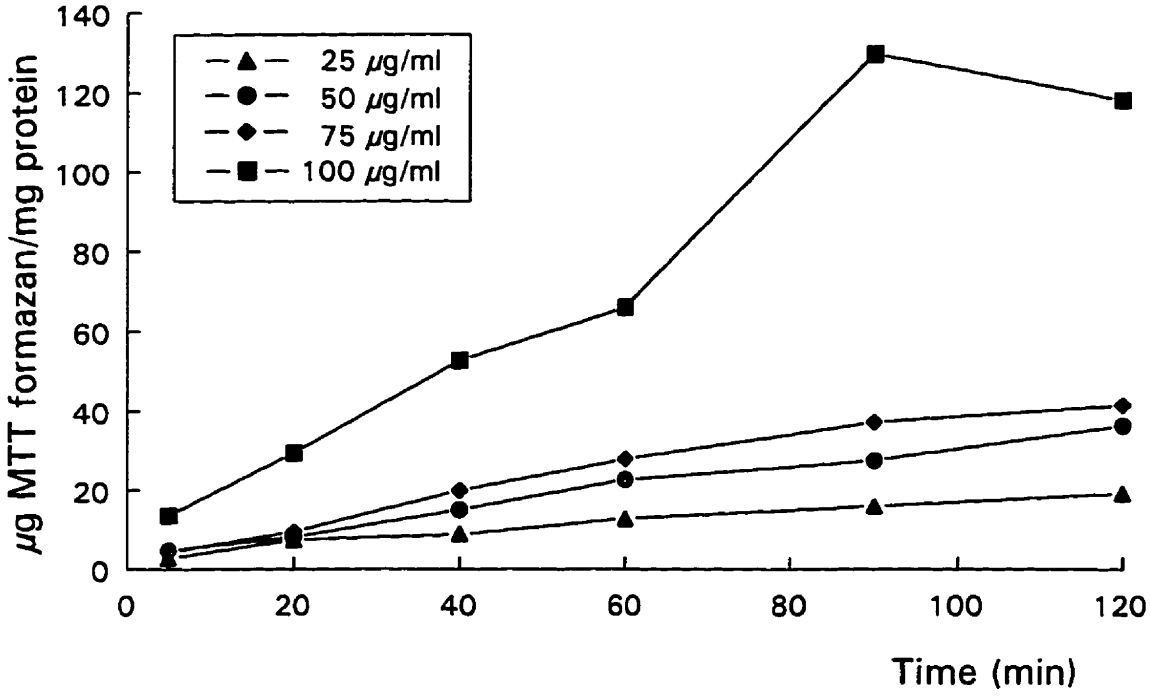

4.2 Characterization of the MTT cytotoxicity assay in control cultured hamster lung slices. Lung slices were incubated with varying MTT tetrazolium concentrations. Results are representative of a typical experiment using 2 slices per data point.

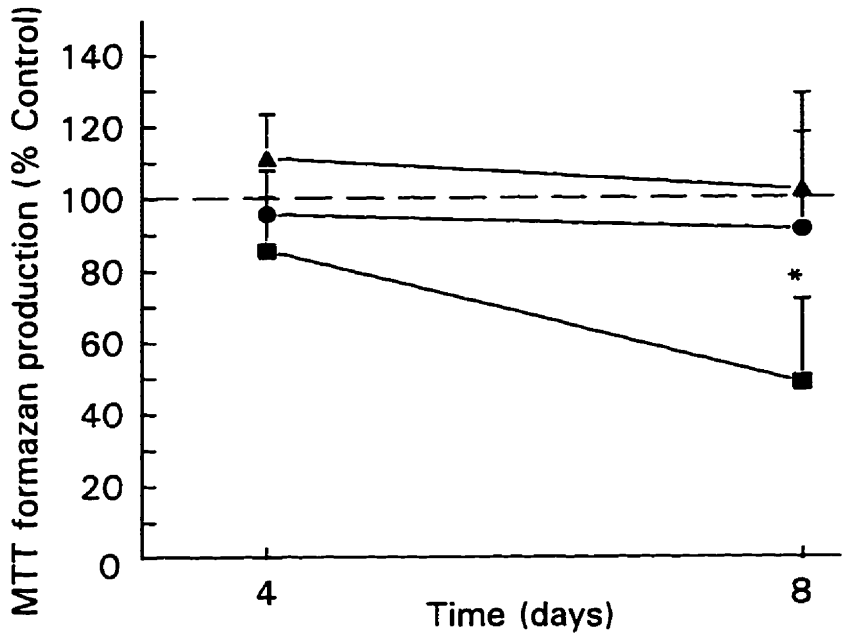

Fig. 4.3 Cytotoxicity in cultured lung slices as assessed by the MTT assay. Lung slices were incubated with 200 μM AM (●) 10 μM PQ (▲) and 200 μM PQ (■). Cytotoxicity is expressed as a percentage of formazan production in control slices, n=4 separate experiments; * significant difference from control, $p < 0.05$.

Fig. 4.4 Electron micrograph of lung alveoli from cultured hamster lung slices incubated for 8 days (Control). Cells and architecture are well preserved. A type I (arrow) and a type II cell (arrowhead) are evident. Magnification: 3600X.

Fig. 4.5 Electron micrograph of lung alveoli from cultured hamster lung slices incubated for 2 weeks (Control). Cells and architecture are well preserved. Numerous cytoplasmic vacuoles (arrows) are present in various cells. Type II cell spreading (arrowhead) is also evident. Magnification: 3600X.

200 μM AM for 8 days as indicated by the MTT assay (Fig. 4.3). Generally, good preservation of architecture was evident at 2 and 4 days of AM treatment, although focal blebbing of Type I cells was visible as early as 2 days following AM incubation (Fig. 4.6). At 4 days, some loss of type I cells with lateral spreading of type II cells was observed and type II cells contained a few lamellar bodies (Figs. 4.7). At 8 days of incubation, AM treated lung slices demonstrated type I cell loss and lateral spreading of type II cells. Degenerating cells were characterized by pyknotic nuclei, cytoplasmic vacuolation, lysis and loss of cytoplasmic contents (Figs. 4.8a and 4.8b). Following 2 weeks of AM treatment, numerous cytoplasmic vacuoles were present in extensively degenerating component cells (Fig. 4.9). There was, however, no evidence of fibrosis in AM treated lung slices.

Incubation of lung slices with 200 μM PQ for 2 days resulted in vacuolation and blebbing of type I and II cells with a loss of cytoplasm into the alveolar lumen (Fig. 4.10). At 4 days, most alveolar cells had undergone degenerative changes which included nuclear pyknosis, cytoplasmic vacuolation and lysis (Fig. 4.11). At 8 days of incubation with 200 μM PQ, all alveolar cells were swollen and extensive degenerative alterations included karyolysis of nuclei, lysis of cytoplasmic components and loss of plasma membranes, with the resultant death of alveolar cells and destruction of alveolar architecture (Fig. 4.12). Accordingly, MTT formazan production was considerably reduced in lung slices treated with 200 μM PQ at 8 days, but not in those incubated with 10 μM PQ (Fig. 4.3). Electron microscopy supported this finding, as alveolar

Fig. 4.6 Electron micrograph of lung alveoli from cultured hamster lung slices incubated with 200 μM AM for 2 days. Cells and architecture are well preserved. Focal blebbing of type I alveolar cell (arrow) is evident. Magnification: 3600X.

Fig. 4.7 Electron micrograph of lung alveoli from cultured hamster lung slices incubated with 200 μM AM for 4 days. Lateral spreading of a type II cell (arrow). Type II cell contains a few lamellar bodies (arrowhead). Magnification: 3600X.

Fig. 4.8A Electron micrograph of lung alveoli from cultured hamster lung slices incubated with 200 μM AM for 8 days. Lateral spreading of a type II cell (arrows). Magnification: 3600X.

Fig. 4.8B Electron micrograph of lung alveoli from cultured hamster lung slices incubated with 200 μM AM for 8 days. Degeneration of alveolar cells characterized by pyknotic nuclei (arrowhead) and cytoplasmic vacuolation, lysis and loss of component structures (*). Attenuated type II cells containing lamellar bodies (arrows) are present. Magnification: 3600X.

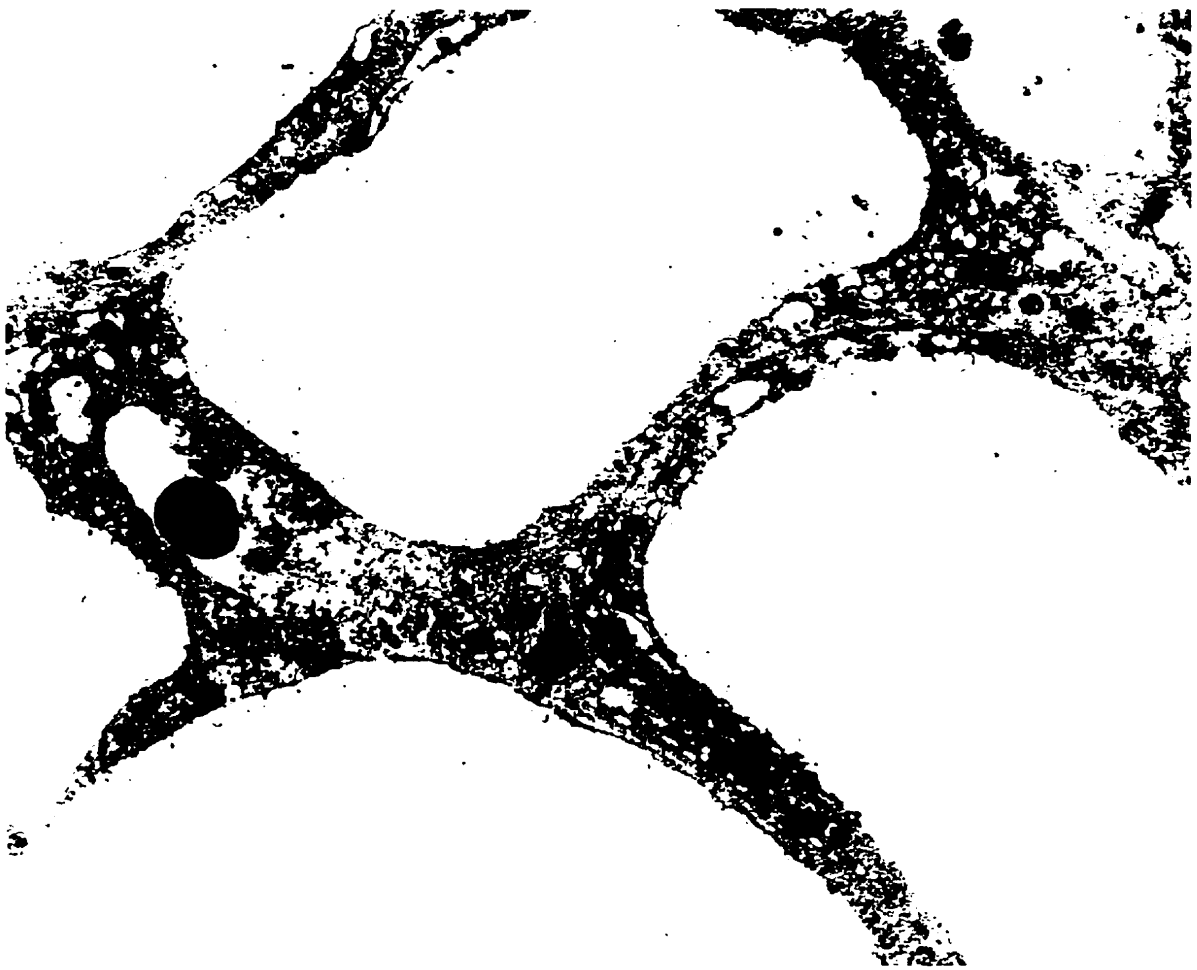

Fig. 4.9 Electron micrograph of lung alveoli from cultured hamster lung slices incubated with 200 μM AM for 2 weeks. Architecture is well preserved. Cells show degenerative changes and cytoplasmic vacuolation. Magnification: 3600X.

Fig. 4.10 Electron micrograph of lung alveoli from cultured hamster lung slices incubated with 200 μM PQ for 2 days. Vacuolation and blebbing of a type I cell (arrows) is evident. Magnification: 3600X.

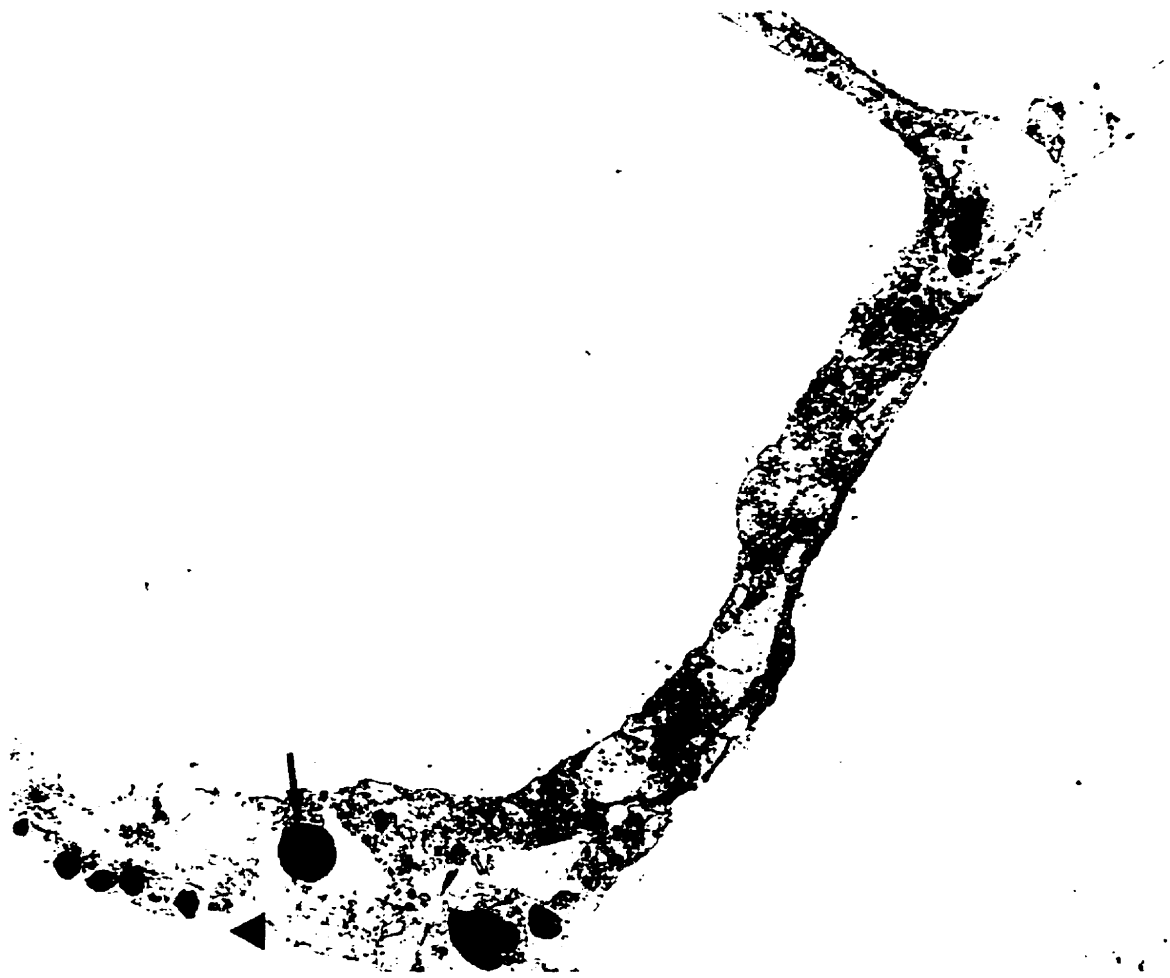

Fig. 4.11 Electron micrograph of lung alveoli from cultured hamster lung slices incubated with 200 μM PQ for 4 days. Most cells have degenerated and nuclear pyknosis (arrow), cytoplasmic vacuolation and lysis (arrowhead) are evident. Magnification: 3600X.

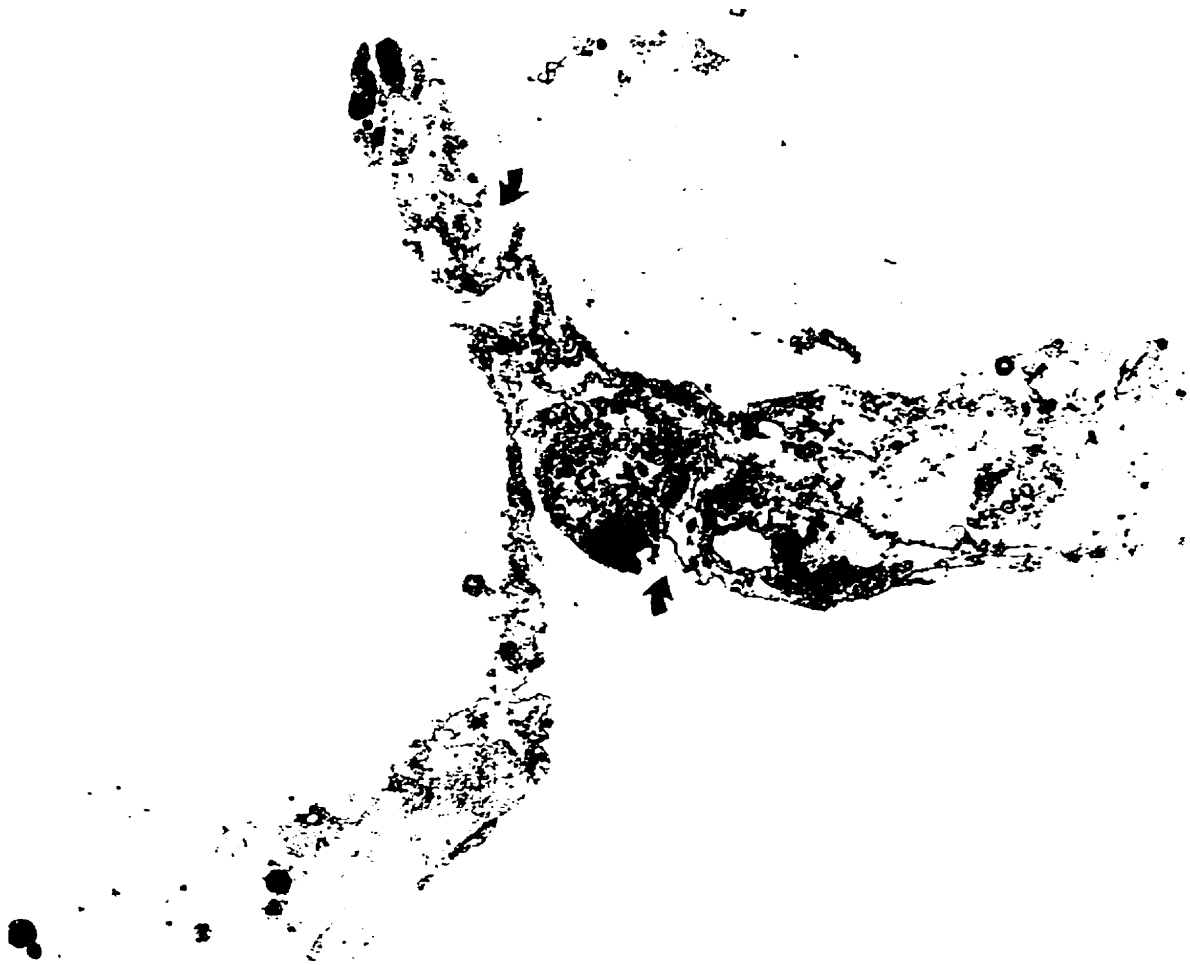

Fig. 4.12 Electron micrograph of lung alveoli from cultured hamster lung slices incubated with 200 μM PQ for 8 days. All alveolar cells are swollen and extensively deteriorated. Loss of cytoplasmic contents and plasma membrane rupture (arrows) are evident. Magnification: 3600X.

septa of 10 μM PQ treated slices were similar to those observed in control slices after 8 days of incubation (not shown).

GSSG reductase activity increased from the beginning of incubation throughout 8 days of incubation in control, 200 μM AM and 10 μM PQ treated lung slices. GSSG reductase activity was not altered in lung slices incubated with 200 μM AM or 10 μM PQ when compared to control. However, GSSG reductase activity was significantly reduced in slices treated with 200 μM PQ at 2,4, 6 and 8 days compared to all treatment groups (Fig. 4.13).

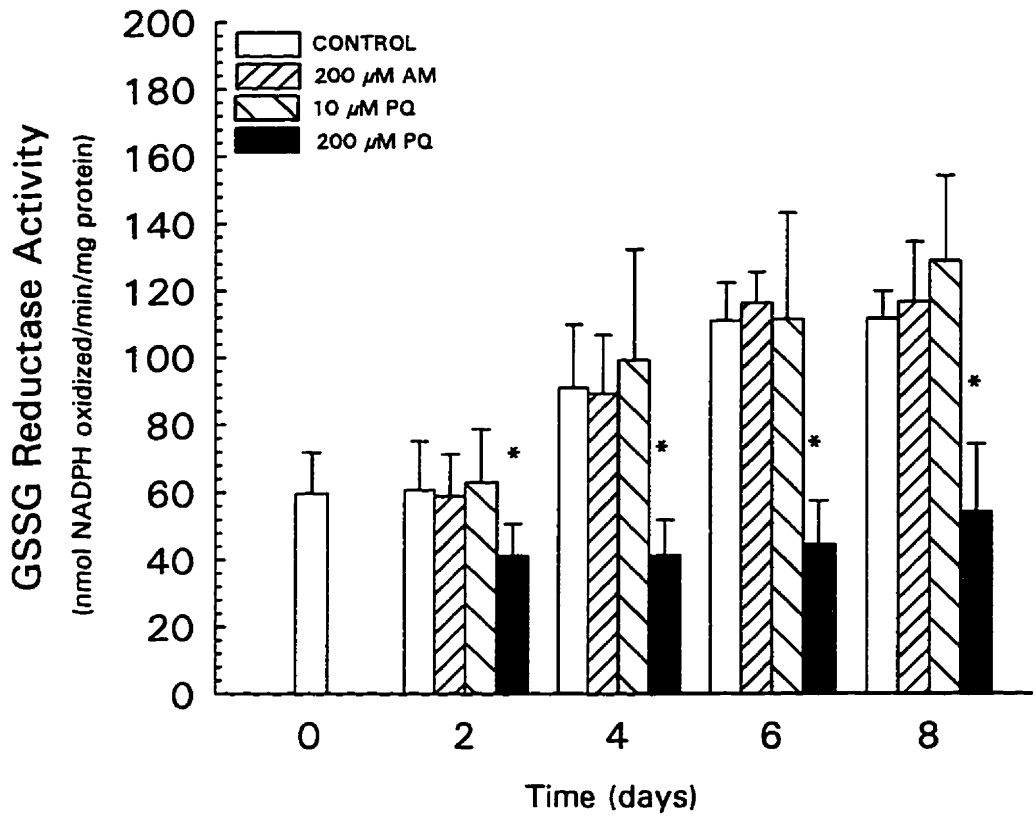

Fig. 4.13 GSSG reductase activity in cultured hamster lung slices. Lung slices were incubated with 200 μM AM, 10 μM PQ or 200 μM PQ. GSSG reductase activity is expressed as nmol NADPH oxidized/min/mg protein. * significant difference from control, $p<0.05$, $n=4$ separate experiments.

4.4 DISCUSSION

Adult peripheral lung slices are difficult to maintain in culture due to alveolar collapse and their predisposition to central tissue necrosis (Adamson and Bowden, 1975; Stoner *et al.*, 1978). Placke and Fisher (1987a) were able to maintain adult peripheral lung slices in culture for up to 4 weeks with the introduction of a new technique that involves inflation of airways and alveolar spaces with agarose and serum-free culture medium, followed by culture of slices on porous gelatin sponges. This cultured lung slice system has been adopted by other investigators (Stefaniak *et al.*, 1992; Kinnard *et al.*, 1994; Shapiro *et al.*, 1994; Wilde and Upshall, 1994; Sawyer *et al.*, 1995) and with the exception of endothelial cells, normal lung parenchyma has been maintained for up to 60 days (Siminski *et al.*, 1992). Furthermore, the maintenance of DNA and protein synthesis suggests that essential anabolic and catabolic processes are operational in this cultured lung slice system (Placke and Fisher, 1987a).

The MTT cytotoxicity assay has been shown to be a sensitive and reproducible indicator of viability in monolayer cell cultures (Mosmann, 1983; Denizot and Lang, 1986; Arnould *et al.*, 1993), and more recently, in cultured lung slices (Wilde and Upshall, 1994; Sawyer *et al.*, 1995). The present study, as well as other studies, have shown that potassium content and enzyme leakage assays are not good indicators of toxicity in cultured lung slices due to contamination by culture medium and entrapment in agarose, respectively (Stefaniak *et al.*, 1992; Fisher *et al.*, 1994).

Cell viability in control lung slices was maintained for the duration of the 8 day

incubation period as assessed by the MTT cytotoxicity assay and electron microscopy. However, numerous cytoplasmic vacuoles in various cell types were observed in lung slices incubated for 2 weeks suggesting that optimal conditions for incubation of hamster lung slices for longer than 8 days had not been achieved.

In the present study, type I cells appeared to be more susceptible to AM than were other cell types in the lung. At the earliest time examined (2 days), focal blebbing of type I cells was observed, which progressed to further cell damage and death by 8 days. Both swelling of type I cells (Cantor *et al.*, 1984) and proliferation of type II cells have been observed in animal models of AIPT (Cantor *et al.*, 1984; Heath *et al.*, 1985; Riva *et al.*, 1987) and in humans (Marchlinski *et al.*, 1982; VanZandwijk *et al.*, 1983; Cazzadori *et al.*, 1986; Dean *et al.*, 1987; Myers *et al.*, 1987). It is well known that type II cells proliferate and differentiate into type I cells in response to type I cell damage, as has been demonstrated in various kinds of chemically induced lung injury (Mason and Williams, 1991; Schneeberger, 1991).

As mentioned previously, AM has been shown to be directly cytotoxic to several lung cell types *in vitro* including fibroblasts, endothelial cells, type II cells, macrophages (Martin and Howard, 1985; Kachel *et al.*, 1990; Wilson and Lippmann, 1996) and most recently, Clara cells (Bolt *et al.*, 1997). In an *in vitro* study by Bolt and coworkers (1997) designed to examine differential lung cell susceptibility to AM, cell specific toxicity to AM was dependent on AM concentration in the incubation medium. Clara cells were the most susceptible cell type to AM toxicity at a lower AM concentration (50 μM) and alveolar macrophages were most susceptible at higher AM

concentrations (100 and 200 μM). However, differences in drug uptake by cells could not fully explain the relative cell susceptibilities to AM-induced cytotoxicity (Wilson and Lippmann, 1996; Bolt *et al.*, 1997). The susceptibility of type I cells to AM has not been addressed in *in vitro* studies most likely because other cell types such as macrophages and type II cells show more conspicuous changes, such as accumulation of phospholipid inclusion bodies (Reasor *et al.*, 1988).

Type I cell damage in AM treated lung slices observed by electron microscopy at 8 days, was not detected as a significant reduction in MTT formazan production. Thus, it appears that the MTT cytotoxicity assay was not sufficiently sensitive to detect a small amount of cell damage or death. Moreover, Type I cells comprise only 8.9% of the total cell population in rat lung (Crapo *et al.*, 1982). Thus, the MTT assay when used as a single indicator of cytotoxicity may result in the oversight of important toxicant effects, particularly cell-specific effects.

By 3 days, slices exposed to 200 μM AM contained approximately 11 μg AM per g lung. AM content in lung slices was not measured beyond 3 days, however, a trend toward AM accumulation in lung slices was demonstrated. It is likely that AM content increased with further incubation, as AM is known to accumulate in the lung and ranges from 20 to 734 μg/g (Haffajee *et al.*, 1983; Heger *et al.*, 1983; Holt *et al.*, 1983; Maggioni *et al.*, 1983; Plomp *et al.*, 1984; Brien *et al.*, 1987; Nalos *et al.*, 1987).

There was no evidence of fibrosis during incubation of cultured lung slices with AM for 2 weeks. However, incubation of lung slices with AM for a greater duration

would most likely be necessary for the development of fibrosis in this system. Although pulmonary fibrosis was discernible by 2 weeks in an *in vivo* hamster model of AIPT, marked deposition of collagen did not occur until 3 weeks post dosing (single intratracheal instillation) (Cantor *et al.*, 1984; Daniels *et al.*, 1989).

Incubation of cultured lung slices with 200 μM PQ also did not lead to fibrosis. It is likely that the massive cell necrosis produced by 200 μM PQ did not allow repair processes, including fibrosis, to occur. On the other hand, PQ at 10 μM, was not a high enough concentration to produce significant cell toxicity at 8 days. It is possible that a longer duration of incubation of lung slices with 10 μM PQ, a intermediate concentration between 10 and 200 μM PQ, or a shorter exposure to 200 μM PQ would eventually lead to the production of fibrosis. Fisher and Placke (1987) did not observe PQ-induced fibrosis in cultured hamster lung slices until 4 weeks of incubation. Other fibrogenic compounds (ie., bleomycin, asbestos and silica) produced interstitial fibrosis in cultured hamster lung slices following a 3-4 week incubation period (Placke and Fisher, 1987b; Fisher and Placke, 1988). The development of fibrosis in cultured lung slices suggests that inflammatory cell influx is not necessary for fibrosis to occur, but may modulate or exacerbate primary tissue damage (Fisher and Placke, 1988).

An increase in lung AM content in cultured lung slices may be attained by filling the lungs directly with AM and agarose instead of incubating slices in culture medium containing AM. This may also lead to accelerated development of cytotoxicity as well as fibrosis.

A significant reduction in MTT formazan production and electron microscopy

revealed epithelial cell necrosis in cultured lung slices treated with 200 μM PQ. The development of PQ-induced pulmonary toxicity is believed to be linked to its ability to redox cycle and produce oxidative stress (Bus and Gibson, 1984). The extensive lung damage produced by PQ treatment suggests that cultured hamster lung slices possess sufficient enzyme activity to catalyze the redox cycling of PQ. Hamster lung slices have recently been shown to possess the polyamine uptake system required for PQ transport into cells (Hoet *et al.*, 1995). Vacuolization and blebbing of alveolar type I and II cells observed in the present study were consistent with PQ mediated effects observed *in vivo* (Last, 1989). This damage progressed to extensive degeneration of most alveolar cells and loss of alveolar architecture.

In vivo studies have shown an induction of antioxidant enzyme activities following intratracheal AM administration to the hamster and, accordingly have suggested that oxidative stress has an initiating role to play in AIPT (Wang *et al.*, 1992; Leeder *et al.*, 1994). However, it is unknown whether the increase in lung antioxidant enzyme activities is attributed to an influx of inflammatory cells that occurs subsequent to AM treatment. Consequently, lung slices which are devoid of an inflammatory component were used to investigate the basis of the increase in antioxidant enzyme activities observed in the lung following intratracheal administration of AM to the hamster (Leeder *et al.*, 1994). Increased GSSG reductase activity was demonstrated in control lung slices as well as in slices incubated with 10 μM PQ and 200 μM AM. Thus, it is unknown whether oxidative stress was produced in lung slices exposed to AM or 10 μM PQ since even the control lung slices may have

been subjected to oxidative stress under these culture conditions. Electron microscopy, however, did not reveal any overt cell damage in control lung slices at 8 days. Alternatively, GSSG reductase activity may have been reduced during lung slice preparation and the elevation observed at 4 days may have been a consequence of restoration to normal "pre-culture" levels. Other studies of cultured lung slices have not included measurement of antioxidant enzyme activities, so it is unknown whether the apparent induction of antioxidant enzyme activity in control lung slices is unique to this study. Oxidative stress should have been minimized under the incubation conditions of the present study, since 95% air was used instead of 95% O_2.

The decrease in glutathione reductase activity present in slices incubated with 200 μM PQ can be attributed to cell death, since it coincided with a decrease in MTT formazan production as well as cell damage at the electron microscopic level.

Agarose instilled cultured rat lung slices possessed both Phase I and Phase II dependent biotransformation activities at 4 h (Price *et al.*, 1995a). It would be interesting to determine whether cultured hamster lung slices maintain these and other enzyme activities for prolonged periods of incubation. Many pulmonary toxicants must be converted to electrophiles and free radicals by biotransformation enzymes for toxicity to be manifested (Parkinson, 1996). Cultured lung slices could therefore serve as a valuable model for mechanistic studies involving pulmonary toxicants if biotransformation activities are maintained.

The utility of this system was assessed by both biochemical and morphological parameters. The cytotoxic responses of AM and PQ were similar to those observed in

other *in vitro* as well as *in vivo* models of toxicity. Although *in vivo* studies have indicated that the type I cell is damaged in AIPT, this cultured lung slice system demonstrated that the type I cell may be the earliest target for AIPT. Thus, cultured lung slices provide an alternative approach for the study of AIPT. However, their extended maintenance in culture requires further investigation.

CHAPTER 5

EFFECT OF *IN VITRO* AMIODARONE ON LUNG MITOCHONDRIAL RESPIRATION

5.1 INTRODUCTION

The mitochondrial electron transport chain releases free energy which is conserved in the form of the phosphate bond energy of ATP, an essential fuel for most cellular processes. The coupling of electron transport to ATP synthesis is referred to as oxidative phosphorylation. The respiratory chain of the inner mitchondrial membrane consists of four enzyme complexes which act as electron carriers to transfer electrons down the chain, ultimately resulting in the reduction of O_2 to H_2O (Fig. 5.1) and concomitantly pumping H^+ out of the mitochondrial matrix. The electrochemical H^+ gradient is harnessed to produce ATP by ATP synthase (Stryer, 1988).

Lipophilic basic drugs accumulate in lung mitochondria (Hori *et al.*, 1987). Accordingly, AM has been shown to accumulate in lung mitochondria (Hostetler *et al.*, 1988). However, the consequences of AM accumulation on mitochondrial function in the lung have not been examined.

In liver mitochondria, AM inhibited the tricarboxylic acid cycle and the respiratory chain, and uncoupled oxidative phosphorylation. Specifically, AM exerted a biphasic effect (stimulation followed by inhibition) on state 4 respiration of complexes I and II of the respiratory chain as well as an inhibitory effect on state 3 respiration (Fromenty *et al.*, 1990b). State 3 respiration refers to the respiratory rate in

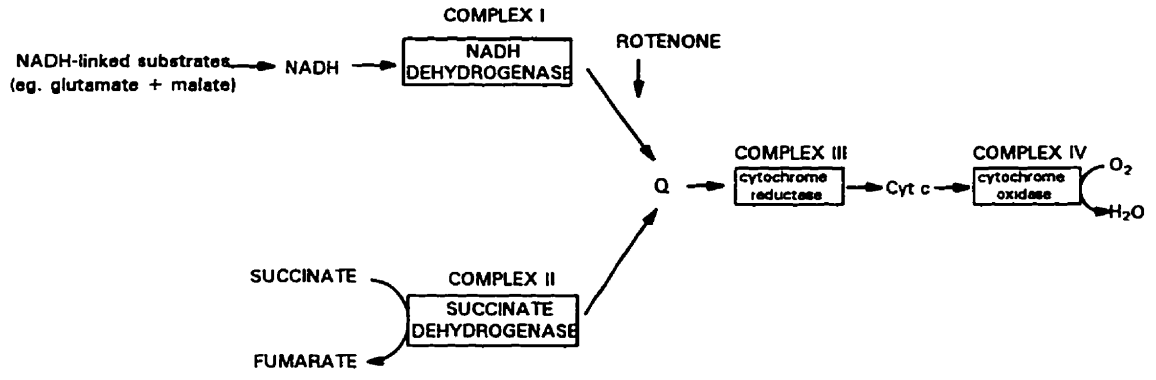

Fig. 5.1 Schematic representation of the mitochondrial electron transport chain. Q= ubiquinone or coenzyme Q, cyt c= cytochrome c

the absence of ADP and is also referred to as the resting rate (Nedergaard and Cannon, 1979). AM also inhibited the mitochondrial β-oxidation of fatty acids both *in vivo* and *in vitro,* effects that correlated with the production of microvesicular steatosis in mouse liver (Fromenty *et al.*, 1990a). AM also accumulated in liver mitochondria and produced a collapse of the mitochondrial membrane potential, resulting in ATP depletion (Fromenty *et al.*, 1990b). In human lymphocytes, AM-induced ATP depletion occurred prior to the onset of a loss in viability (Fromenty *et al.*, 1993).

Morphologically, AM produced mitochondrial swelling in isolated hepatocytes and lymphocytes prior to the onset of significant cytotoxicity (Gross *et al.*, 1989; Yashuda *et al.*, 1996). Glucose partially restored the depleted ATP and protected lymphocytes from AM toxicity (Fromenty *et al.*, 1993). Niacin treatment has also been shown to partially ameloriate AM-induced pulmonary fibrosis. Although the mechanism of niacin protection against AIPT is currently unknown, it has been suggested to exert protective effects by maintaining lung NAD and/or ATP levels (Wang *et al.*, 1991; O'Neill and Giri, 1994).

The purpose of this preliminary study was to determine whether AM produces lung mitochondrial dysfunction at the level of complexes I and II of the respiratory chain. Specifically, the objectives of this study were to determine the effects of AM on: 1) state 4 of complex I of the respiratory chain; and 2) state 4 of complex II of the respiratory chain.

5.2 MATERIALS AND METHODS

5.2.1 Chemical sources

Chemicals were obtained as follows: ethylene glycol-bis-(β-aminoethyl ether)N,N,N',N'-tetraacetic acid (EGTA), 3-[N-morpholino]propanesulfonic acid (MOPS), D-mannitol, L-glutamate (monosodium salt), L(-) malate (monosodium salt), succinate (disodium salt, hexahydrate), rotenone (95-98%), adenosine 5'-diphosphate (ADP, free acid), antimycin A (*Streptomyces* sp.) and fatty acid free bovine serum albumin from Sigma Chemical Co., St. Louis, MO. All other chemicals were of reagent grade and obtained from common commercial suppliers.

5.2.2 Animals

Male golden Syrian hamsters (140-160g) were obtained and cared for as described in Section 2.2.2.

5.2.3 Preparation of isolated lung mitochondria

Mitochondria were isolated by differential centrifugation as described by Fisher *et al.* (1973). Solutions were kept ice cold and procedures for mitochondrial preparation were performed at 4°C. Hamsters were killed by pentobarbital injection (300 mg/kg ip). The thoracic cavity was exposed and the lungs were perfused *in situ* with ice-cold isotonic saline (0.9 % NaCl) via the pulmonary artery. Following removal of blood, lungs were excised, rinsed in 0.9% NaCl, blotted dry and weighed. Extrapulmonary tissue was removed and the lungs were minced with scissors and

homogenized (homogenization buffer: 225 mM mannitol, 75 mM sucrose, 20 mM EGTA, pH 7.2 plus 5 mM MOPS and 2% fatty acid free BSA) (4.0 ml/g tissue, wet weight) by using a motorized Potter-Elvehjem® teflon pestle-glass tube homogenizer. The homogenate was centrifuged at 1300 x g for 5 min, the supernatant was collected and centrifuged at 13 000 x g for 10 min to precipitate the mitochondrial pellet. The resultant pellet was washed twice with approximately half of the original volume of homogenization buffer (excluding MOPS and BSA) and centrifuged (13 000 x g, 10 min). The final pellet was gently resuspended in 0.35 ml homogenization buffer using a teflon pestle and glass homogenization tube (manual) and kept on ice until measurement of oxygen consumption. Mitochondrial protein concentration was determined by the method of Lowry *et al.* (1951) and ranged from 10-15 mg/ml. This method typically yielded 10-15 mg of mitochondrial protein from 8 hamster lungs.

5.2.4 Polarographic measurement of oxygen consumption

Oxygen consumption was measured using a biological oxygen monitor (Model 5300) connected to a chart recorder (Fisher Recordall Series 5000) and a Clark-type polarographic oxygen electrode (Model 5331) (Yellow Springs Instrument Co., Inc., Yellow Springs, OH). Sample chambers were mounted in a 4 chamber standard water-jacketed bath assembly (Model 5301). The electrode was immersed in a magnetically stirred sample chamber containing respiratory buffer (145 mM KCl, 5 mM KH_2PO_4, 20 mM Tris-Cl, pH 7.2) (Fisher *et al.*, 1973) saturated with room air and maintained at 30°C using a circulating waterbath.

Lung mitochondrial protein (1.0-1.5 mg protein) was added to 3.0 ml respiratory buffer. Respiration at complex I was assessed by using glutamate (5 mM) and malate (5 mM) as substrates. Respiration at complex II was assessed by using succinate (10 mM final concentration, 50 μl) as a substrate. Rotenone (3 μM final concentration, 50 μl of 0.2 mM in 3% ethanol), was added to block electron flow from complex I of the mitochondrial oxidative phosphorylation system to ubiquinone. To test the effect of AM on state 4 respiration of complexes I and II, AM (15-30 μl of 12.5 or 50 mM stock solution in distilled H_2O) was added to the medium at a final concentration of 50-400 μM, at least 2 min following the total expenditure of 0.2 mM ADP (50 μl).

The respiratory control ratio (RCR) was calculated as the ratio of the respiratory rate (rate of oxygen consumption) in the presence of added ADP (state 3) to the rate subsequently obtained when added ADP is consumed (state 4). This ratio assesses the coupling of electron transport to the phosphorylation of ADP (Fromenty *et al.*, 1993). The ADP:O ratio was calculated as the total amount of ADP added, divided by the total amount of oxygen consumption during state 3 respiration (Nedergaard and Cannon, 1979). State 3 and state 4 respiration rates were expressed as nmol atomic oxygen consumed/min/mg mitochondrial protein.

5.2.5 Statistical analysis

The results were expressed as $\bar{x} \pm$ SD. Group means were analyzed by the unpaired Student's t test. Differences were considered statistically significant when

$p<0.05$.

5.3 RESULTS

5.3.1 Effect of AM on complex I state 4 respiration

Respiration at complex I was examined by using glutamate and malate as substrates. AM (50-400 μM) stimulated state 4 respiration. However, at higher concentrations (200 and 400 μM), this initial stimulation of state 4 was followed by inhibition. These effects were observed in mitochondria with a relatively high RCR (ie., tightly coupled mitochondria, RCR=2.80 $\pm$ 0.14, n=3) (Fig. 5.2). AM solely induced inhibition of state 4 respiration in mitochondria with an RCR of 2.06 $\pm$ 0.18 (n=3). This inhibition occurred at all concentrations of AM (100-400 μM) tested. Fifty μM AM did not appear to have an affect on respiration in mitochondria with lower RCRs (ie. non-tightly coupled mitochondria) (Fig. 5.3).

5.3.2 Effect of AM on complex II state 4 respiration

Succinate supported state 4 respiration was stimulated by all concentrations of AM tested (50-400 μM). At 200 and 400 μM AM, the initial stimulatory effect was followed by a progressive decrease in the respiratory rate, culminating in its inhibition (Fig. 5.4). The stimulatory effect was observed in mitochondria with an RCR of 2.63 (n=1). In contrast, only inhibition was produced by AM (50-400 μM) in mitochondrial preparations with lower RCRs (1.33 $\pm$ 0.16, n=6) (Fig. 5.5).

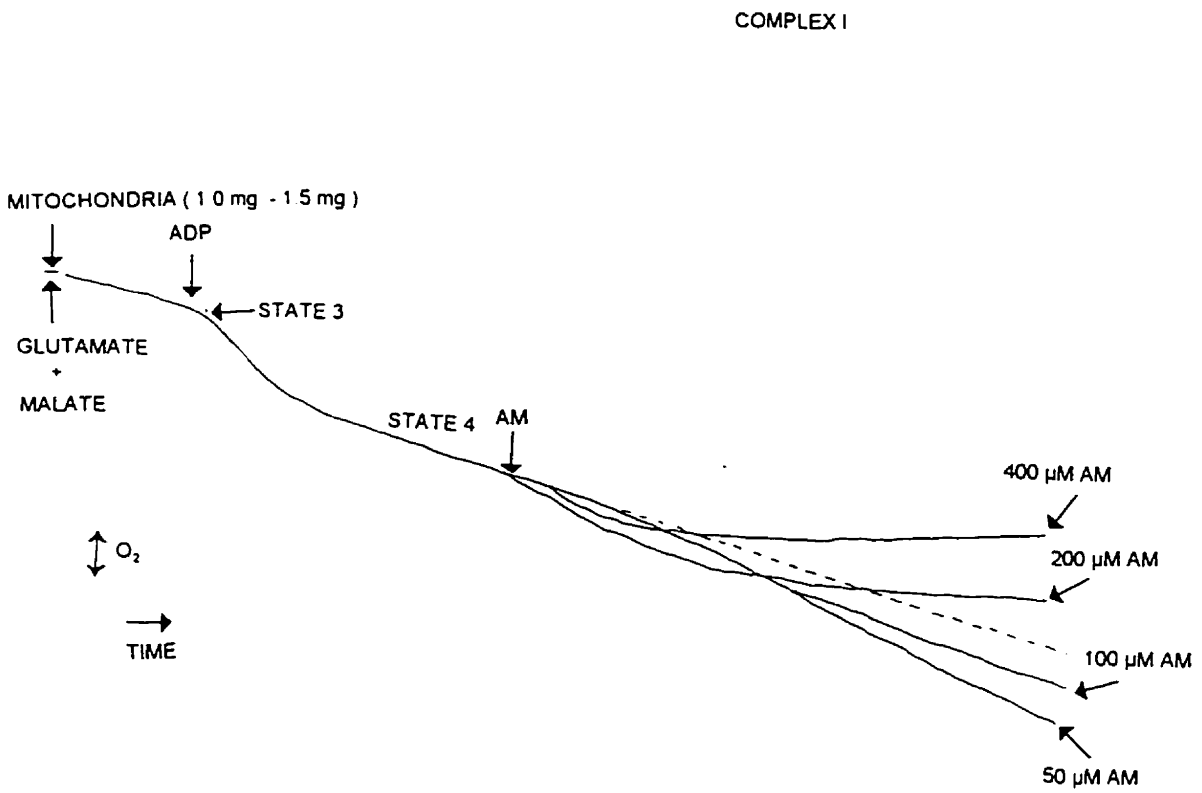

Fig. 5.2 Effects of various concentrations of AM on state 4 respiration supported by glutamate and malate. Hamster lung mitochondria (1.0-1.5 mg protein) with RCR=2.74 were incubated in respiration buffer containing glutamate (5 mM) and malate (5 mM), followed by the addition of ADP. AM was added at least 2 min following the total expenditure of 0.2 mM ADP. Tracing represents the oxygen consumption obtained with different concentrations of AM superimposed on the figure.

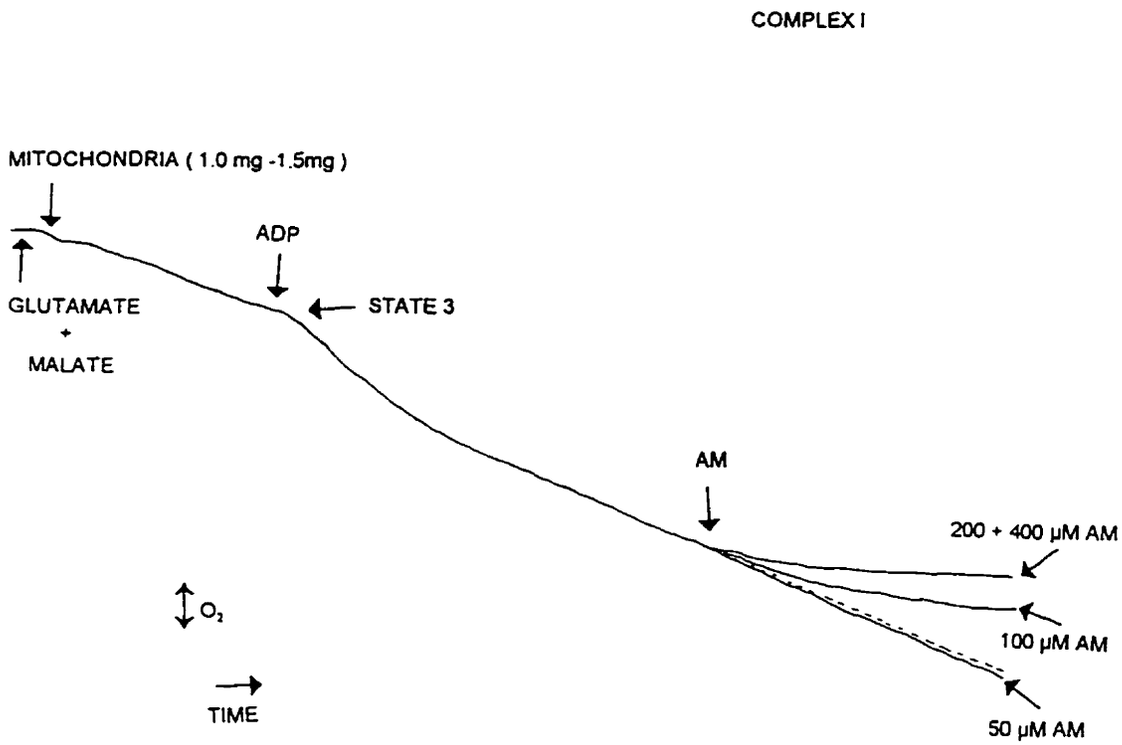

Fig. 5.3 Effects of various concentrations of AM on state 4 respiration supported by glutamate and malate. Hamster lung mitochondria (1.0-1.5 mg protein) with RCR=2.24 were incubated in respiration buffer containing glutamate (5 mM) and malate (5 mM), followed by the addition of ADP. AM was added at least 2 min following the total expenditure of 0.2 mM ADP. Tracing represents the oxygen consumption obtained with different concentrations of AM superimposed on the figure.

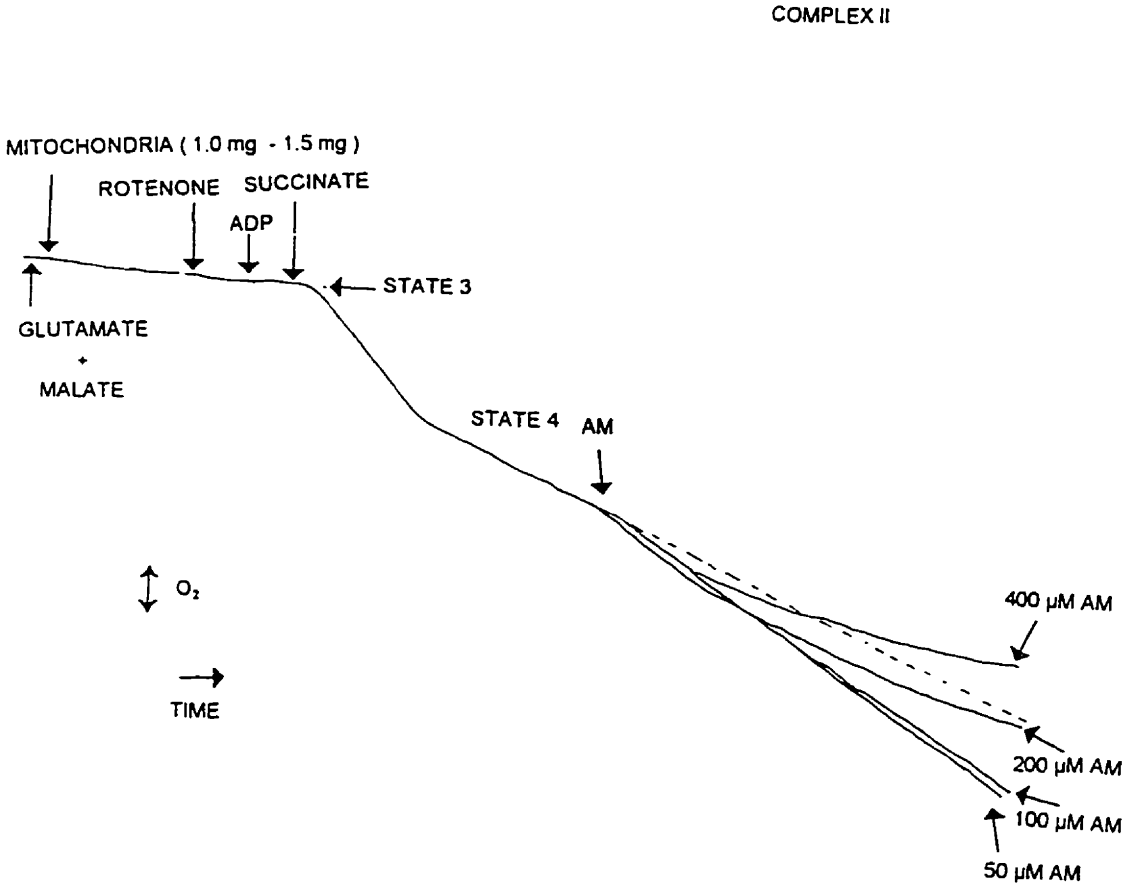

Fig. 5.4 Effects of various concentrations of AM on state 4 respiration supported by succinate. Hamster lung mitochondria (1.0-1.5 mg protein) with RCR= 2.63 were incubated in respiration buffer containing succinate (10 mM), followed by the addition of ADP. AM was added at least 2 min following the total expenditure of 0.2 mM ADP. Tracing represents the oxygen consumption obtained with different concentrations of AM superimposed on the figure.

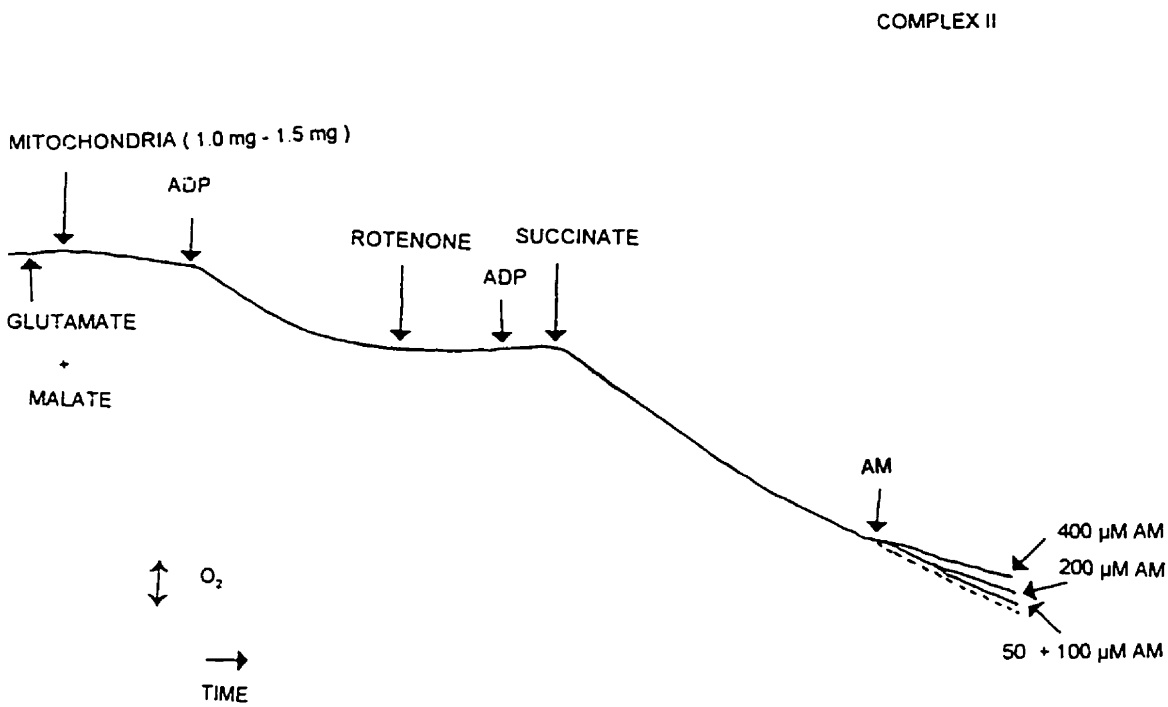

Fig. 5.5 Effects of various concentrations of AM on state 4 respiration supported by succinate. Hamster lung mitochondria (1.0-1.5 mg protein) with RCR = 1.36 were incubated in respiration buffer containing succinate (10 mM), followed by the addition of ADP. AM was added at least 2 min following the total expenditure of 0.2 mM ADP. Tracing represents the oxygen consumption obtained with different concentrations of AM superimposed on the figure.

5.3.3 Respiratory rate and oxidative phosphorylation of hamster lung mitochondria

RCRs were used to assess the tightness of coupling (ie., coupling of electron transport to the phosphorylation of ADP) in each lung mitochondrial preparation. It was difficult to isolate hamster lung mitochondria with high RCRs for both complexes I and II. However, the success rate with complex I was higher than with complex II. In addition, the likelihood of isolating mitochondrial fractions with high RCRs from liver was greater than isolation from lung.

Both the stimulatory and inhibitory effects of AM were observed at complex I of the respiratory chain in tightly coupled mitochondrial fractions which possessed significantly greater RCR and ADP:O values than non tightly coupled mitochondria (Table 5.1). Respiration rates of states 3 and 4 did not differ between tightly coupled and non-tightly coupled mitochondrial preparations.

At complex II, only one experiment was conducted in which AM exerted its biphasic effect on respiration. Therefore, statistical analysis could not be performed to compare differences between tightly coupled and non-tightly coupled mitochondrial fractions.

Table 5.1 State 3 and state 4 respiration rates, respiratory control and ADP/O ratios in hamster lung mitochondria (no AM treatment).

Complex I	state 3	state 4	RCR	ADP/O
tightly coupled	87.9 ± 24.6	32.2 ± 9.1	2.80 ± 0.14*	4.63 ± 0.25*
non-tightly coupled	86.1 ± 15.4	43.0 ± 2.9	2.06 ± 0.18	3.40 ± 0.46
Complex II	state 3	state 4	RCR	ADP/O
tightly coupled	134.5 ± 23.6	51.5 ± 8.5	2.63 ± 0.36	2.50 ± 0.30
non-tightly coupled	96.9 ± 7.7	73.5 ±10.5	1.33 ± 0.16	2.28 ± 0.41

state 3 and state 4 respiration rates are expressed as nmol atomic oxygen consumed/min/mg mitochondrial protein

Complex I (n=3)
* indicates significant difference from non-tightly coupled mitochondria (unpaired Student's t test, $p<0.05$)

Complex II (n=1) (tightly coupled) and n=6 (non-tightly coupled)

5.4 DISCUSSION

AM exerted a biphasic effect on state 4 respiration at complexes I and II of the respiratory chain when lung mitochondria were tightly coupled (ie. higher RCRs). AM initially stimulated state 4 respiration at all concentrations tested and then inhibited state 4 respiration at higher concentrations. These results are similar to the effects of AM observed in liver mitochondria (Fromenty *et al.*, 1990b). AM was proposed to stimulate respiration by acting as an uncoupler, a substance which dissipates the proton-motive force by transporting protons across the inner mitochondrial membrane into the mitochondrial matrix. These investigators suggested that AM (pK_a 6.6), a lipophilic molecule that is partly protonated in the incubation medium (or in the cytosol), enters mitochondria by diffusion along the mitochondrial membrane potential, as do many other lipophilic cationic amines (Garlid and Nakashima, 1983). Protonated AM then dissociates into a proton and uncharged AM in the relatively alkaline mitochondrial matrix. As a result, AM accumulates in the mitochondria at concentrations higher than in the incubation medium. The protonophoric effect of protonated AM has an uncoupling effect resulting in increased oxygen consumption. The secondary inhibitory effect was explained by the progressive entry of AM into the mitochondria, which leads to its accumulation in the inner membrane and in the matrix, subsequently resulting in the inhibition of the respiratory chain (Fromenty *et al.*, 1990b).

AM at lower concentrations (50 and 100 μM) did not produce an inhibitory effect, possibly due to insufficent accumulation of AM in the mitochondria or an insufficient time period to allow adequate drug accumulation to occur. At these lower

concentrations, however, AM directly inhibited the β-oxidation of fatty acids in liver mitochondria (Fromenty *et al.*, 1990a).

AM did not have an initial stimulatory effect on state 4 respiration in isolated lung mitochondrial fractions with lower RCRs. This difference is likely attributable to the inability to observe the uncoupling effect of AM in mitochondrial preparations that are not tightly coupled. Therefore, only AM's inhibitory effect on the respiratory chain is observed.

In this study, it was much easier to obtain tightly coupled (ie., high RCRs) liver mitochondria as compared to lung mitochondria. The coupling of respiration to phosphorylation is lost when the integrity of the mitochondrial inner membrane is disrupted. Other researchers have stated that tightly coupled lung mitochondria are more difficult to isolate than liver mitochondria (Reiss, 1966). Fisher *et al.* (1973) suggested that the isolation of lung mitochondrial fractions posed difficulties due to the collagenous nature of lung tissue and the high tissue content of lipids and lysosomal enzymes which often contaminate mitochondrial fractions. Thus, isolated lung mitochondrial fractions may be less pure than liver mitochondria (Spear and Lumeng, 1978) and prone to damage and degradation during isolation. Nonetheless, some investigators were able to isolate mitochondria-rich fractions from lung with reproducible rates of substrate oxidation and RCRs (Fisher *et al.*, 1973; Spear and Lumeng, 1978; Rossouw and Engelbrecht, 1987). However, lung mitochondrial RCRs for glutamate and succinate supported respiration varied remarkably both within and among species. RCRs for glutamate plus malate and succinate supported respiration

concentrations, however, AM directly inhibited the β-oxidation of fatty acids in liver mitochondria (Fromenty *et al.*, 1990a).

AM did not have an initial stimulatory effect on state 4 respiration in isolated lung mitochondrial fractions with lower RCRs. This difference is likely attributable to the inability to observe the uncoupling effect of AM in mitochondrial preparations that are not tightly coupled. Therefore, only AM's inhibitory effect on the respiratory chain is observed.

In this study, it was much easier to obtain tightly coupled (ie., high RCRs) liver mitochondria as compared to lung mitochondria. The coupling of respiration to phosphorylation is lost when the integrity of the mitochondrial inner membrane is disrupted. Other researchers have stated that tightly coupled lung mitochondria are more difficult to isolate than liver mitochondria (Reiss, 1966). Fisher *et al.* (1973) suggested that the isolation of lung mitochondrial fractions posed difficulties due to the collagenous nature of lung tissue and the high tissue content of lipids and lysosomal enzymes which often contaminate mitochondrial fractions. Thus, isolated lung mitochondrial fractions may be less pure than liver mitochondria (Spear and Lumeng, 1978) and prone to damage and degradation during isolation. Nonetheless, some investigators were able to isolate mitochondria-rich fractions from lung with reproducible rates of substrate oxidation and RCRs (Fisher *et al.*, 1973; Spear and Lumeng, 1978; Rossouw and Engelbrecht, 1987). However, lung mitochondrial RCRs for glutamate and succinate supported respiration varied remarkably both within and among species. RCRs for glutamate plus malate and succinate supported respiration

transport chain resulting in the reduction of AM to an AM radical, as has been shown to occur with CCl_4 in isolated rat liver mitochondria (Tomasi *et al.*, 1987). Electron leakage may also occur via the mitochondrial CYP450 system, another site of electron transport (Kubow *et al.*, 1985; Davies, 1995). The free radical could then destroy proteins or initiate LPO. Since complexes III and IV were unaffected by AM in liver mitochondria, it is likely that AM may also produce a specific effect in lung mitochondria.

AM has been reported to accumulate in isolated rat lung mitochondria (Hostetler *et al.*, 1988). Several other lipophilic basic drugs (eg., imipramine, quinine, chlorphentermine) have been shown to accumulate in rat lung mitochondria (Minchin *et al.*, 1978; Hori *et al.*, 1987). The accumulation of these drugs in the lung can be predicted on the basis of their mitochondrial binding (Hori *et al.*, 1987). However, drug accumulation in lung mitochondria alone is not sufficient to produce the cell injury that progresses to pneumonitis and pulmonary fibrosis characteristic of AIPT.

Chlorphentermine, like AM, is an uncoupler of oxidative phosphorylation. Chlorphentermine treatment of rats stimulated state 4 respiration and reduced the RCR and the ADP:O ratio, but did not affect respiration in state 3 and the uncoupled state at complexes I and II of lung mitochondria (Zychlinski *et al.*, 1983). This anorectic drug also binds to mitochondria (Minchin *et al.*, 1978) and disrupts mitochondrial membranes (Zychlinski *et al.*, 1983). Interestingly, chlorphentermine, like AM, is a cationic amphiphilic amine which also produces phospholipidosis in the lung. Chlorphentermine may produce its effects on specific components of the mitochondrial

respiratory chain. Alternatively, alterations in membrane lipids may be induced which may have led to the observed changes in mitochondrial structure and function (Zychlinski *et al.*, 1983).

In the liver, AM also reduced state 3 respiration at complexes I and II of the mitochondrial respiratory chain. However, AM did not alter respiration at complexes III and IV (Fromenty *et al.*, 1990b). It would be interesting to determine the effects of AM on state 3 respiration and on complexes III and IV of the lung mitochondrial respiratory chain. Thus, the specificity of AM with respect to its actions on the different mitochondrial complexes could be resolved.

In conclusion, AM has a biphasic effect on state 4 respiration in tightly coupled lung mitochondria. This biphasic effect is also observed in liver mitochondria. AM affects the transfer of electrons to, in or from complexes I and II. The relationship of these mitochondrial alterations to mitochondrial structure and function, and their relationship to cell death and AIPT remain to be determined.

CHAPTER 6

GENERAL DISCUSSION AND FUTURE DIRECTIONS

6.1 GENERAL DISCUSSION

The keto oxygen of AM was proposed to be a key site for free radical formation and the production of AIPT (Bennett *et al.*, 1987). However, the present study demonstrated that this structural component of the AM molecule is not a critical determinant of AIPT since DOAM, a derivative of AM lacking this group also produced pulmonary toxicity including fibrosis in the hamster (Chapter 2). If AM-derived free radicals were involved in AIPT, it was likely that generation of free radicals at a site(s) other than the keto oxygen played an important role in the production of AIPT.

The ESR spin trapping study demonstrated that incubation of AM with pulmonary or hepatic microsomes resulted in the generation of a free radical. Based on the hfsc's and the chemical structure of AM, the PBN-free radical adduct was most consistent with a carbon-centred phenyl radical, which was likely to be derived from the AM molecule. DOAM and DEA were also capable of generating free radicals possessing hfsc's that were very similar to the free radical generated by AM (Chapter 3). Interestingly, both these agents also produce pulmonary toxicity, including fibrosis. Thus, a free radical mechanism may be involved in the production of pulmonary toxicity by AM, DEA and DOAM. However, a direct correlation between free radical production and pulmonary toxicity has yet to be established.

The type I alveolar cell was an early target of AM toxicity in cultured hamster lung slices (Chapter 4). Type I cell damage has previously been observed in *in vivo* animal models of AIPT as well as in humans with AIPT. However, ultrastructural time course studies have not been performed prior to inflammation in order to determine the earliest target cell of AM-induced toxicity *in vivo*. Certain populations of cells such as type I cells and pulmonary capillary endothelial cells appear to be susceptible to oxidant injury (Martin, 1991). Both these cell types are targets of bleomycin and butylated hydroxytoluene (BHT). BHT, a food preservative has been suggested to induce pulmonary toxicity via the formation of a highly reactive, electrophilic quinone methide metabolite and a phenoxy radical(Witschi *et al.*, 1989). Bleomycin, a chemotherapeutic agent, releases hydroxyl radicals and other ROS following ternary complex formation with DNA, Fe^{2+} and O_2 (Hay *et al.*, 1991). If free radical generation plays an important role in AIPT *in vivo*, it is possible that AM-generated radicals may preferentially target the type I cell. It is unlikely, however, that the type I cell would be involved in the production of this radical because it possesses relatively small amounts of endoplasmic reticulum. On the other hand, type II cells possess relatively more endoplasmic reticulum (Simon, 1992). If a free radical mechanism is involved in AIPT, it may lead to the production of LPO. The release of toxic products of LPO may damage other cell types. The type I cell may be preferentially susceptible to AM toxicity compared to other cell types in the lung because it possesses low detoxification capabilities. Indeed, the type I cell possesses low antioxidant enzyme activities compared to the type II cell (Forman and Fisher,

1981).

In a preliminary study, AM stimulated and subsequently inhibited state 4 respiration in hamster lung mitochondria *in vitro* (Chapter 5). Fromenty and coworkers (1990b) observed the stimulatory effect of AM on liver mitochondrial respiration and suggested that it was induced by uncoupling of oxidative phosphorylation. Uncoupling of oxidative phosphorylation was thought to be due to a protonophoric effect of AM, leading to the entry of its protonated form into the mitochondria (Fromenty *et al.*, 1990b). Protons are then released from the AM molecule due to the relatively basic milieu of the mitochondria. The entry of protons in this manner leads to the uncoupling effect of AM. Inhibition of mitochondrial oxygen consumption that occurred subsequent to the uncoupling of oxidative phosphorylation may be due to either an effect of the parent AM molecule itself or due an AM free radical generated *in situ*. The donation of an electron to AM from electron transport sites in the mitochondria may result in the generation of a free radical.

In conclusion, this research was the first to demonstrate that DOAM is a toxic derivative of AM *in vivo*. More importantly, the keto oxygen was not a critical factor in the development of AIPT. This research also provided the first direct evidence for an AM generated free radical in biological tissue. The free radical behaved very similarly to a carbon centred phenyl radical. Furthermore, the type I cell, which has been shown to susceptible to different kinds of free radical mediated toxicity, was also a target for AM toxicity in cultured hamster lung slices. A preliminary investigation also revealed for the first time, that AM inhibits lung mitochondrial respiration. It is

possible that AM may be inhibiting lung mitochondrial function by a free radical mechanism. Further investigation based on these findings is necessary to determine whether the free radical generated by AM is involved in the production of AIPT. If the free radical mechanism is involved in AIPT, is it an initiating mechanism?

6.2 FUTURE DIRECTIONS

6.2.1 Cultured hamster lung slices and AIPT

Cultured hamster lung slices were shown to be a valuable model for the study of AIPT. It would be advantageous to maintain lung slices in culture for a longer duration, if possible, for at least 4 weeks to determine whether fibrosis can be produced by AM in this system. The cause of the elevation in GSSG reductase activity in control lung slices needs to be determined. The possible role of oxidative stress could be confirmed in this system by the measurement of total glutathione (GSH and GSSG).

Cells containing several cytoplasmic vacuoles as well as type II cell spreading were evident in hamster lung slices maintained in culture for 2 weeks. Thus, it is necessary to improve culture conditions such that these ultrastructural alterations do not occur, if cultures are to be maintained for prolonged periods.

Since type I cells were selectively damaged by AM in the cultured lung slice system, it would be interesting to conduct an electron microscopic time course study to thoroughly examine the alterations produced in the type I cell *in vivo*.

6.2.2 An ESR spin trapping study of AIPT

The structural identity of the free radicals generated by AM, DEA and DOAM remains to be elucidated. Structural identification requires chromatographic separation to isolate the PBN spin adduct of interest, followed by mass spectrometry. Preliminary experiments showed that the PBN-free radical adduct of interest can be separated by HPLC (Chapter 3). The use of deuterated PBN can aid in mass spectral analysis since the masses of the parent ion and/or fragment peaks increase by the amount of deuteration (ie., an increase of 14 for PBN-d_{14} (both phenyl and *tert*-butyl deuteration)). Identification of the free radical would allow a better understanding of the mechanisms of generation of free radicals as well as their role in pulmonary toxicity. Since it has been proposed that AM can gain an electron to form a free radical, it would be interesting to determine whether free radicals are produced in lung mitochondria incubated with AM. Mitochondria are major sites of electron transport processes, both via the mitochondrial CYP450 system and the respiratory chain, from which electron leakage can occur (Kubow *et al.*, 1985; Davies, 1995). Also, a comparison of the characteristics of the free radical generated by UV irradiation of an AM solution with those of the free radical generated in microsomes and possibly mitochondria would provide additional information on the types of radicals generated by different mechanisms.

Addition of glutathione or cysteine, both thiol containing compounds, or vitamin E to a system containing AM-generated free radicals could be performed to determine their abilities to affect radical levels. PBN and other nitrones have been used

to prevent or reduce the damage produced by radicals in biological systems (Wells *et al.*, 1989). The role of free radicals in AIPT would be further defined by determining whether AM-induced toxicity could be prevented in lung cells that are also incubated with PBN.

6.2.3 The mitochondrion as a target organelle in AIPT

A comprehensive investigation of the mitochondrion as a target organelle in AIPT is warranted. Preliminary results have shown that AM uncouples phosphorylation and inhibits state 4 respiration at complexes I and II of the respiratory chain. The effects of AM on state 3 respiration of complexes I and II should also be determined. In addition, the effects of AM on complexes III and IV of the mitochondrial respiratory chain have yet to be examined.

Tetraphenylboron, a lipophilic anion which favours the mitochondrial uptake of lipophilic cationic amines (Garlid and Nakashima, 1983), has been shown to form an ion pair with AM and increase AM entry into liver mitochondria (Fromenty *et al.*, 1990b). It would be worthwhile to determine whether AM accumulates in hamster lung mitochondria and whether tetraphenylboron increases its uncoupling effect and its entry into the mitochondria. Further experimentation would determine whether mitochondrial AM accumulation was associated with a decrease in the mitochondrial membrane potential and an inhibition of ATP synthesis.

If a free radical(s) was detected in isolated lung mitochondria incubated with AM (as discussed in section 6.2.2), then the ability of AM to induce mitochondrial

lipid peroxidation, protein oxidation or binding via free radical production could be examined. Following an investigation of the effects of AM on the various components of mitochondrial function, it will be crucial to determine whether mitochondrial dysfunction and subsequent loss of ATP occurs prior to lung cell death. If mitochondrial dysfunction proves to be instrumental in AIPT, then the effects of various agents that act to maintain cell ATP levels should be determined in an *in vivo* model of AIPT.

REFERENCES

Adams, P.C., Gibson, G.J., Morley, A.R., Wright, A.J., Corris, P.A., Reid, D.S. and Campbell, R.W.F. (1986). Amiodarone pulmonary toxicity: clinical and subclinical features. Quarterly J. Med. 59(229): 449-71.

Adams, G.D., Kehoe, R.F., Lesch, M. *et al.* (1988). Amiodarone induced pneumonitis: assessment of risk factors and possible risk reduction. Chest 93: 254-63.

Adamson, I.Y.R. and Bowden, D.H. (1975). Reaction of cultured adult and fetal lung to prednisolone and thyroxine. Arch. Pathol. 99: 80-85.

Akoun, G.M., Gauthier-Rahman, S., Milleron, B., Perrot, J. and Mayaud, C. (1984). Amiodarone-induced hypersensitivity pneumonitis. Chest 85: 133-135.

Akoun, G.M., Cadranel, J.L., Blanchette, G., Milleron,B.J. and Mayaud, C.M. (1991). Bronchoalveolar lavage cell data in amiodarone-associated pneumonitis: evaluation in 22 patients. Chest 99: 1177-1182.

Altman, F.P. (1976). Tetrazoliums and formazans. Progr. Histochem. Cytochem. 9(3): 1-56.

Anastasiou-Nana, M., Levis, G.M. and Moulopoulos, S. (1982). Pharmacokinetics of amiodarone after intravenous and oral administration. Int. J. Clin. Pharmacol. Ther. Toxicol. 20: 524-529.

Anderson, K.P., Walker, R., Dustman, T., Lux, R.L., Ershler, P.R., Kates, R.E. et al. (1989). Rate-related electrophysiologic effects of long-term administration of amiodarone on canine ventricular myocardium *in vivo*. Circulation 79: 948-958.

Andreasen, F., Agerbaek, H., Bjerregaard, P. and Gotzsche, H. (1981). Pharmacokinetics of amiodarone after intravenous and oral administration. Eur. J. Clin. Pharmacol. 19: 293-299.

Antonini, J.M., McCloud, C.M. and Reasor, M.J. (1994). Acute silica toxicity: attenuation by amiodarone-induced pulmonary phospholipidosis. Environ. Health Perspect. 102: 372-378.

Antunes-Madeira, M.C., Videira, R.A., Kluppel, M.L.W. and Madeira, V.V.M.C. (1995). Amiodarone effects on membrane organization evaluated by fluoresence polarization. Int. J. Cardiol. 48: 211-18.

Arnould, R., Dubois, J., Abikhalil, F., Libert, A., Ghanem, G., Atassi, G., Hanocq,

M. and Lejeune, F.J. (1990). Comparison of two cytotoxicity assays- Tetrazolium derivative reduction (MTT) and tritiated thymidine uptake-on three malignant mouse cell lines using chemotherapeutic agents and investigational drugs. Anticancer Res. 10: 145-154.

Aust, S.D., Chignell, C.F.., Bray, T.M., Kalyanaraman, B. and Mason, R.P. (1993). Contemporary issues in toxicology. Toxicol.Appl. Pharmacol. 120:168-178.

Bassett, D.J.P., Elbon, C.L. and Reichenbaugh, S.S. (1992). Respiratory activity of lung mitochondria isolated from oxygen-exposed rats. Am. J. Physiol. 263(Lung Cell. Mol. Physiol. 7): L439-445.

Bast, A., Guido, R., Haenen, M. and Doelman, C.J.A. (1991). Oxidants and antioxidants: State of the art. Am. J. Med. 91(suppl 3C): 2S-12S.

Baudin, B., Beneteau-Burnat, B. and Giboudeau, J. (1996). Cytotoxicity of amiodarone in cultured human endothelial cells. Cardiovasc. Drugs Therapy 10: 557-560.

Beddows, S.A., Page, S.R., Taylor, A.H., McNerney, R., Whitley, G.S., Johnstone, A.P. and Nussey, S.S. (1989). Cytotoxic effects of amiodarone and desethylamiodarone on human thyrocytes. Biochem. Pharmacol. 38: 4397-4403.

Bellomo, 1991 Cell damage by oxygen free radicals. Cytotechnol. 5: S71-73.

Bennett, P.B., Kabalka, G.W., Kennedy, T.P., Woosley, R.L. and Hondeghem, L.M. (1987). An amiodarone derivative with reduced toxicity and Na-channel blocking properties. Circulation 76: VI-150.

Bennett, P.B., Valenzuela, C. and Hondeghem, L.M. (1989). Modulation of cardiac Na, Ca and K currents by amiodarone and des-oxo-amiodarone. Biophys. J. 55: 295a.

Blake, T.L. and Reasor, M.J. (1995). Acute pulmonary inflammation in hamsters following intratracheal administration of amiodarone. Inflammation 19(1): 55-65.

Blake, T.L. and Reasor, M.J. (1996). Pulmonary responses to amiodarone in hamsters: comparison of intratracheal and oral administrations. Toxicol. Appl. Pharmacol. 131: 325-331.

Bolt, M.W., Racz, W.J., Brien, J.F., Bray, T.M. and Massey, T.E. (1997). Differential susceptibilities of isolated hamster lung cell types to amiodarone cytotoxicity. (manuscript submitted for publication)

Bonati, M., Gaspari, F., D'Aranno, V., Benfenati, E., Neyroz, P., Galletti, F. and Tognoni, G. (1983). Physicochemical and analytical characteristics of amiodarone. J. Pharm. Sci. 73: 829-31.

Borg, D.C. (1976). Applications of electron spin resonance in biology. In: Free radicals in biology, Vol. 1, pp 69, Pryor, W.A., ed., Academic Press, New York.

Boyd, M. (1984). Metabolic activation and lung toxicity: A basis for cell-selective pulmonary damage by foreign chemicals. Environ. Health. Perspec. 55: 47-51.

Bray, T.M. and Kubow, S. (1985). Involvement of free radicals in the mechanism of 3-methylindole-induced pulmonary toxicity: and example of metabolic activation in chemically induced lung disease. Environ. Health Perspect 64: 61.

Brent,J.A. and Rumack, B.H. (1993). Role of free radicals in toxic hepatic injury. I. Free radical biochemistry. Clin. Toxicol. 31(1): 139-171.

Brien, J.F., Jimmo, S., Brennan, F.J., Ford, S.E. and Armstrong, P.W. (1987). Distribution of amiodarone and its metabolite, desethylamiodarone in human tissues. Can J. Physiol. Pharmacol. 65: 360-4.

Brien, J.F., Jimmo, S., Brennan, F.J., Armstrong, P.W. and Abdollah, H. (1990). Disposition of amiodarone and its proximate metabolite, desethylamiodarone in the dog for oral administration of single-dose and short-term drug regimens. Drug Metab. Dispos. 18: 846-51.

Bus, J.S. and Gibson, J.E. (1984). Paraquat: Model for oxidant-initiated toxicity. Environ. Health Perspec. 55: 37-46.

Cairns, J.A., Connolly, S.J., Roberts, R. and Gent, M. (1991). Post-myocardial infarction mortality in patients with ventricular premature depolarizations: Canadian Amiodarone Myocardial Infarction Arrhythmia Trial Pilot Study. Circulation 84: 550-557.

Cairns, J.A., Connolly, S.J., Roberts, R. and Gent, M. (1997). Randomised trial of outcome after myocardial infarction in patients with frequent or repetitive ventricular premature depolarisations: CAMIAT. Lancet 349: 675-82.

Camus, P. and Mehendale, H.M. (1986). Pulmonary sequestration of amiodarone and desethylamiodarone. J. Pharmacol. Exp. Ther. 237: 867-73.

Cantor, J.O., Osman, M., Cerreta, J.M., Suárez, R., Mandl, I. and Turino, G.M. (1984). Amiodarone-induced pulmonary fibrosis in hamsters. Exp. Lung Res. 6: 1-10.

Cazzadori, A., Braggio, P. and Ganassini, A. (1986). Amiodarone-induced pulmonary toxicity. Respiration 49: 157-60.

Chamulitrat, W., Jordan, S.J., Mason, R.P., Saito, K. and Cutler, R.G. (1993). Nitric oxide formation during light-induced decomposition of phenyl N-*tert*-butylnitrone. J. Biol. Chem. 268(16): 11520-11527.

Charlier, R., Deltour, G. and Tondeur, R. et al. (1962). Recherche dans la serie des benzofuranes. VII. Etude pharmacologique preliminaire du butyl-2(diiodo 3'5'-β-N-diethylaminoethoxy-4'benzoyl)-3 benzofurannes. Arch. Int. Pharmacodyn. Ther. 139: 255-262.

Charlier, R., Delaunois, G., Bauthier, J. and Deltour, G. (1969). Recherches dans la serie des benzofuranes. XL. Propietes antiarythmiques de l'amiodarone. Cardiologia 54: 83-90.

Chatelain, P. and Brotelle, R. (1985). Phospholipid composition of rat lung after amiodarone treatment. Res. Commun. Chem. Pathol. Pharmacol. 50(3): 407-18.

Chatelain, P. and Laruel, R. (1985). Amiodarone partitioning with phospholipid bilayers and erythrocyte membranes. J. Pharmaceut. Sci. 74(7): 783-784.

Chatelain, P., Laruel, R. and Gillard, M. (1985). Effect of amiodarone on membrane fluidity and Na^+/K^+ ATPase activity in rat brain synaptic membranes. Biochem. Biophys. Res. Commun. 129(1): 148-154.

Chatelain, P., Ferreira, J., Laruel, R., Ruysschaer, J.M. (1986). Amiodarone induced modification of the phospholipid physical state: A fluoresence polarization study. Biochem. Pharmacol. 35(18): 3007-3013.

Cheeseman, K.H., Albano, E.F., Tomasi, A., Dianzani, M.U. and Slater, T.F. (1985). The effects of the spin traps PBN and 4-POBN on microsomal drug metabolism and hepatocyte viability. Life Chem. Rep. 3: 259-264.

Chen, G., Bray, T.M. and Janzen, E.G. (1991). The role of mixed function oxidase (MFO) in the metabolism of the spin trapping agent α-phenyl-N-tert-butyl-nitrone (PBN) in rats. Free Rad. Res. Comms. 14(1): 9-16.

Colgan, T., Simon, G.T., Kay, J.M., Pugsley, S.O. and Eydt, J. (1984). Amiodarone pulmonary toxicity. Ultrastruct. Pathol. 6: 199-207.

Cooper, J.A.D., White, D.A. and Matthay, R.A. (1986). Drug-induced pulmonary disease. Part 2: Non cytotoxic drugs. Am. Rev. Respir. Dis. 133: 488-505.

Costa-Jussà, F.R., Corrin, B. and Jacobs, J.M. (1984). Amiodarone lung toxicity: a human and experimental study. J. Pathol. 143: 73-9.

Cotgreave, I.A., Moldeus, P. and Orrenius, S. (1988). Host biochemical defence mechanisms against prooxidants. Ann. Rev. Pharmacol. Toxicol. 28: 189-212.

Coudert, B., Bailly, F., Lombard, J.N., Andre, F. and Camus, P. (1992). Amiodarone pneumonitis. Bronchoalveolar lavage findings in 15 patients and review of the literature. Chest 102(4): 1005-12.

Crapo, J.D., Barrey, B.E., Gehr,P., Bachofen, M. and Weibel, E.R. (1982). Cell number and cell characteristics of the normal human lung. Am. Rev. Respir. Dis. 125: 740.

Crawford, D.R. and Davies, K.J. (1994). Adaptive response and oxidative stress. Environ. Health. Perspec. 102(10): 25-28.

Crystal, R.G., Ferrans, V.J. and Basset, F. (1991). Biological basis of pulmonary fibrosis. In: The Lung: Scientific Foundations (R.G. Crystal and J.B. West, Eds.) pp. 2031-2046, Raven Press, New York.

Dake, M.D., Madison, J.M., Montgomery, C.K., Shellito, J.E., Hinchcliffe, W.A., Winkler, M.L. and Bainton, D.F. (1985). Electron microscopic demonstration of lysosomal inclusion bodies in lung, liver, lymph nodes, and blood leukocytes of patients with amiodarone pulmonary toxicity. Am. J. Med. 78: 506-512.

D'Amico, D.J., Kenyon, K.R. and Ruskin, J.N. (1981). Amiodarone keratopathy: drug-induced lipid storage disease. Arch. Ophthalmol. 99(2):257-261.

Daniels, J.M., Brien, J.F., and Massey, T.E. (1989). Pulmonary fibrosis induced in the hamster by amiodarone and desethylamiodarone. Toxicol. Appl. Pharmacol. 100: 350-9.

Daniels, J.M., Leeder, R.G., Brien, J.F. and Massey, T.E. (1990). Repeated amiodarone exposure in the rat: toxicity and effects on hepatic and extrahepatic monooxygenase activities. Can. J. Physiol. Pharmacol. 68: 1261-8.

Darmanata, J., van Zandwijk, N., Duren, D., van Royen, E., Mooi, W., Plomp, T.A., Jansen, H. and Durrer, D. (1984). Amiodarone pneumonitis: three further cases with a review of published reports. Thorax 39: 57-64.

Davies, K.J.A. (1995). Oxidative stress: the paradox of aerobic life. Biochem. Soc. Symp. 61: 1-31.

Dean, P.J., Gorshart, K.D., Poerterfield, J.G., Iansmith, D.H. and Golden, E.B. (1987). Amiodarone-associated pulmonary toxicity; a clinical and pathological study of eleven cases. Am. J. Clin. Pathol. 87: 7-13.

Denizot, F. and Lang, R. (1986). Rapid colorimetric assay for cell growth and survival. Modifications to the tetrazolium dye procedure giving improved sensitivity and reliability. J. Immunol. Meth. 89: 271-277.

Dudognon, P., Hauw, J.J., de Baecque, C., Escourolle, R., Derride, J.P. and Nick, J. (1979). Amiodarone neuropathy: drug-induced lipidosis (author's trans letter). Nouvelle Presse Medicale 8(21): 1766-1767.

Duenas-Laita, A., Barry, M.G., Mac Mathuna, P. and Feely, J. (1987). Effects of chronic treatment with amiodarone on hepatic demethylation and cytochrome P450. J. Pharm. Pharmacol. 39: 757-759.

Dunn, M. and Glassroth, J. (1989). Pulmonary complications of amiodarone toxicity. Prog. Cardiovasc. Dis. 31(6): 447-53.

Dusman, R.E., Stanton, M.S., Miles, W.M., Klein, L.S., Zipes, D.P. et al. (1990). Clinical features of amiodarone-induced pulmonary toxicity. Circulation 82(1): 51-59.

Dzimiri, N. and Almotrefi, A.A. (1993). Actions of amiodarone on mitochondrial ATPase and lactate dehydrogenase activities in guinea pig heart preparations. Eur. J. Pharmacol. 242: 113-118.

Fan, K., Bell, R., Eudy, S. and Fullenwider, J. (1987). Amiodarone-associated pulmonary fibrosis. Evidence of an immunologically mediated mechanism. Chest 92: 625-30.

Federico,A., Battisti, C., Manneschi, L., Gaggelli, E., Tassini, M., Valensin, G. and Vivi, A. (1996). Amiodarone effects membrane water permeability properties of human erythrocytes and rat mitochondria. Eur. J. Pharmacol. 304: 237-241.

Fisher, A.B., Scarpa, A., LaNoue, K.F., Bassett, D. and Williamson, J.R. (1973). Respiration of rat lung mitochondria and the influence of Ca^{2+} on substrate utilization. Biochem. 12(7): 1438-1445.

Fisher, G.L. and Placke, M.E. (1987). *In vitro* models of lung toxicity. Toxicology 47: 71-93.

Fisher, G.L. and Placke, M.E. (1988). Cell and organ culture models of respiratory toxicity. In: Toxicology of the Lung, pp285-314; Gardner, D.L., Crapo, J.D. and

Massaro, E.J., eds., Raven Press, NY.

Fisher, R.L., Smith, M.S., Hasal, S.J., Hasal, K.S., Gandolfi, A.J. and Brendel, K. (1994). The use of human lung slices in toxicology. Human Exp. Toxicol. 13: 466-471.

Forman, H.J. and Fisher, A.B. (1981). Antioxidant enzymes of rat granular pneumocytes. Constitutive levels and effect of hyperoxia. Lab. Invest. 45:1

Fraire, A.E., Guntupalli, K.K., Greenberg, S.D., Cartwright, J. and Chasen, M.H. (1993). Amiodarone pulmonary toxicity: A multidisciplinary review of current status. South. Med. J. 86(1): 67-77.

Freeman, B.A. and Crapo, J.D. (1982). Biology of disease. Free radicals and tissue injury. Lab. Invest. 47: 412-426.

Fromenty, B., Fisch, C., Labbe, G., Degott,C., Deschamps, D., Berson, A., Letteron, P. and Pessayre, D. (1990a). Amiodarone inhibits the mitochondrial oxidation of fatty acids and produces microvesicular steatosis of the liver in mice. J. Pharmacol. Exp. Ther. 255(3): 1371-1376.

Fromenty, B., Fisch, C., Berson, A., Letteron, P., Larrey, D. and Pessayre, D. (1990b). Dual effect of amiodarone on mitochondrial respiration. Initial protonophoric uncoupling effect followed by inhibition of the respiratory chain at the levels of complex I and complex II. J. Pharmacol. Exp. Ther. 255(3): 1377-1384.

Fromenty, B., Letteron, P., Fisch, C., Berson, A., Deschamps, D. and Pessayre, D. (1993). Evaluation of human blood lymphocytes as a model to study the effects of drugs on human mitochondria. Effects of low concentrations of amiodarone on fatty acid oxidation, ATP levels and cell survival. Biochem. Pharmacol. 46(3): 421-432.

Futamura, Y. (1995). Effect of amiodarone on release of cytokines from mouse alveolar macrophages pretreated with eicosapentaenoic acid. Jpn. J. Pharmacol. 69: 335-341.

Futamura, Y. (1996). Effect of amiodarone on cytokine release and on enzyme activities of mouse alveolar macrophages, bone marrow macrophages, and blood monocytes. J. Toxicol. Sci. 21: 125-134.

Garlid, K.D. and Nakashima, R.A. (1983). Studies on the mechanism of uncoupling by amine local anesthetics. Evidence for mitochondrial proton transport mediated by lipophilic ion pairs. J. Biol. Chem. 258(13): 7974-7980.

Gefter, W.B., Epstein, D.M., Pietra, G.G. and Miller, W.T. (1983). Lung disease caused by amiodarone, a new antiarrhythmic agent. Radiology 147: 339-44.

Gibb, P. and Melendez, L.J. (1986). Segmental pulmonary consolidation due to amiodarone. Can. Med. Assoc. J. 134: 611-613.

Gill, J., Heel, R.C. and Fitton, A. (1992). Amiodarone- An overview of its pharmacological properties, and review of its therapeutic use in cardiac arrhythmias. Drugs 43(1): 69-110.

Giri, S.N. and Wang, Q. (1989). Mechanisms of bleomycin-induced lung injury. Comments Toxicol. 3: 145-176.

Goeptar, A.R., Scheerens, H. and Vermeulen, N.P.E. (1995). Oxygen and xenobiotic reductase activities of cytochrome P450. Crit. Rev. Toxicol. 25(1): 25-65.

Gottlieb, S.S. (1997). Dead is dead-artificial definitions are no substitute. Lancet 349: 662-663.

Grech-Bélanger, O. (1984). Depressive effect of amiodarone on hepatic drug metabolism in the rat. Res. Commun. Chem. Pathol. Pharmacol. 44(1): 15-30.

Greenberg, M.L., Lerman, B.B., Shipe, J.R., Kaiser, D.L. and DiMarco, J.P. (1987). Relation between amiodarone and desethylamiodarone plasma concentrations and electrophysiologic effects, efficacy and toxicity. J. Am. Coll. Cardiol. 9(5): 1148-55.

Greenspon, A.J., Kidwell, G.A., Hurley, W., and Mannion, J. (1991). Amiodarone-related postoperative adult respiratory distress syndrome. Circulation 84: III407-III415.

Gross, I., Walker Smith, G.L., Maniscalco, W.M., Czajka, M.R., Wilson, G.M. and Rooney, S.A. (1978). An organ culture model for study of biochemical development of fetal rat lung. Amer. Physiol. Soc. 45(3): 335-352.

Gross, I., Walker Smith, G.L., Wilson, G.M., Maniscalco, W.M., Ingleson, L.D., Brehier, A. and Rooney, S.A. (1980). The influence of hormones on the biochemical development of fetal rat lung in organ culture. II. Insulin. Pediatr. Res. 14: 834-838.

Gross, S.A., Bandyopadhyay, S., Klaunig, J.E. and Somani, P. (1989). Amiodarone and desethylamiodarone toxicity in isolated hepatocytes in culture. Proc. Soc. Exp. Biol. Med. 190: 163-169.

Guerreiro, H., Campello, A., Lopes, L. and Kluppel, L. (1986a). Effect of amiodarone on mitochondrial energy-linked reactions and on mitochondria

morphology. Arq. Biol. Tecnol. 29(4): 621-631.

Guerreiro, H., Campello, A., Lopes, L. and Kluppel, L. (1986b). Effect of amiodarone on mitochondrial membranes. Arq. Biol. Tecnol. 29(4): 675-684.

Gutteridge, J.M.C. (1994). Biological origin of free radicals, and mechanisms of antioxidant protection. Chem.-Biol. Interac. 91: 133-140.

Ha, H.R., Wyss, P.A., Stieger, B., Meier, P.J., Meyer, U.A. and Follath, F. (1992). Amiodarone metabolism in human liver metabolism. FASEB J. 6(5) Part II: A1845.

Haffajee, C.I., Love, J.C., Canada, A.T., Lesko, L.J., Asdourian, G. and Alpert, J.S. (1983). Clinical pharmacokinetics and efficacy of amiodarone for refractory tachyarrhythmias. Circulation 67(6): 1347-1355.

Hageluken, A., Nurnberg, B., Harhammer, R., Grunbaum, L., Schunack, W. and Seifert, R. (1995). The class III antiarrhythmic drug amiodarone directly activates pertussis toxin-sensitive G proteins. Mol. Pharmacol. 47: 234-240.

Haire, D.L., Oehler, U.M., Krygsman, P.H. and Janzen, E.G. (1988). Correlation of radical structure with EPR spin adduct parameters: utility of the ^{1}H, ^{13}C, and ^{14}N hyperfine splitting constants of aminoxyl adducts of PBN-nitronyl-^{13}C for three-parameter scatter plots. J. Org. Chem. 53: 4535-4542.

Halliwell, B. (1989). Current status review: Free radicals, reactive oxygen species and human disease: a critcal evaluation with special reference to atherosclerosis. Br. J. Exp. Path. 70: 737-757.

Halliwell, B. (1991). Reactive oxygen species in living systems: Source, biochemistry, and role in human disease. The American Journal of Medicine. 91(suppl 3C): 14S-21S.

Halliwell, B. and Chirico, S. (1993). Lipid peroxidation: its mechanism, measurement and significance. Am. J. Clin. Nutr. 57(suppl): 715S-725S.

Halliwell, B. and Cross, C.E. (1994). Oxygen-derived species: Their relation to human disease and environmental stress. Environ. Health Prespect 102(suppl 10): 15-12.

Hanelt, M., Gareis, M. and Kollarczik, B. (1994). Cytotoxicity of mycotoxins evaluated by the MTT-cell culture assay. Mycopathologia 128: 167-174.

Hasan, T., Kochevar, I.E. and Abdulah, D. (1984). Amiodarone phototoxicity to

human erythrocytes and lymphocytes. Photochem. Photobiol. 40(6): 715-719.

Hay, J., Shahzeidi, S. and Laurent, G. (1991). Mechanisms of bleomycin-induced lung damage. Arch. Toxicol. 65(2): 81-94.

Heath, D., Smith, P., and Hasleton, P.S. (1973). Effects of chlorphentermine on the rat lung. Thorax 28: 551-558.

Heath, M.F., Costa-Jussa, F.R., Jacobs, J.M. and Jacobson, W. (1985). The induction of pulmonary phospholipidosis and the inhibition of lysosomal phospholipases by amiodarone. Brit. J. Exp. Pathol. 66: 391-397.

Heger, J.J., Prystowsky, E.N., and Zipes, D.P. (1983). Relationships between amiodarone dosage, drug concentrations, and adverse side effects. Am. Heart. J. 106: 931-935.

Herbette, L.G., Trumbore, M., Chester, D.W. and Katz, A.M. (1988). Possible molecular basis for the pharmacokinetics and pharmacodynamics of three membrane-active drugs: propranolol, nimodipine and amiodarone. J. Mol. Cell. Cardiol. 20: 373-378.

Herndon, J.C., Cook, A.O., Ramsay, M.A.E., Swygert, T.H. and Capehart, J. (1992). Postoperative unilateral pulmonary edema: Possible amiodarone pulmonary toxicity. Anaesthesiology 76: 308-312.

Hoet, P.H.M., Lewis, C.P.L., Dinsdale, D., Demedts, M. and Nemery, B. (1995). Putrescine uptake in hamster lung slices and primary cultures of type II pneumocytes. Am. J. Physiol. 269 (Lung Cell. Mol. Physiol. 13): L681-689.

Hollán, S. (1995). Free radicals in health and disease. Haematologia 26: 177-189.

Holt, D.W., Tucker, G.T., Jackson, P.R. and Storey, G.C.A. (1983). Amiodarone pharmacokinetics. Am. Heart J. 106: 840-846.

Honegger, U.E., Zuehlke, R.D., Scuntaro, I., Schaefer, M.H.A., Toplak, H. and Wiesmann, U.N. (1993). Cellular accumulation of amiodarone and desethylamiodarone in cultured human cells. Consequences of drug accumulation on cellular lipid metabolism and plasma membrane properties of chronically exposed cells. Biochem. Pharmacol. 45(2): 349-356.

Honegger, U.E., Scuntaro, I. and Wiesmann, U.N. (1995). Vitamin E reduces accumulation of amiodarone and desethylamiodarone and inhibits phospholipidosis in cultured human cells. Biochem. Pharmacol. 49(12): 1741-1745.

Hori, R., Okumura, K. and Yoshida, H. (1987). Binding of basic drugs to rat lung mitochondria. Pharmaceutical Res. 4(2): 142-146.

Hostetler, K.Y., and Matsuzawa, Y. (1981). Studies on the mechanism of drug-induced lipidosis: Cationic amphiphilic drug inhibition of lysosomal phospholipases A and C. Biochem. Pharmacol. 30: 1121-1126.

Hostetler, K.Y., Reasor, M.J., Walker, E.R., Yazaki, P.J. and Frazee, B.W. (1986). Role of phospholipase A inhibition in amiodarone pulmonary toxicity in rats. Biochim. Biophys. Acta 875: 400-405.

Hostetler, K.Y., Giordano, J.R. and Jellison, E.J. (1988). In vitro inhibition of lysosomal phospholipase A1 of rat lung by amiodarone and desethylamiodarone. Biochim. Biophys. Acta 959: 316-321.

Ignatowicz, E. and Rybczynska, M. (1994). Some biochemical and pharmacological aspects of free radical-mediated tissue damage. Pol. J. Pharmacol. 46: 103-114.

Israel-Biet, D., Venet, A., Caubarrere, I., Bonan, G., Bennewald, G., Pechaud, D., Danel, C. and Chretien, J. (1985). Amiodarone pneumonitis mechanism: evaluation by bronchoalveolar lavage (BAL). Am. J. Resp. Dis. 131: A74.

Israel-Biet, D., Venet, A., Caubarrere, I., Bonan, G., Danel, C., Chretien, J. and Hance, A.J. (1987). Bronchoalveolar lavage in amiodarone pneumonitis. Cellular abnormalities and their relevance to pathogenesis. Chest 91: 214-21.

Jandrisits, L.T. (1988). A study of the spin adducts produced during the respiratory burst of canine neutrophils. MSc thesis, University of Guelph.

Janzen, E.G. and Blackburn, B.J. (1969). Detection and identification of short-lied free radicals by electron spin resonance trapping techniques (spin trapping). Photolysis of organolead, tin and mercury compounds. J. Am. Chem. Soc. 91: 4481-4490.

Janzen, E.G., Coulter, G.A., Oehler, U.M., Bergsma, J.P. (1982). Solvent effects on the nitrogen and β-hydrogen hyperfine splitting constants of aminoxyl radicals obtained in spin trapping experiments. Can. J. Chem. 60: 2725-2733.

Janzen, E.G. (1984). Spin trapping. Meth. Enzymol. 105: 188-198.

Janzen, E.G., Towner, R.A. and Haire, D.L. (1987). Detection of free radicals generated from the *in vitro* metabolism of carbon tetrachloride using improved ESR spin trapping techniques. Free Rad. Res. Commun. 3(6): 357-364.

Janzen, E.G. (1990). Spin trapping associated vocabulary. Free Rad. Res. Commun. 9: 163-167.

Janzen, E.G. and Haire, D.L. (1990). Two decades of spin trapping. Adv. Free Rad. Chem. 1: 253-295.

Janzen, E.G., Poyer, J.L., West, M.S., Crossley, C. and McCay, P.B. (1994). Study of the reproducibility of spin trapping results in the use of C-phenyl-N-tert-butylnitrone (PBN) for trichloromethyl radical detection in CCl_4 metabolism by rat liver microsomal dispersions. Biological spin trapping I. J. Biochem. Biophys. Meth. 29(3-4): 189-205.

Joelson, J., Kluger, J., Cole, S. and Conway, M. (1984). Possible recurrence of amiodarone pulmonary toxicity following corticosteroid therapy. Chest 85: 284-6.

Joshi, U.M., Rao, P., Kodavanti, S., Coudert, B., Dwyer, T.M. and Mehendale, H.M. (1988). Types of interaction of amphiphilic drugs with phospholipid vesicles. J. Pharmacol. Exp. Ther. 246(1): 150-157.

Joyce, D. (1987). Oxygen radicals in disease. Adverse Drug Reaction Bulletin. 127: 476-479.

Julian, D.G., Camm, A.J., Frangin, G., Janse, M.J., Munoz, A., Schwartz, P.J. and Simon, P. for the European Myocardial Infarct Amiodarone Trial Investigators (1997). Randomised trial of effect of amiodarone on mortality in patients with left-ventricular dysfunction after recent myocardial infarction: EMIAT. Lancet 349: 667-74.

Kabalka, G.W., Kennedy, T.P., Goudgaon, N.M. and Varma, R.S. (1989). Synthesis of (2-butyl-3-benzofuranyl){4-[2-(diethylamino)ethoxy]-3,5-diiodo phenyl}methane derivatives. Org. Prep. Proced. Int. 21: 348-351.

Kachel, D.L., Moyer, T.P. and Martin, W.J. (1990). Amiodarone-induced injury of human pulmonary artery endothelial cells: protection by α-tocopherol. J. Pharmacol. Exp. Therap. 254(3): 1107-1112.

Kannan, R., Miller, S. and Singh, B.N. (1985). Tissue uptake and metabolism of amiodarone after chronic administration in rabbits. Drug Metab. Disp. 13(6): 646-650.

Kannan, R., Sarma, J.S., Guha, M. and Venkataraman, K. (1989). Tissue drug accumulation and ultrastructural changes during amiodarone administration in rats. Fundam. Appl. Toxicol. 13: 793-803.

Kannan, R., Sarma, J.S.M., Guha, M., and Venkataraman, K. (1990). Desethylamiodarone-induced phospholipidsosis in lung, liver, and pulmonary

macrophages and its relationship to tissue drug accumulation in rats. Eur. J. Pharmacol. 183: 2452-2453.

Karpel, J.P., Mitsudo, S. and Norin, A.J. (1991). Natural killer cell activity in a rat model of amiodarone-induced interstitial lung disease. Chest 99: 230-4.

Kay, G.N., Epstein, A.E., Kirklin, J.K., Diethelm, A.G., Graybar, G. and Plumb, V.J. (1988). Fatal postoperative amiodarone pulmonary toxicity. Am. J. Cardiol. 62: 490-492.

Kehrer, J.P. (1988). Contemporary issues in toxicology. Toxicol. Appl. Pharmacol. 95: 349-362.

Kehrer, J.P. (1993). Free radicals as mediators of tissue injury and disease. Crit. Rev.Toxicol. 23(1): 21-48.

Kennedy, T.P., Gordon, G.B., Paky, A., McShane, A., Adkinson, N.F., Peters, S.P., Friday, K., Jackman, W., Sciuto, A.M. and Gurtner, G.H. (1988). Amiodarone causes acute oxidant lung injury in ventilated and perfused rabbit lungs. J. Cardiovasc. Pharmacol. 12: 23-36.

Kinnard, W.V., Tuder, R., Papst, P. and Fisher, J.H. (1994). Regulation of alveolar type II cell differentiation and proliferation in adult rat lung explants. Am. J. Respir. Cell Mol. Biol. 11: 416-425.

Kinnula, V.L., Crapo, J.D. and Raivio, K.O. (1995). Biology of Disease: Generation and disposal of the reactive oxygen metabolites in the lung. Lab.Invest. 73(1): 3-19.

Knecht, K.T. and Mason, R.P. (1993). *In vivo* spin trapping of xenobiotic free radical metabolites. Arch. Biochem. Biophys. 303(2): 185-194.

Kodavanti, U.P. and Mehendale, H.M. (1991). Amiodarone- and desethylamiodarone-induced pulmonary phospholipidosis, inhibition of phospholipases *in vivo*, and alteration of [^{14}C]amiodarone uptake by perfused lung. Am. J. Respir. Cell Mol. Biol. 4: 369-378.

Kubow, S.J. (1984). An ESR spin trapping study on the role of free radicals, glutathione and vitamin E in 3-methylindole-induced lung disease. PhD thesis, University of Guelph, ON, Canada.

Kubow, S., Janzen, E.G. and Bray, T.M. (1984). Spin-trapping of free radicals formed during *in vitro* and *in vivo* metabolism of 3-methylindole. J. Biol. Chem. 259(7): 4447-4451.

Kubow, S., Bray, T.M. and Janzen, E.G. (1985). Spin-trapping studies on the effects of vitamin E and glutathion on free radical production induced by 3-methylindole. Biochem. Pharmacol. 34: 1117-1119.

Kubow, S. and Bray, T.M. (1988). The effect of lung concentrations of glutathione and vitamin E on the pulmonary toxicity of 3-methylindole. Can. J. Physiol. Pharmacol. 66(7): 863-867.

Kudenchuk, P., Pierson, D., Greene, H., Graham, E., Sears, G. and Trobaugh, G. (1984). Prospective evaluation of amiodarone pulmonary toxicity. Chest 86: 541-548.

Larrey, D., Tinel, M., Letteron, P., Geneve, J., Descatoire, V. and Pessayre, D. (1986). Formation of an inactive cytochrome P-450Fe(II)-metabolite complex after administration of amiodarone in rats, mice and hamsters. Biochem. Pharmacol. 35(13): 2213-2220.

Last, J.A. (1989). The paraquat model of lung fibrosis. In: Handbook of animal models of pulmonary disease; volume 1, pp 151-164, Cantor, J.O., ed., CRC Press, Boca Raton, FL.Latini, R., Tognoni, G. and Kates, R.E. (1984). Clinical pharmacokinetics of amiodarone. Clin. Pharmacokin. 9: 136-156.

Latini, R., Tognoni, G. and Kates, R. (1984). Clinical pharmacokinetics of amiodarone. Clin. Pharmacokin. 9: 136-156.

Leech, J., Gallastegui, J. and Swiryn, S. (1984). Pulmonary toxicity of amiodarone. Chest 85(3): 444-5.

Leeder, R.G., Brien, J.F. and Massey, T.E. (1994). Investigation of the role of oxidative stress in amiodarone-induced pulmonary toxicity in the hamster. Can. J. Physiol. Pharmacol. 72: 613-621.

Leeder, R.G., Rafeiro, E., Brien, J.F., Mandin, C.C. and Massey, T.E. (1996). Evaluation of reactive oxygen species involvement in amiodarone pulmonary toxicity in vivo and in vitro. J.Biochem. Toxicol.11:147-159.

Levy, A., Meyerstein, D. and Ottolenghi, M. (1973). Photodissociation of iodoaromatics in solution. J. Phys. Chem. 77: 3044-3047.

Li, A.S.W. and Chignell, C.F. (1987). Spectroscopic studies of cutaneous photosensitizing agents-IX. A spin trapping study of the photolysis of amiodarone and desethylamiodarone. Photochem. Photobiol. 45(2): 191-197.

Lindenschmidt, R.C., and Witschi, H.P. (1985). Propranolol-induced elevation of

pulmonary collagen. J. Pharmocol. Exp. Ther. 232: 346-350.

Liu, F.L., Cohen, R.D., Downar, E., Butany, J.W., Edelson, J.D. and Rebuck, A.S. (1986). Amiodarone pulmonary toxicity: functional and ultrastructural evaluation. Thorax 41: 100-105.

Lowry, O.H., Rosebrough, N.J., Farr, A.L. and Randall, J.R. (1951). J.Biol. Chem. 193: 265-275.

Lüllmann, H., Lullmann-Rauch, R., and Wasserman, O. (1978). Lipidosis induced by amphiphilic cationic drugs. Biochem. Pharmacol. 27: 1103-1108.

Maggioni, A.P., Maggi, A., Volpi, A., D'Aranno, V., Tognoni, G. and Giani, P. (1983). Amiodarone distribution in human tissues after sudden death during Holter recording. Am. J. Cardiol. 52: 217-218.

Maling, T. (1988). Amiodarone therapeutic plasma concentration monitoring. Is it practical? Clin. Pharmacokin. 14: 321-324.

Manicardi, V., Bernini, G., Bossini, P., Bertorelli, G. Pesci, A. and Bellodi, G. (1989). Low-dose amiodarone-induced pneumonitis: evidence of an immunologic pathogenetic mechanism. Am. J. Med. 86: 134-135.

Mansuy, D. and Fontecave, M. (1983). Reduction of benzyl halides by liver microsomes. Formation of 478 nm-absorbing alkyl-ferric cytochrome P450 complexes. Biochem. Pharmacol. 32(12): 1871-1879.

Marchlinski, F.E., Gansler, T.S., Waxman, H.L. and Josephson, M.E. (1982). Amiodarone pulmonary toxicity. Annals Intern. Med. 97: 839-45.

Marchlinski, F.E. (1987). Amiodarone: therapeutic but toxic. New York State J. Med. 87(6): 322-324.

Martin, W.J.II and Howard, D.M. (1985). Amiodarone-induced lung toxicity. *In vitro* evidence for the direct toxicity of the drug. Am. J. Pathol. 120: 344-350.

Martin, W.J. II and Rosenow, E.C. III (1988a). Amiodarone pulmonary toxicity: recognition and pathogenesis (Part 1). Chest 93(5): 1067-75.

Martin, W.J. II and Rosenow, E.C. III (1988b). Amiodarone pulmonary toxicity: recognition and pathogenesis (Part 2). Chest 93(6): 1242-8.

Martin, W.J. II, Kachel, D.L., Standing, J.E., Olsen, R. and Powis, G.W. (1989).

Alpha tocopherol prevents amiodarone-mediated increase in cytosolic Ca^{2+} and toxicity in cultured human pulmonary endothelial cells. Am. Rev. Resp. Dis. 139: A423.

Martin,W.J. (1990). Mechanisms of amiodarone pulmonary toxicity. Clin.Chest Med. 11(1): 131-8.

Martinez-Cayuela, M. (1995). Oxygen free radicals and human disease. Biochimie 77: 147-161.

Mason, J.W., Hondeghem, L.M. and Katzung, B.G. (1983). Amiodarone blocks inactivated cardiac sodium channels. Pflugers Arch. 396: 79-81.

Mason, J.W. (1987). Amiodarone. New Eng. J. Med. 316(8): 455-466.

Mason, R.J. and Williams, M.C. (1991). Alveolar type II cells. In: The Lung: Scientific Foundations, R.G. Crystal and J.B. West et al., eds, Raven Press Ltd., New York.

Mason, R.P. and Chignell, C.F. (1994). Free radicals in toxicology with an emphasis on electron spin resonance investigations, pp 319-332. In: Free radical damage and its control. Rice, C.A. and Burdon, R.H. (eds), Elsevier Science.

Massey, T.E., Leeder, R.G., Rafeiro, E. and Brien, J.F. (1995). The 1994 Veylien Henderson Award of the Society of Toxicology of Canada. Mechanisms in the pathogenesis of amiodarone-induced pulmonary toxicity. Can. J. Physiol. Pharmacol. 73: 1675-1685.

Mazel, P. (1971). General principles and procedures for drug metabolism in vitro. In: Fundamentals of drug metabolism and disposition, LaDu and Mandel, Eds., pp 527-545.

Mazue, G., Vic, P., Gouy, D., Remandet, B., Lacheretz, F., Berthe, J., Barchewitz, G. and Gagnol, J.P. (1984). Recovery from amiodarone-induced lipidosis in laboratory animals: a toxicological study. Fund. Appl. Toxicol. 4: 992-999.

McCay, P.B., Noguchi, T., Fong, K-L., Lai, E.K. and Poyer, J.L. (1980). Production of radicals from enzyme systems and the use of spin traps, pp 155-186. In "Free Radicals in Biology" Volume IV, pp 155-186, W.A. Pryor, Ed.

McCay, P.B. (1987). Application of ESR spectroscopy in toxicology. Arch. Toxicol. 60: 133-137.

McKenna, W.J., Rowland, E. and Krikler, D.M. (1983). Amiodarone: the experience

of the past decade. Br. Med. J. 287: 1654-1656.

McNeil, K.D., Firouz-Abadi, A., Oliver, W. and Zimmerman, P.V. (1992). Amiodarone pulmonary toxicity-three unusual manifestations. Aust. N.Z. J. Med. 22: 14-18.

Minchin, R.F., Ilett, K.F. and Madsen, B.W. (1978). Chlorphentermine binding in rat lung subcellular fractions and its displacement by desmethylimpramine. Biochem. Pharmacol. 28: 2273-2278.

Moldéus, P., Hogberg, J. and Orrenius, S. (1978). Isolation and use of liver cells. Meth. Enzymol. 52: 60-71.

Montgomery, M.R., Furry, J.M. and Reasor, M.J. (1982). Chlorphentermine inhibits oxidative energy metabolism in rat lung slices. Tox. Appl. Pharmacol. 65: 63-68.

Mosmann, T. (1983). Rapid colorimetric assay for cellular growth and survival: application to proliferation and cytotoxicity assays. J. Immunol. Meth. 65: 55-63.

Myers, J.L., Kennedy, J.I. and Plumb, V.J. (1987). Amiodarone lung: Pathologic findings in clinically toxic patients. Hum. Pathol. 18: 349-354.

Nademanee, K., Singh, B.N., Callahan, B., Hendrickson, J.A. and Hershman, J.M. (1986). Amiodarone, thyroid hormone indexes, and altered thyroid function: long-term serial effects in patients with cardiac arrhythmias. Am. J. Cardiol. 58: 981-986.

Nagai, A., Matsumiya, H., Hayashi, M., Yasui, S., Okamoto, H. and Konno, K. (1994). Effects of nictotinamide and niacin on bleomycin-induced acute injury and subsequent fibrosis in hamster lungs. Exp. Lung Res. 20: 263-281.

Nalos, P.C., Kass, R.M., Gang, E.S., Fishbein, M.C., Mandel, W.J. and Peter, T. (1987). Life-threatening postoperative pulmonary complications in patients with previous amiodarone pulmonary toxicity undergoing cardiothoracic operations. J. Thorac. Cardiovasc. Surg. 93: 904-912.

Nattel, S. and Talajic, M. (1988). Recent advances in understanding the pharmacology of amiodarone. Drugs 36: 121-131.

Nedergaard, J. and Cannon, B. (1979). Overview- Preparation and properties of mitochondria from different sources. Meth. Enzymol. 55: 3-12.

Nicolet-Chatelain, G., Prevost, M.C., Escamilla, R. and Migueres, J. (1991). Amiodarone-induced pulmonary toxicity. Immunoallergologic tests and

bronchoalveolar lavage phospholipid content. Chest 99(2): 363-9.

Nicotera, P., Bellomo, G. and Orrenius, S. (1992). Calcium-mediated mechanisms in chemically induced cell death. Annu. Rev. Pharmacol. Toxicol. 32: 449-70.

Ogle, C.L. and Reasor, M.J. (1990). Response of aveolar macrophages to amiodarone and desethylamiodarone, in vitro. Toxicology: 62: 227-238.

Ohar, J.A., Jackson, F., Dettenmeier, P.A., Bedrossian, C.W., Tricomi, S.M., and Evans, R.G. (1992). Bronchoalveolar lavage cell counts and differential are not reliable indicators of amiodarone-induced pneumonitis. Chest 102: 999-1004.

O'Neill, C.A. and Giri, S.N. (1994). Biochemical mechanisms for the attenuation of bleomycin-induced lung fibrosis by treatment with niacin in hamsters: The role of NAD and ATP. Exp. Lung Res. 20: 41-56.

Padmavathy, B., Devaraj, H. and Devaraj, N. (1993). Amiodarone-induced changes in surfactant phospholipids of rat lung. Naunyn-Schmiedeberg's Arch. Pharmacol. 347: 421-424.

Paillous, N. and Verrier, M. (1988). Photolysis of amiodarone, an antiarrhythmic drug. Photochem. Photobiol. 47(3): 337-343.

Paillous, N. and Fery-Forgues, S. (1994). Is there a link between the phototoxic or antioxidant properties of amiodarone, an antiarrhythmic drug, and its lipophilic character? Biochem. Pharmacol. 48(5): 851-857.

Parkinson, A. (1996). Biotransformation of xenobiotics. In: Casarett & Doull's Toxicology: The basic science of poisons, Vol. 6, pp 113-186, C. Klassen, ed, The McGraw-Hill Cos., Inc., USA.

Pessayre, D. (1992). Mechanisms for drug-induced hepatic injury. In: Drug-induced hepatic injury, Vol. 2, pp 23-49; Stricker, ed., Elsevier Science, Amsterdam.

Pilcher, W.J., Schlinder, L., Staubli, M., Stadler, B.M. and de Weck, A.L. (1988). Anti-amiodarone antibodies: detection and relationship to the development of side effects. Am. J. Med. 85: 197-202.

Pirovino, M., Muller, O., Zysset, T. and Honegger, U. (1988). Amiodarone-induced hepatic phospholipidosis: Correlation of morphological and biochemical findings in an animal model. Hepatology 8(3): 591-598.

Pitcher, W.D. (1992). Southwestern Internal Medical Conference: Amiodarone

pulmonary toxicity. Am. J. Med. Sci. 303(3): 206-12.

Placke, M.E. and Fisher, G.L. (1987a). Adult peripheral lung organ culture-A model for respiratory tract toxicology. Toxicol. Appl. Pharmacol. 90: 284-298.

Placke, M.E. and Fisher, G.L. (1987b). Asbestos in peripheral lung culture. A species comparison of pulmonary tissue response. Drug Chemical Toxicol.

Plomp, T.A., van Rossum, J.M., Robles de Medina, E.O., van Lier, T. and Maes, R.A.A. (1984). Pharmacokinetics and body distribution of amiodarone in man. Arzneim.-Forsch./Drug Res. 34(I): 513-520.

Plomp, T.A., van Rossum, J.M., Robles de Medina, E.O., van Lier, T. and Maes, R.A.A. (1985). Pharmacokinetics and body distribution of amiodarone in man. Arzneimittelforschung 35: 513-520.

Podrid, P.J. (1995). Amiodarone: Reevaluation of an old drug. Ann. Intern. Med. 122: 689-700.

Pollak, P.T. and Sami, M. (1984). Acute necrotinizing pneumonitis and hyperglycemia after amiodarone therapy. Case report and review of amiodarone-associated pulmonary disease. Am. J. Med. 76: 935-939.

Pollak, P.T., Sharma, A.D., Delmaestro, R.F. and Carruthers, S.G. (1986). Amiodarone alters superoxide dismutase activity in human red blood cells. J. Am. Coll. Cardiol. 7: 92A.

Pollak, P.T., Sharma, A.D., and Carruthers, S.G. (1990). Relation of amiodarone hepatic and pulmonary toxicity to serum drup concentrations and superoxide dismutase activity. Am. J. Cardiol. 65: 1185-1191.

Poucell, S., Iretcon, J., Downer, E., Larratt, L., Patterson, J., Blendis, L. and Phillips, M.J. (1984). Amiodarone-associated phospholipidosis and fibrosis of the liver. Gastronenterology 86: 926-936.

Powis, G., Olsen, R., Standing, J.E., Kachel, D. and Martin, W.J. II (1990). Amiodarone-mediated increase in intracellular free Ca^{2+} associated with cellular injury to human pulmonary artery endothelial cells. Toxicol. Appl. Pharmacol. 103: 156-164.

Price, R.J., Renwick, A.B., Beamand, J.A., Esclangon, F., Wield, P.T., Walters, D.G. and Lake, B.G. (1995a). Comparison of the metabolism of 7-ethoxycoumarin and coumarin in precision-cut rat liver and lung slices. Fd. Chem. Toxic. 33(3): 233-237.

Price, R.J., Renwick, A.B., Wield, P.T., Beamand, J.A. and Lake, B.G. (1995b). Toxicity of 3-methylindole, 1-nitronaphthalene and paraquat in precision-cut rat lung slices. Arch. Toxicol. 69: 405-409.

Prasada Rao, K.S., Rao, S.B., Camus, P.H. and Mehendale, H.M. (1986). Effect of amiodarone on Na^+,K^+ATPase and Mg^{2+}-ATPase activities in rat brain synaptosomes. Cell. Biochem. Funct. 4: 143-51.

Rafeiro, E., Leeder, R.G., Daniels, J.M., Brien, J.F. and Massey, T.E. (1990). *In vitro* hepatic, renal, and pulmonary N-dealkylation of amiodarone. Biochem. Pharmacol. 39(10): 1627-1629.

Rakita, L., Sobol, S.M., Mostow, N. and Vrobel, T. (1983). Amiodarone pulmonary toxicity. Am. Heart J. 106: 906-916.

Rakita, L. and Mostow, N.D. (1988). Side effect profile of amiodarone and approaches to optimal dosing, pp 509-541. In: Control of cardiac arrhythmias by lengthening repolarization. Singh, B.N. ed., Mount Kisco NY, Futura Publishing.

Rao, R.H., McCready, V.R. and Spathis, G.S. (1986). Iodine kinetic studies during amiodarone treatment. J. Clin. Endocrinol. Met. 62(3): 563-568.

Reasor, M.J., Ogle, C.L., Walker, E.R. and Kacew, S. (1988). Amiodarone-induced phospholipidosis in rat alveolar macrophages. Am. Rev. Respir. Dis. 137: 510-518.

Reasor, M.J. (1989). A review of the biology and toxicologic implications of the induction of lysosomal lamellar bodies by drugs. Toxicol. Appl. Pharmacol. 97: 47-56.

Reasor, M.J., Ogle, C.L. and Kacew, S. (1989). Amiodarone-induced pulmonary toxicity in rats: biochemical and pharmacological considerations. Toxicol. Appl. Pharmacol. 97: 124-133.

Reasor, M.J., Ogle, C.L. and Miles, P.R. (1990). Response of rat lungs to amiodarone: preferential accumulation of amiodarone and desethylamiodarone in alveolar macrophages. Exp. Lung Res. 16: 577-591.

Reasor, M.J. and Kacew, S. (1991). Amiodarone pulmonary toxicity: morphological and biochemical features. Proc. Soc. Exp. Biol. Med. 196: 1-7.

Reasor, M.J., McCloud, C.M., Beard, T.L., Ebert, D.C., Kacew, S., Gardner, M.F., Aldern, K.A. and Hostetler, K.Y. (1996a). Comparative evaluation of amiodarone-induced phospholipidosis and drug accumulation in Fischer-344 and Sprague-Dawley rats. Toxicol. 106: 139-147.

Reasor, M.J., McCloud, C.M., DiMatteo, M., Schafer, R. Ima, A. and Lemaire, I. (1996b). Effects of amiodarone-induced phospholipidosis on pulmonary host defense functions in rats. Proc. Soc. Exp. Biol. Med. 211: 346-352.

Reasor, M.J. and Kacew, S. (1996). An evaluation of possible mechanisms underlying amiodarone-induced pulmonary toxicity. Proc. Soc. Exp. Biol. Med. 212: 297-304.

Reilly, P.M., and Bulkley, G.B. (1990). Tissue injury by free radicals and other toxic oxygen metabolites. Br.J. Surg. 77: 1324-1325.

Reinhart, P.G., Lai, Y.L. and Gairola, C.G. (1996). Amiodarone-induced fibrosis in Fisher 344 rats. Toxicology 110: 95-101.

Reiser, K.M. and Last, J.A. (1986). Early cellular events in pulmonary fibrosis. Exp. Lung Res. 10: 331-355.

Reiss, O.K. (1966). Studies of lung metabolism. Isolation and properties of subcellular fractions from rabbit lung. J. Cell Biol. 30: 45-57.

Rekka, E., Mannhold, R.M., Bast, A. and Timmerman, H. (1990). Molecular pharmacological aspects of antiarrhythmic activity I. Class I and Class III compounds and lipid peroxidation. Biochem. Pharmacol. 39(1): 95-100.

Riley, P.A. (1994). Free radicals in biology: oxidative stress and the effects of ionizing radiation. Int. J. Biol. 66(1): 27-33.

Riva, E., Gerna, M., Neyroz, P., Urso, R., Bartosek, I. and Guaitani, A. (1982). Pharmacokinetics of amiodarone in rats. J. Cardiovasc. Pharmacol. 4: 270-275.

Riva, E., Marchi, S., Pesenti, A., Bizzi, A., Cini, M., Veneroni, E., Tavbani, E., Boeri, R., Bertani, T. and Latini, R. (1987). Amiodarone induced phospholipidosis. Biochemical, morphological and functional changes in the lungs of rats chronically treated with amiodarone. Biochem. Pharmacol. 36(19): 3209-3214.

Roden, D.M. (1993). Pharmacokinetics of amiodarone: implications for drug therapy. Am. J. Cardiol. 72: 45F-50F.

Rosenow, E.C. III and Martin, W.J. II (1988). Drug-induced interstitial disease. In Interstitial lung disease. Schwarz M.A. et al. eds. BC Becker, Toronto.

Rossouw, D.J. and Engelbrecht, F.M. (1978). The effect of paraquat on the respiration of lung cell fractions. S. Afr. Med. J. 54: 1101-1104.

Rothenberg, F., Franklin, J.O. and DeMaio, S.J. (1994). Use, value and toxicity of amiodarone. Heart Dis. Stroke 3: 19-23.

Rotmensch, H.H., Belhassen, B., Swanson, B.N., Shoshani, D., Spielman, S.R., Greenspon, A.J., Greenspan, A.M., Vlasses, P.H. and Harowitz, L.N. (1984). Steady-state serum amiodarone concentrations: relationships with antiarrhythmic efficacy and toxicity. Ann. Intern. Med. 101: 462-469.

Ruangyuttikarn, W., Skiles, G.L. and Yost, G.S. (1992). Identification of a cysteninyl adduct of oxidized 3-methylindole from goat lung and human liver microsomal ptns. Chem. Res. Toxicol. 5: 713.

Ruch, R.J., Bandyopadhyay, S., Somani, P. and Klaunig, J.E. (1991). Evaluation of amiodarone free radical toxicity in rat hepatocytes. Tox. Lett. 56: 117-126.

Sandron, D., Israel-Biet, D., Venet, A. and Chretien, J. (1986). Immunoglobulin abnormalities in bronchoalveolar lavage specimens from amiodarone-treated subjects. Chest 89: 617-618.

Sautereau, A.M., Tournaire, C., Suares, M., Tocanne, J.F. and Paillous, N. (1992). Interactions of amiodarone with model membranes and amiodarone-photoinduced peroxidation of lipids. Biochem. Pharmacol. 43(12): 2559-66.

Saussine, M., Colson, P., Alauzen, M. and Mary, H. (1992). Postoperative acute respiratory distress syndrome: a complication of amiodarone associated with 100 percent oxygen ventilation. Chest. 102: 980-981.

Sawyer, T.W., Wilde, P.E., Rice, P. and Weiss, M.T. (1995). Toxicity of sulphur mustard in adult rat lung organ culture. Toxicol. 100: 39-49.

Schneeberger, E.E. (1991). Alveolar type I cells. In: The Lung: Scientific Foundations, Crystal, R.G. and West, J.B. et al., eds, Raven Press Ltd., New York.

Schwartz, A., Shen, E., Morady, F., Gillespie, K., Scheinman, M. and Chatterjee, K. (1983). Hemodynamic effects of intravenous amiodarone in patients with depressed left ventricular function and recurrent ventricular with 100 percent oxygen ventilation. Chest 102: 980-981.

Shapiro, P.S., Casty, F.E., Stirewalt, W.S., Leslie, K.O., Absher, M.P. and Evans, J.N. (1994). Oxygen-induced changes in protein synthesis and cell proliferation in cultured lung slices. Am. J. Physiol. 267 (Lung Cell. Mol. Physiol. 11): L720-L727.

Sharma, R.K. and Kharasch, N. (1968). The photolysis of iodoaromatic compounds.

Angew. Chem. Internat. Edit. 7: 36-44.

Sies, H. (1991). Oxidative Stress: From basic research to clinical application. Am. J.f Med. 91(suppl 3C): 31S-38S.

Siminski, J.T., Kavanagh, T.J., Chi, E. and Raghu, G. (1992). Long-term maintenance of mature pulmonary parenchyma cultured in serum-free conditions. Am. J. Physiol. 262 (Lung Cell Mol. Physiol. 6): L105-L110.

Simon, R.H. (1992). The biology and biochemistry of pulmonary alveolar epithelial cells. In: Treatise on pulmonary toxicology: Comparative biology of the normal lung. Vol 1, Chapter 29, pp 545-564, R.A. Parent, Ed., CRC Press, Boca Raton, FLA.

Singh, B.N. and Vaughan-Williams, E.M. (1970). The effect of amiodarone, a new anti-anginal drug, on cardiac muscle. Br. J. Pharmacol. 39: 657-667.

Singh, B.N., Venkatesh, N., Nademanee, K., Josephson, M.A. and Kannan, R. (1989). The historical development, cellular electrophysiology and pharmacology of amiodarone. Prog. Cardiovasc. Dis. 31: 249-280.

Singh, B.N. (1996). Antiarrhythmic actions of amiodarone: A profile of a paradoxical agent. Am. J. Cardiol. 78(4A): 41-53.

Slater, T.F. (1984). Free-radical mechanisms in tissue injury. Biochem. J. 222: 1-15.

Smith,A.C. and Boyd, M.R. (1984). Preferential effects of 1,3-bis(2-chloroethyl)-1-nitrosourea (BCNU) on pulmonary glutathione reductase and glutathione/glutathione disulfide ratios: Possible implications for lung toxicity. J. Pharmacol. Exp. Ther. 229(3): 658-663.

Snider, G.L., Hayes, J.A. and Korthy, A.L. (1978). Chronic interstitial pulmonary fibrosis produced in hamsters by endotracheal bleomycin. Am. Rev. Respir. Dis. 117: 1099-1108.

Sobol, S.M. and Rakita, L. (1982). Pneumonitis and pulmonary fibrosis associated with amiodarone treatment: a possible complication of a new antiarrhythmic drug. Circulation 65: 819-824.

Somani, P., Bandyopadhyay, S., Klawnig, J.E., and Gross, S.A. (1990). Amiodarone- and desethylamiodarone-induced myelinoid inclusion bodies and toxicity in cultured rat hepatocytes. Hepatology 11: 81-92.

Southorn, P.A. and Powis, G. (1988). Free radicals in medicine. I. chemical nature

and biologic reactions. Mayo. Clin. Proc. 63: 381-389.

Spear, R.K. and Lumeng, L. (1978). A method for isolating lung mitochondria from rabbits, rats and mice with improved respiratory characteristics. Anal. Biochem. 90: 211-219.

Staiger, Ch., Jauernig, R., De Vries, J. and Weber, E. (1984). Influence of amiodarone on antipyrine pharmacokinetics in three patients with ventricular tachycardia. Br. J. Clin Pharmac. 18: 263-264.

Staübli, M., Troendle, A., Schmid, B., Balmer, P., Kohler, B., Studer, H. and Bircher, J. (1985). Pharmacokinetics of amiodarone, desethylamiodarone and other iodine-containing amiodarone metabolites. Eur. J. Clin. Pharmacol. 29: 417-423.

Stefaniak, M.S., Krumdiek, C.L., Spall, R.D., Gandolfi, A.J. and Brendel, K. (1992). Biochemical and histological characterization of agar-filled precision cut rat lung slices in dynamic organ culture as an *in vitro* tool. *In Vitro* Toxicol. 5(1): 7-19.

Stoner, G.D., Harris, C.C., Authrup, H. Trump, B.F., Kingsbury, E.W. and Myers, G.A. (1978). Explant cultures of human peripheral lung. I. Metabolism of benzo[a]pyrene. Lab. Invest. 38: 685-692.

Stryer, L. (1988). Oxidative phosphorylation. In:Biochemistry 1st ed. W.H. Freeman and Co. New York Chapter 17: 397-448.

Suarez, L.D., Poderoso, J.J., Elsner, B., Bunster, A.M., Esteva, H. and Bellotti, M. (1983). Subacute pneumopathy during amiodarone therapy. Chest 83: 566-568.

Swartz, H.M. (1990). Principles of the metabolism of nitroxides and their implications for spin trapping. Free Rad. Res. Commun. 9(3-6): 399-405.

Tomasi, A., Albano, E., Banni, S., Botti, B., Corongiu, F., Dessi, M.A., Iannone, A., Vannini, V. and Dianzani, M.U. (1987). Free radical metabolism of carbon tetrachloride in rat liver mitochondria. A study of the mechanism of activation. Biochem. J. 246: 313-317.

Trivier, J.M., Libersa, C., Belloc, C. and Lhermitte, M. (1993). Amiodarone N-deethylation in human liver microsomes: Involvement of cytochrome P450 3A enzymes (First report). Life Sci. 52: PL91-96.

Trush, M.A., Seed, J.L. and Kensler, T.W. (1985). Oxidant-dependent metabolic activation of polycyclic aromatic hydrocarbons by phorbol ester-stimulated human polymorphonuclear leukocytes: possible link between inflammation and cancer. Proc.

Nat. Acad. Sci. USA 82(15): 5194-5198.

Valenzuela, C., and Bennett, P.B. (1991). Voltage- and use-dependent modulation of calcium channel current in guinea pig ventricular cells by amiodarone and des-oxo-amiodarone. J. Cardiovasc. Pharmacol. 17: 894-902.

Van Mieghem, W., Coolen, L., Malysse, I., Lacquet, L.M., Deneffe, G.J.D. and Dermedts, M.G.P. (1994). Amiodarone and the development of ARDS after lung surgery. Chest 105: 1642-1645.

Van Schepdael, I. and Solvay, H. (1970). Etude clinique de l'amiodarone dans les troubles du rythme cardiaque. Presse Medicale 78: 1849-50.

Van Zandwijk, N., Darmanata, J.I., Duren, D.R., Alberts, C., Durrer, D. and Wagenvoort, C.A. (1983). Amiodarone pneumonitis. Eur. J. Respir. Dis. 64: 313-317.

Venet, A., Bonan, G. and Caubarrere, I. (1984). Five cases of immune-mediated amiodarone pneumonitis. Lancet 1: 962-3.

Vereckei, A., Blazovics, A., Gyorgy, I., Feher, E., Toth, M., Szenasi, G., Zsinka, A., Foldiak, G. and Feher, J. (1993). The role of free radicals in the pathogenesis of amiodarone toxicity. J. Cardiovasc. Electrophysiol. 4: 161-177.

Vig, P.J.S., Yallapragada, P.R., Kodavanti, P.R.S. and Desaiah, D. (1991). Modulation of calmodulin properties by amiodarone and its major metabolite desethylamiodarone. Pharmacol. Toxicol. 68: 26-33.

Vrobel, T.R., Miller, P.E., Mostow, N.D. and Rakita, L. (1989). A general overview of amiodarone toxicity: its prevention, detection, and management. Prog. Cardiovasc. Dis. 31(6): 393-426.

Wang, Q., Giri, S.N., Hyde, D.M. and Li, C. (1991). Amelioration of bleomycin-induced pulmonary fibrosis in hamsters by combined treatment with taurine and niacin. Biochem. Pharmacol. 42: 1115-1122.

Wang, Q., Hollinger, M.A. and Giri, S.N. (1992). Attenuation of amiodarone-induced lung fibrosis and phospholipidosis in hamsters by taurine and/or niacin treatment. J. Pharmacol. Exp. Ther. 262(1): 127-132.

Wells, P., Zubovits, J.T., Wong, S.T., Molinari, L.M. and Ali, S. (1989). Modulation of phenytoin teratogenicity and embryonic covalent binding by acetylsalicylic acid, caffeic acid, and α-phenyl-N-t-butylnitrone: Implications for

bioactivation by prostaglandin synthetase. Toxicol. Appl. Pharmacol. 97: 192-202.

Wertz, J.E. and Bolton, J.R. (1986). Basic principles of electron spin resonance pp 1-71. In: Electron spin resonance-elementary theory and practical applications.

Wilde, P.E. and Upshall, D.G. (1994). Cysteine esters protect cultured rodent lung slices from sulphur mustard. Human Exp. Toxicol. 13: 743-748.

Wilson, B.D., Jaworski, A.J., Donner, M.E. and Lippman, M.L. (1989). Amiodarone-induced pulmonary toxicity in the rat. Lung 167: 301-311.

Wilson, B.D. and Lippmann, M.L. (1990). Pulmonary accumulation of amiodarone and N-desethylamiodarone. Relationship to the development of pulmonary toxicity. Am. Rev. Respir. Dis. 141: 1553-1558.

Wilson, B.D., Clarkson, C.E. and Lippmann, M.L. (1991). Amiodarone-induced pulmonary inflammation. Correlation with drug dose and lung levels of drug, metabolite, and phospholipid. Am. Rev. Respir. Dis. 143: 1110-1114.

Wilson, B.D. and Lippmann, M.L. (1993). Amiodarone pulmonary toxicity in the rat is associated with increased lavage immunoglobulin and alveolar macrophages primed for increased Il-1 secretion. Am. J. Respir. Cell. Mol. Biol. 9: 295-299.

Wilson, B.D. and Lippmann, M.L. (1996). Susceptibility to amiodarone-induced pulmonary toxicity: relationship to the uptake of amiodarone by isolated lung cells. Lung 174: 31-41.

Witschi, H., Malkinson, A.M. and Thompson, J.A. (1989). Metabolism and pulmonary toxicity of butylated hydroxytoluene (BHT). Pharmacol. Therapeut. 42(1): 89-113.

Wood, D.L., Osborn, M.J., Rooke, J. and Holmes, D.R. (1985). Amiodarone pulmonary toxicity: Report of two cases associated with rapidly progressive fatal adult respiratory distress syndrome after pulmonary angiography. Mayo Clin. Proc. 60: 601-603.

Yasuda, S.U., Sausville, E.A., Hutchins, J.B., Kennedy, T. and Woolsley, R.L. (1996). Amiodarone-induced lymphocyte toxicity and mitochondrial function. J. Cardiovasc. Pharacol. 28: 94-100.

Young, R.A. and Mehendale, H.M. (1986). *In vitro* metabolism of amiodarone by rabbit and rat liver and small intestine. Drug Metab. Disp. 14(4): 423-429.

Young, R.A. and Mehendale, H.M. (1987). Effect of cytochrome P-450 and flavin-containing monooxygenase modifying factors on the *in vitro* metabolism of amiodarone by rat and rabbit. Drug Metab. Disp. 15(4): 511-517.

Zitnik, R.J., Cooper, J.A.D., Rankin, J.A. and Sussman, J. (1992). Effects of *in vitro* amiodarone exposure on alveolar macrophage inflammatory mediator production. Am. J. Med. Sci. 304: 352-6.

Zychlinski, L., Montgomery, M.R., Shamblin, P.B. and Reasor, M.J. (1983). Impairment in pulmonary bioenergetics following chlorphentermine administration to rats. Fund. Appl. Toxicol. 3: 192-198.

APPENDIX I

ELECTRON MICROSCOPY METHODS

Buffer Preparation

A. 0.2 M STOCK PHOSPHATE BUFFER

1. Prepare 1 liter of 0.2 M sodium dihydrogen phosphate (NaH_2PO_4) by weighing out any of the following:

   24.0 g NaH_2PO_4 (anhydrous)
   or 27.6 g $NaH_2PO_4.H_2O$,
   or 31.2 g $NaH_2PO_4.2H_2O$

   Add sufficient deionized/distilled water to make 1 liter. This is Part A (monobasic sodium phosphate).

2. Prepare 1 liter of 0.2 M disodium hydrogen phosphate (Na_2HPO_4) by weighing out any of the following:

   28.4 g Na_2HPO_4 (anhydrous)
   or 35.6 g $Na_2HPO_4.2H_2O$
   or 53.6 g $Na_2HPO_4.7H_2O$
   or 71.6 g $Na_2HPO_4.12H_2O$

   Add sufficient deionized/distilled water to make 1 liter. This is Part B (dibasic sodium phosphate).

3. Prepare the buffer at the required pH (usuallly 7.2 to 7.4) by mixing Part A and Part B together in the following proportions: (Note: usually go with 7.4)

pH	6.4	6.8	7.0	7.2	7.4	7.6	7.8
mL of A	73.5	51.0	39.0	28.0	19.0	13.0	8.5
mL of B	26.5	49.0	61.0	72.0	81.0	87.0	91.5

4. Check the pH and adjust as required using the acid (Part A) or alkaline (Part B) component.

B. 0.1 M PHOSPHATE BUFFER WASH

1. To 50 mL 0.2 M phosphate buffer add 50 mL deionized/distilled water.

2. Check the pH.

NOTES:

a) Store all solutions in appropriately labelled containers at 4°C.

b) These solutions are stable for several weeks or months at 4°C. Be sure to check the pH before use.

c) Any cloudiness or the presence of a precipitate indicates decomposition, and the solution should be discarded.

GENERAL NOTES:

a) All chemicals used should be Analytical Grade or better.

b) All solutions should be made using distilled or deionized water.

Fixative Preparation

A. 3% GLUTARALDEHYDE (your preparation method)

B. 1% OSMIUM TETROXIDE FIXATIVE

1. In a fumehood, carefully score and break a sealed glass ampoule of 10 mL of 4% OsO_4. Using a pasteur pipette, transfer the contents to a 50 mL amber bottle.

2. Add 20 mL of the appropriate 0.2 M buffer (Procedure 63.250.02), plus 10 ml of deionized/distilled water to make a total volume of 40 mL.

3. Label the bottle appropriately and store at 4°C.

4. Wash the broken glass ampoule well with water (in the fumehood) before discarding into the appropriate container.

FIXATION OF TISSUES FOR ULTRASTRUCTURAL EVALUATION:

Double-Fixation Procedure:

1. Select suitable vials to contain the tissue during processing. The vials must be able to hold fluid to at least 20 times the volume of the tissue being processed, and they must be resistant to the chemicals used during fixation, processing and embedding. The most convenient are 4 mL (1 dram) glass vials with vinyl-lined plastic screw caps.

2. Fill the vials with the primary (glutaraldehyde-containing) fixative.

NOTE: 3% Glutaraldehyde in 0.1 M phosphate buffer at pH 7.2 to 7.4 is used routinely as the primary fixative.

3. Label each vial. Use adhesive paper labels and cover with transparent tape.

4. Keep the vials at 4°C until needed.

5. Using a clean scalpel, remove a thin slice from the tissue, organ or tumor to be fixed. Trim away excess fat and connective tissue.

NOTE: The remaining steps should be carried out in a fumehood.

6. Place the tissue on a sheet of dental wax or parafilm, and cover it with several drops of the primary glutaraldehyde fixative.

7. If the structures in the tissue are randomly orientated, cut the tissue into cubes of 1 mm or less with a clean sharp scalpel or razor blade.

NOTES:

a) Glutaraldehyde and osmium tetroxide have very poor penetrating abilities in tissue, hence the necessity for the tissue cubes or slices to be 1 mm or less in thickness.

b) Tissues must be collected and fixed as quickly as possible to prevent post-mortem changes.

8. Transfer the tissue cubes or slices to a vial containing the primary glutaraldehyde fixative.

9. Fix the specimen at room temperature with agitation for a minimum of 2 hours.

NOTE: If fixation is to continue overnight or longer store the vials at 4°C.

10. Replace the fixative with 0.1 M buffer wash at pH 7.2 to 7.4. Agitate for 15 to 30 minutes at room temperature.

11. Repeat Step 6 twice more.

NOTE: The specimens may be stored in the second or third buffer wash at 4°C until further processing is desired.

12. Secondary (Post-) Fixation

NOTE: The following steps must be carried out in a fumehood as the vapors of osmium tetroxide are extremely toxic. After the third buffer wash, siphon off the buffer, and fill the vials with 1% osmium tetroxide in the same phophate buffer.

13. Allow to fix for 1 to 2 hours at room temperature with agitation.

NOTE: To prevent the precipitation of excess osmium in the tissues, do not fix for longer than 2 hours.

14. Replace the osmium tetroxide with 50% ethanol, and proceed with dehydration and embedding procedure below.

NOTES:

a) The first three ethanol steps of the dehydration and embedding serve as washes to remove excess osmium tetroxide from the tissues. Perform in a fumehood.

b) The specimens may be stored temporarily at 4°C in the 70% ethanol step.

REFERENCES:

1. Fixation, Dehydration and Embedding of Biological Specimens. In: Practical Methods in Electron Microscopy, Vol 3, Part I. Audrey M. Glauert, North Holland Publishing Co., 1975.

2. Principles and Techniques of Electron Microscopy - Biological Applications. Volume 1. MA Hayat, Van Nostrand Reinhold Co., 1970.

3. Histologic Fixatives Suitable for Diagnostic Light and Electron Microscopy. Elizabeth M. McDowell, Benjamin F. Trump. Arch Pathol Lab Med 100, 405,

1976.

4. Glutaraldehyde Fixation in Routine Histopathology Robert W Chambers, et al. Arch Pathol 85, 18, 1958.

5. The Influence of Different Fixatives and Fixation Methods on the Ultrastructure of Rat Kidney Proximal Tubule Cells. 1. Comparison of Different Perfusion Fixation Methods and of Glutaraldehyde, Formaldehyde and Osmium Tetroxide Fixatives. Avrid B Maunsbach. J Ultrastruct Res 15, 242, 1966.

6. Fixation for Electron Microscopy - MA Hayat, Academic Press, 1981.

7. Reynold ES. J Cell Biol 17: 208, 1963.

8. Venable JH and Coggeshall R. J Cell Biol 25: 407, 1965.

PROCEDURE FOR THE DEHYDRATION AND EMBEDDING OF TISSUES FOR ELECTRON MICROSCOPIC STUDIES:

A. PREPARATION OF 100 mL OF EPON-ARALDITE EMBEDDING RESIN

1. Weigh out and combine the following:
   - Araldite 502 - 15.75g
   - Epon 812 - 31.25g
   - Dodecenyl succinic anhydride (DDSA) - 56.00 g

2. Stir at room temperature until the mixture is homogeneous.

3. Add 2.0 mL of 2,4,6-Tri(dimethyl-amino methyl) phenol (DMP-30) to the mixture and stir gently to ensure complete blending of components.

B. DEHYDRATION AND EMBEDDING

NOTE:

The following scheme indicates steps and time periods used in the standard dehydration/embedding process. At the end of each step, the processing solution is siphoned off and replaced with the next processing fluid at a volume of at least 20 times the volume of the tissue being processed. All steps are carried out at room temperature. The tissue used at this point will have been fixed and ususally post-fixed in the appropriate fixative.

Standard Alcohol Dehydration:

1. Fill vial with 50% ethanol and agitate for 15 minutes.
2. Fill vial with 70% ethanol and agitate for 15 minutes.
3. Fill vial with 90% ethanol and agitate for 15 minutes.
4. Fill vial with 95% ethanol and agitate for 15 minutes.
5. Fill vial with 100% ethanol and agitate for 15 minutes.
6. Repeat step 5 two more times.
7. Fill vial with propylene oxide and agitate for 20 minutes.
8. Repeat Step 7 above.
9. Fill vial with 1:1 propylene oxide: Epon-Araldite mixture and agitate for 60 minutes.
10. Fill vial with 1:2 propylene oxide: Epon-Araldite mixture and agitate for 1.5 hours.
11. Fill vial with 100% Epon-Araldite mixture and agitate for 2 hours at room temperature.

NOTES:

a) The tissue may be left overnight at 4°C without agitation at the end of steps 2 and 10 above. Keep the vials well sealed.

b) 100% ethanol, propylene oxide and all the resin components are hygroscopic and must be kept well sealed from the atmosphere.

C. EMBEDDING

1. Place a paper strip labeled with the assigned EM laboratory sequential block number into each depression according to the number of blocks to be embedded. Record the block numbers assigned to each specimen in the EM Records notebook.

2. Pre-dry the molds and paper strips in the 60°C oven for at least 1 hour.

3. Remove from the oven and cool.

4. Partially fill the capsules or depressions with Epon-Araldite, being careful to avoid air bubbles.

5. Place one cube (i.e. block) of tissue at both ends of each depression in the required orientation.

6. Completely fill the capsules or depressions with Epon-Araldite, again being careful to avoid air bubbles.

7. Polymerize the resin by placing the molds in a 60°C to 65°C oven for 48-72 hours.

8. After cooking to room temperature, remove the blocks from the capsules by pressing them out with a pair of wide-nosed pliers. Flat-embedded blocks can simply be snapped out of the molds.

NOTES:

a) Propylene oxide (1,2 epoxy propane) is highly flammable and toxic. All work with this compound should be done in a fumehood.

b) All components of the plastic monomer mixture are toxic, allergenic, and potentially carcinogenic. Handle with rubber gloves. Prepare in a fumehood.

c) All waste propylene oxide:resin mixtures should be put into a sealable container especially marked for that purpose. Mixtures should be concentrated by evaporating off most of the propylene oxide in the fumehood. When full, the sealed container is turned over to a waste disposal company.

d) Left-over Epon:Araldite should be polymerized in the oven before being discarded.

PROCEDURE FOR THE TRIMMING, SECTIONING AND STAINING OF TISSUE FOR ELECTRON MICROSCOPIC STUDIES:

General Information:

This procedure describes the routine normally carried out by the Electron Microscopy Laboratory for:

a) preparation of stains for thick and thin sections;
b) trimming of specimen blocks;
c) cutting and staining of thick sections; and
d) cutting and staining of thin sections.

NOTE: Unless otherwise stated in this procedure, distilled water denotes distilled, deionized water.

Equipment:

1. Ultramicrotome (Reichert OM-U2 and Reichert-Jung Ultracut E)
2. Hot Plate
3. Heat Pen

4. Glass slides and coverslips
5. 200-mesh copper grids
6. Plastic petri dishes

A. PREPARATION OF STAINS

I) Toluidine Blue O:

1. Prepare 250 mL of a 1% sodium borate solution. This is Stock Solution A.

2. Prepare 250 mL of a 1% Toluidine Blue O solution. This is Stock Solution B.

3. Combine 50 mL of Stock A and 50 mL of Stock B, and stir to ensure adequate mixing.

4. Label appropriately, and store at room temperature.

ii) Reynolds Lead Citrate:

1. In a 500 mL Erlenmeyer flask boil 200 mL distilled water for 15 minutes to make it CO_2 free, cool to room temperature, and use throughout the stain formulation.

2. In a 50 mL volumetric flask, dissolve 1.33 g of lead nitrate in 15 mL of distilled CO_2-free water.

3. In a 50 mL beaker, dissolve 1.76 g of anhydrous sodium citrate (1.89g of dihydrate) in 15 mL of distilled CO_2-free water.

4. Add the sodium citrate solution to the lead nitrate solution. Rinse the beaker with 10 mL of distilled water and add to flask. Stopper the flask and shake intermittently for 20 min.

5. Add 8 ml of 1 N sodium hydroxide and gently swirl until solution clears. Add water to bring volume to 50 mL. Store stoppered, labeled flask at 4°C.

NOTE: Stain containing any white precipitate should be discarded.

6. Stain can be drawn off directly into an appropriately labeled 5 mL syringe. Cap the syringe with a disposable filter and cap (0.22 mμ pore size). The capped syringe can then be used repeatedly. Discard the first 2 drops of stain before each use.

NOTES:

a) This is a modification of the preparation method of Reynolds E.S., J. Cell Biol. 17: 208, (1963).

b) Lead citrate stain is extremely sensitive to atmospheric carbon dioxide. Avoid prolonged air exposure.

iii) Uranyl Acetate:

1. Weigh out 2.5 g of uranyl acetate (EM grade) and dilute with 100 mL of 70% ethyl (or methyl) alcohol.

2. Store in an appropriately-labeled amber bottle at 4°C.

NOTE: Uranyl acetate is light sensitive.

B. TRIMMING OF SPECIMEN BLOCKS

1. Trim blocks by hand on the stage of the ultramicrotome using a degreased razor blade.

C. CUTTING AND STAINING OF THICK SECTIONS

NOTE:
Thick sections or blues denote plastic embedded material sectioned at 0.5 to 1 μm thickness and stained with Toluidine Blue stain. Thick sections are examined by light microscopy to asssess the quality and suitability of the tissue specimen. The examination of these sections minimizes the number of thin sections to be cut for viewing under the electron microscope. Thick sections may also be used to reveal structures which are not ordinarily visible in routine paraffin-embedded sections.

1. The controls and operation of the ultramicrotome are described in the manufacturer's operations manual.

2. Mount the block in its chuck into the microtome specimen arm.

3. Mount a diamond histoknife in the knife holder.

4. Fill the trough with distilled water until a positive meniscus is formed.

5. Remove water from the trough until the water forms a reflective surface.

6. Align the block face so that the wide side of the trapezoid is parallel to the knife edge.

7. Use the manual handwheel of the microtome and the fine feed to rough cut the block in order to remove any surface marks.

8. Using the handwheel and fine manual feed, proceed to cut sections at thicknesses of 0.25, 0.50, and 0.75 μm.

9. Use a metal wire loop to pick up the sections and transfer to a glass slide.

10. Place the slide on a hot plate at 70°C and allow to stretch and dry for at least 5 minutes.

11. While still on the hot plate, cover the surface of the slide with Toluidine Blue stain.

12. Allow to stain for about 45 seconds.

13. Wash the slide with deionized/distilled water from a squirt bottle. Dip slides 7 to 10 times in deionized/distilled water. Differentiate stain by dipping 7 to 10 times in acetone. Rinse by dipping 7 to 10 times in water taking care not to disrupt the sections, wipe off excess water and air dry.

14. Coverslip using Permount mounting media and a #1 cover glass.

15. Label the slide.

D. CUTTING OF THIN SECTIONS

NOTE:

Thin or ultrathin sections denote plastic embedded material sectioned at approximately 120 - 140 nm ($\pm$10 nm) thickness; these sections reveal a gold interference color when viewed through the eyepiece of the ultramicrotome.

1. The controls and operation of the ultramicrotome are described in the manufacturer's operation manual.

2. Mount a diamond knife in the knife holder, and adjust the knife angle to that recommended by the manufacturer. This is indicated on the container.

3. Fill the knife boat with deionized/distilled water which has been filtered through a

0.22μm pore filter. Follow Steps 4 and 5 of Section C.

4. Orient the knife so that the knife edge and its reflection in the block face are parallel.

5. Slowly approach the block using the fine feed control.

6. Proceed to cut ultrathin sections following the instructions of the manufacturer's operation manual.

7. Flatten the sections using the pre-heated filament of a heat pen.

8. Pick up the sections from below using 200 mesh, hexagon, thin-bar copper grids (J.B. EM Services, JBS #G2OOHH).

9. Transfer the grids to a silicone rubber pad (grid-gripper with numbered squares) in a covered petri dish.

10. Label the petri dish with the study number, animal number, group, sex, and block number.

E. STAINING OF THIN SECTIONS

1. Prepare boiled cooled (CO_2-free) deionized/distilled water as in Steps 1 and 2 of Part A (ii) of this procedure.

2. Take up a portion of the CO_2-free deionized/distilled water into a disposable syringe. Attach a 0.22 μm pore size disposable syringe filter to the tip.

3. Using 4, 50 mL Tri-Pour beakers, prepare grid washing solutions:
   a) 70% ethanol.
   b) alkaline H_2O (2 small pellets NaOH in 50 mL filtered H_2O).
   c) filtered H_2O in 2 beakers.

4. Using a Pasteur pipette, draw off a small amount of stain from beneath the surface of the uranyl acetate staining solution. Place one drop per grid on a flat piece of parafilm in a petri dish.

5. Float a single grid, sections-side down, on each drop of uranyl acetate. Replace the opaque cover, and stain for 15 minutes.

6. Using clean forceps, pick up each grid and gently dip 8 to 10 times in 70% ethanol and 8 to 10 times in each of two H_2O rinses. Transfer to filter paper.

7. Immediately transfer each grid to a single drop of filtered (0.22 μm) lead citrate stain in a second petri dish staining vessel with fresh NaOH pellets placed in center depression. Stain for 5 to 7 minutes.

8. Using clean forceps, quickly pick up each grid and gently dip 8 to 10 times in alkaline H_2O and 8 to 10 times each in the final two H_2O rinses; allow the grids to dry on clean filter paper.

9. Transfer the grids back to their original places in the labeled petri dishes.

REFERENCES:

1. Reynolds ES. J. Cell Biol. 17: 208, 1963.

ROUTINE EXAMINATION AND PHOTOGRAPHY OF TISSUES USING THE PHILLIPS CM10 ELECTRON MICROSCOPE

PROCEDURE:

A. TURNING ON THE MICROSCOPE

1. The microscope is fully operational at all times.

B. INSERTING THE GRID

1. Remove the specimen holder from the microscope by pulling it out until it stops rotating 90° clockwise and drawing straight out. Store in the appropriate holder on the bench top.

2. Using the tool provided, lift the specimen clamp.

3. Place the grid specimen (section side up) into the cavity of the specimen holder.

4. Lower the specimen clamp and gently squeeze down with forceps to ensure true clamping of grid.

5. Insert the specimen holder into the airlock very gently until locating pin activates

pump; wait until red warning light on airlock is out.

6. While holding the specimen holder with both hands, rotate slowly 90° counterclockwise.

7. Slowly push the specimen holder in as far as it will go, while gently resisting the movement of the specimen holder as it is drawn into position. (DO NOT RELEASE!)

8. To remove the specimen holder, repeat step 1 above.

C. SWITCHING ON THE ILLUMINATION

1. Depress High Tension button (green light will illuminate).

2. Rotate Filament knob clock-wise until a beeping sound is heard.

D. THE PLATE CAMERA: PHOTOGRAPHY, REMOVAL, REINSTALLATION

NOTE:

The plate camera consists of two integrable but separate units. On the top is the plate camera which is capable of holding 56 pre-loaded unexposed photographic plates. On the bottom is the receiver which holds up to 56 exposed plates. The two are held firmly together by easily released side latches. The film of choice is Kodak Electron Microscope Film 4489 3.25" x 4".

(I) PHOTOGRAPHY WITH THE PLATE CAMERA:

1. Set up CM10 and computer according to Section E following.

2. Establish the field to be photographed.

3. Focus using the focus control on the right hand panel; if necessary, use wobbler button on the left hand panel as an aid to focus.

4. Adjust illumination to produce a 2 to 3 second exposure as indicated on the panel screen.

5. Pull left hand lever forward to raise screen.

6. Expose film by pushing illuminated exposure button on the far left of left instrument panel.

7. Lower screen after exposure has been completed (i.e. after room and panel lights return).

8. Record the plate number, study number, animal number, and any relevant details in the EM Film Records book.

NOTE:

After each exposure the newly exposed plate will have been pneumatically transferred from the top assembly - the plate camera, to the lower assembly - the receiver.

(ii) REMOVAL AND REINSTALLATION OF THE PLATE CAMERA AND RECEIVER:

1. Go to the vacuum status page on the CM10 monitor and bring the camera chamber to atmosphere by pushing camera air. (Chamber takes approximately 5 minutes to come to atmosphere.)

2. Remove camera chamber lid by lifting straight up.

3. Remove plate camera - receiver assembly by lifting straight up. (Note the orientation of guide pin.)

4. If necessary, slide the two accessor plates into the slots on the plate camera and the receiver. The plates make each light tight and permit separation and replacement of either the receiver or the plate camera.

5. Reassemble plate camera and receiver.

6. Remove accessory plates and lower the assembly back into the microscope.

7. Replace the camera chamber lid.

8. Evaluate camera chamber by re-pushing camera air button.

E. CM10 COMPUTER LOGGING AND PRINTING OF PHOTOGRAPHIC PARAMETERS

PROCEDURE:

(I) LOGGING OF PHOTOGRAPHIC PARAMETERS:

On CM10:

a) On main menu, select parameters and proceed to second page (press parameters twice).

b) Set general data by selecting operation and camera .

c) Set printing by selecting after exp (if logging is desired after each photo is taken) or direct (log of current EM settings sent to PC without photo taken).

d) On third page of parameters, set for remote control.

On computer:

a) Select CM10 Microscope from menu on dosshell, then select CMONITOR CONTROL SYSTEM.

b) Current Directory (at top of screen) will be C:\CM10\logs for this procedure; F2 may be used to enter new directory name if desired.

c) If creating new log files, use control F9 to set append log files and use F9 to turn logging on (replace only used if previously existing files are to be eliminated).

d) At request, enter new or previous file name. Logging systerm is then ready to receive EM photo data.

e) To view existing log files, toggle logging to OFF using F9. Use control F10 to toggle between SCR (to view log files on screen) or LPT . Press F10 to activate. Enter desired file name.

(ii) EDITING AND PRINTING LABELS FOR ELECTRON MICROGRAPHS

a) Exit CMONITOR (F1) and proceed to WordPerfect (DOS version).

b) List files under C:\CM10\logs and retrieve desired file.

c) Run macro (Alt J) to space information on list to fit onto labels. Move cursor to top of page and delete Exposure No. and next two lines. Move cursor down past study # , then back up one to reset text lines. Enter study # , animal # and block # , information (obtained from EM Film Record Book) when requested, hitting 'enter' after each entry to advance to next step.

NOTE:

When exiting WordPerfect, saving altered WP file under the same name will then over overwrite Cm10 logfiles.